

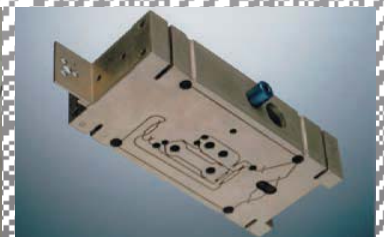
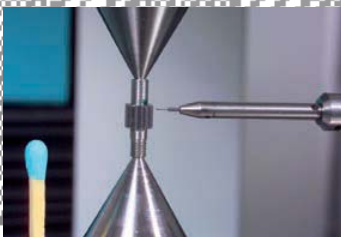
PROFESSIONAL JOURNAL ON PRECISION ENGINEERING

μ MIKRONIEK

ISSUE 4
2013
(VOL. 53)



- **ADVANCED VIRGO INTERFEROMETER** ■ **OPTIMISING FLEXURE GEOMETRY**
- **LOW-FREQUENCY VIBRATION ISOLATION** ■ **WIRE-EDM REVIEW**



Mikroniek is a publication of the DUTCH SOCIETY FOR PRECISION ENGINEERING www.dspe.nl

DSPE

Please join our first

DSPE symposium on Optics & Optomechanics

Where we bring optical and optomechanical experts together, to learn from each other and to increase the economic potential of this area of competence.

The symposium will provide an atmosphere for networking, technical discussion, and sharing the enthusiasm of working in this challenging field. Next to some excellent keynote speakers and business presentations you can get a preview of the book

"A course in lens design" by Chris Velzel

For more information: www.dspe.nl

KEYNOTE SPEAKERS TENTATIVE

Wilhelm Ulrich (Sr. Director Optical Design) Carl Zeiss
"Freeform Optics"

Stefan Sinzinger (Head of Technical Optics) TU Ilmenau
"Freeform surfaces in optical microsystems –
from design to applications"

Wolfgang Vollrath (Chief Scientist) KLA-Tencor
"Optical design and manufacturing requirements
for high-performance microscope objectives"

Arie den Boef (Fellow) ASML
"Optical Metrology of Semiconductor Wafers in Lithography"

Bert van der Pasch (Fellow) ASML
"System stability in a lithography wafer scanner"

Jan Nijenhuis (Sr. System Engineer) TNO

Paul Urbach (President of EOS & Head Optics Research Group TU Delft)

Chairman of the day

Jan Willem Mariani (VP System Engineering) ASML



PUBLICATION INFORMATION

Objective

Professional journal on precision engineering and the official organ of DSPE, the Dutch Society for Precision Engineering. Mikroniek provides current information about scientific, technical and business developments in the fields of precision engineering, mechatronics and optics.

The journal is read by researchers and professionals in charge of the development and realisation of advanced precision machinery.



Publisher

DSPE
High Tech Campus 1, 5656 AE Eindhoven
PO Box 80036, 5600 JW Eindhoven
info@dspe.nl, www.dspe.nl

Editorial board

Ir. Herman Soemers (chairman, University of Twente, Philips Innovation Services), ir.ing. Bert Brals (CCM), dr.ir. Dannis Brouwer (University of Twente), ir. Bart Dirckx (coordinator, WittyWorX), ir. Jos Gungsing (MaromeTech, Avans), ir. Rob van Haendel (Philips Innovation Services), ir. Huub Janssen (Janssen Precision Engineering), ir. Henk Kiela (Opteq, Fontys), ir. Casper Kruijjer, MBI (FEI), ing. Ronald Lamers, M.Sc. (MI-Partners), ir. Piet van Rens (Settels Savenije van Amelsvoort), ir. Ad Vermeer (SoLayTec, Adinsyde)

Editor

Hans van Eerden, hans.vaneerden@dspe.nl

Advertising canvasser

Gerrit Kulsdom, Sales & Services
+31 (0)229 - 211 211, gerrit@salesandservices.nl

Design and realisation

Twin Media bv, Culemborg
+31 (0)345 - 470 500, info@twinmediabv.nl

Subscription costs

The Netherlands € 70.00 (excl. VAT) per year
Europe € 80.00 (excl. VAT) per year
Outside Europe € 70.00 + postage (excl. VAT) per year

Mikroniek appears six times a year.

© Nothing from this publication may be reproduced or copied without the express permission of the publisher.

ISSN 0026-3699



The main cover photo (Hummingbird 2.0 vibration isolation platform) is courtesy of MECAL.

IN THIS ISSUE

ISSUE 4
2013

05

Pushing the Advanced Virgo interferometer to the limit

High-performance vibration isolation for gravitational wave detectors.

12

Wire-EDM review

Electrical Discharge Machining is a competitive technology for serial production of micro-precision components.

18

Robust control of electromagnetic actuators

An outline of system identification experiments as well as a possible robust approach for armature movement control.

24

Large-stroke spatial hinge flexures

A method for optimising the geometry of flexure hinges, aimed at maximising supporting stiffnesses.

31

Measuring small gearwheels

Computer software made it possible to translate a cloud of measuring points into the deviation of a tooth profile from the involute form prescribed.

36

CAD/CAM indispensable time saver or erosion of knowledge and expertise?

Students reporting on the rise of engineering software.

40

Low-frequency vibration isolation

The Hummingbird platform can serve as a vibration filter between a ceiling and a microscope. As a result, microscope users can enjoy a stable image in any building.

45

Progress in energy technologies, optics and measurement

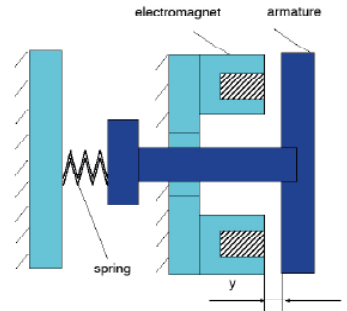
Report of the euspen 13th International Conference.

54

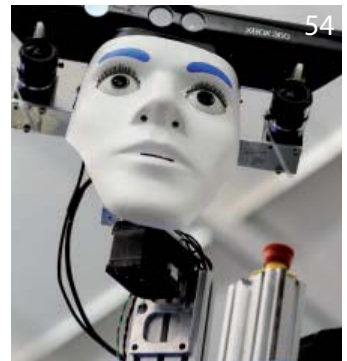
Theme: Robotics

Impressions of the RoboCup 2013 event. The forthcoming issue of Mikroniek will be partly dedicated to robotics, both industrial and non-industrial.

18



54



FEATURES

04 EDITORIAL

Hans Krikhaar, President DSPE and acting as stand-in editorial writer, on DSPE's international ambitions.

39 UPCOMING EVENTS

Including: Electrical Discharge Machining seminar.

51 DSPE

Including: DSPE Symposium Optics & Optomechanics.

53 CPE COURSE CALENDAR

Overview of Certified Precision Engineer courses.

56 NEWS

Including: StartupBootcamp High Tech XL welcomes applications.

EDITORIAL

STAND-IN EDITORIAL WRITER



As you may have noticed, DSPE tries to entice all kinds of people to write an editorial in Mikroniek. Adding new (international) contacts allows us to extend our network of ambition and opportunities. However, sometimes it's not easy to convince a potential editorial writer to submit their contribution on time for the next issue of Mikroniek. The editor then rings me up and we discuss how to solve the matter. This also happened with the present issue, but this time I offered to write the editorial myself. So, now I'm the stand-in editorial writer.

Extending our international network, that is indeed a common theme of many of our activities with various partners. Although the High-Tech Systems conference in April this year was already an international event, next year we want to make a statement by raising the event's international profile. We're also attracting international trainees to our high-end courses on precision engineering and in some cases even delivering the training abroad. This summer, DSPE organised the eighth edition of the Opto-Mechatronics summer school and once again the participants were very enthusiastic in their feedback. All of this is with thanks to the partners who provided the course content.

The first edition of the Manufacturability summer school, which kicked off on 27 August, was oversubscribed. I'm sure it was very cost-effective for companies to send people to this course; it will help designers to save money for their company.

On 7 October, DSPE will be hosting a symposium on Optics & Optomechatronics with a very impressive array of speakers. We think Dutch optical specialists could improve their network by building more contacts and sharing knowledge. Our aim is to become the Dutch optical society partnering with EOS, the European Optical Society. We hope every optical expert in the Netherlands will consider attending the symposium.

And to follow up the very successful 2012 edition, we're already preparing the DSPE Conference 2014.

This summary just goes to show that we're continuously looking for innovation in precision engineering disciplines, currently focusing on high-tech systems, optics & optomechatronics and microsystems applications. But we're also convinced that we should explore the world. During its Golden Age, the Netherlands had very strong maritime trading links with the Far East. Today, we have to exploit our high-tech expertise in the Far East as well. This will allow us to create another Golden Age.

We'll have to keep exploring how to achieve this. From personal experience, I can tell you that it's not easy to figure out what to do. However, once we've learned more, the opportunities will be there. Look at the German automotive industry, it's doing very well. Why? They focus on Asia. Asians like West European high-tech. Why? Because it's high quality. So you see a lot of German cars in China. They've done a good job compared to Japanese and Korean car manufacturers. Learning from the German example, we should try to establish a High-Tech Golden Age for the Netherlands, something I'm convinced we can do.

Hans Krikhaar

DSPE President and stand-in editorial writer

PUSHING THE **ADVANCED VIRGO INTERFEROMETER** TO THE LIMIT

After fifty years of building gravitational wave detectors with ever-increasing sensitivity and bandwidth, the first regular detections are expected in the course of this decade. At frequencies down to 10 Hz, the second generation of interferometric gravitational wave detectors (in Europe, US, India and Japan) requires displacement limits many orders of magnitudes below the level of seismic disturbances. A compact multi-stage, soft-mount suspension was designed and tested for isolating in-vacuum optical benches for the Advanced Virgo interferometer in six degrees of freedom.

ERIC HENNES AND MARK BEKER

Einstein has shown in his theory of General Relativity (1915) that gravity corresponds to deformation of space and time. For instance, two heavy stars, fastly rotating around each other, create large fluctuations in the local gravitational field, and with it, in space itself. These fluctuations propagate outward as a wave, with the speed of light. When the wave reaches the Earth after a long journey, its strength has been reduced to very tiny strain fluctuations. Strain amplitudes of at most 10^{-22} m/m, in the range 10 Hz – 10 kHz, are presumably caused by gravitational waves

originating from pulsars, coalescing binary objects (neutron stars or black holes) or from the early universe (gravitational background radiation).

Gravitational waves were proven to exist in 1974. Nevertheless, until now they have never been directly measured. A key instrumental technique in gravitational wave astronomy is interferometry. Nikhef participates in Virgo, an interferometer with 3km-long arms, located near Pisa in Italy (see Figures 1 and 2).

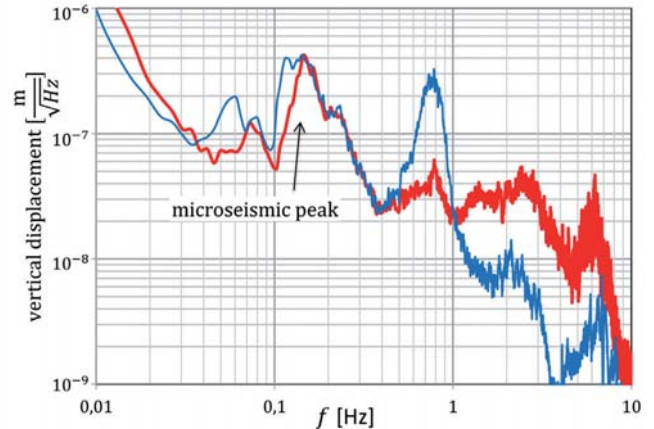
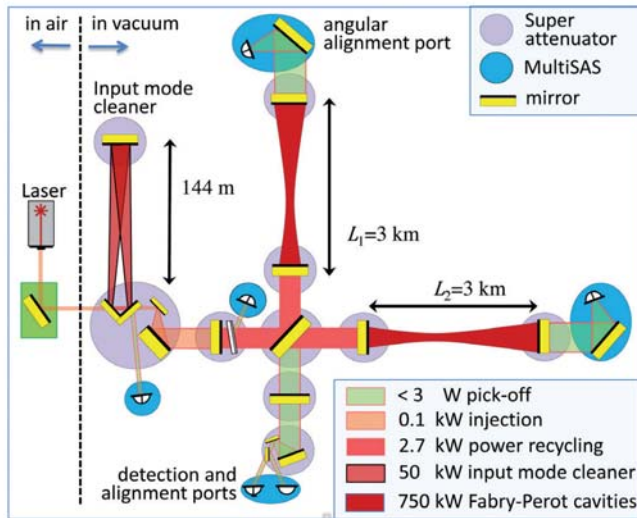
AUTHORS' NOTE

Eric Hennes is working at Nikhef (National Institute for Subatomic Physics), based in Amsterdam, the Netherlands, supporting the Mechanical Technology group. Mark Beker is director of InnoSeis, a spin-off company from Nikhef, specialised in seismic measurements and isolation. This article was, in part, based on presentations at the DSPE Conference, which was held on 4 and 5 September 2012 in Deurne, the Netherlands.

e.hennes@nikhef.nl
www.nikhef.nl
www.innoseis.com



1 Aerial view of the Virgo interferometer near Pisa, Italy.



2

3

The mutually perpendicular arms function as rulers. A passing gravitational wave makes one arm slightly longer (by ΔL_1), while at the same time the other gets shorter (ΔL_2), and vice versa. Typical amplitudes amount to an attometer (10^{-18} m), one thousand times smaller than an atomic nucleus. The difference, $\Delta L = \Delta L_1 - \Delta L_2$, is measured by sending infrared correlated laser beams along both arms. The beams are reflected by mirrors at the ends, and upon return combined into an interferometric signal at the detection port. Analysis of this signal may reveal ΔL , and with it, the gravitational wave strain $\Delta L/2L$.

Note that the arms are nothing more than long evacuated tubes in which a high-power laser beam is running hence and forth between the mirrors of a Fabry-Perot cavity. The output signal can only be ascribed to a gravitational wave if all other mechanisms that (seem to) move the mirrors can be excluded. Typical disturbing sources are thermal noise, photon shot noise, photon scattering, radiation pressure noise and laser power fluctuations. At low frequencies the main disturbance source is seismic motion.

Seism

In Italy, the Earth surface moves randomly in all directions with amplitudes up to several micrometers due to sea swell waves with frequencies between 0.1 and 1 Hz that act on the Atlantic and Mediterranean sea floors and coasts. At higher frequencies the seismic displacement noise level decreases rapidly (see Figure 3). Nevertheless, at 10 Hz it is still 10^{10} (10 billion!) times larger than the allowed displacement of the main mirrors. The high sensitivity requires almost all optical components to be isolated from seismic vibrations.

At Virgo, the required residual vibration levels are reached using low-frequency mechanical oscillators that, by nature, attenuate vibrations above their resonance frequency. The main mirrors are suspended from a so-called super-attenuator, an 8m-long chain of mechanical filters [1]. For the coming upgrade of the interferometer, called Advanced Virgo, Nikhef has designed, built and tested compact in-vacuum seismic attenuation systems (SAS) for a number of auxiliary optical benches that will be installed in 2015.

Passive seismic isolation

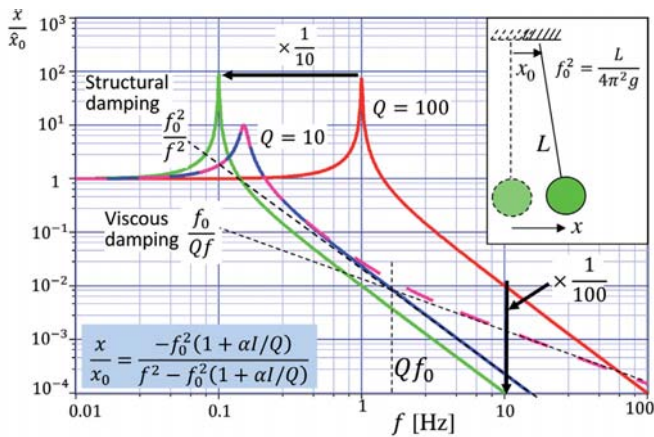
The principle of passive vibration isolation is illustrated by the transfer function of the harmonic oscillator in Figure 4. At frequencies well below resonance ($f \ll f_0$) the mass follows the suspension point: $x/x_0 = 1$. At resonance the oscillator swings up to an amplitude level Q , called the quality factor. Q^{-1} is a measure of the damping. The domain of passive attenuation is clearly above resonance, when the transfer function magnitude drops below unity ($f \gg f_0$).

For a low- Q oscillator the attenuation at higher frequencies depends on the type of damping assumed: viscous ($|x/\dot{x}_0| = f_0/(Qf)$) or structural ($|x/\dot{x}_0| = f_0^2/f^2$). The viscous regime shows up above $f = Qf_0$. For structural damping the attenuation is independent of Q . For example, a 25cm-long pendulum ($f_0 = 1$ Hz) attenuates vibrations at $f = 100$ Hz by a factor $f_0^2/f^2 = 10^4$ (red line in Figure 4). Decreasing the resonance frequency a factor 10 improves the attenuator by a factor 100 (green line). However, this requires a 25m-long pendulum.

The application of anti-springs, discussed below, allows for low resonance frequencies within a compact design. The attenuation can be further improved by putting a number

2 Schematic layout of Advanced Virgo. The input mode cleaner cavity selects a stable Gaussian mode from the laser beam. Both interferometer arms include a 3km-long Fabry-Perot cavity that virtually increases the arm length to 150 km. The new Seismic Attenuation Systems (SAS) are shown in blue.

3 Typical seismic displacement noise spectra at the Virgo site, recorded during a weekday (red) and during a Saturday night (blue).



4

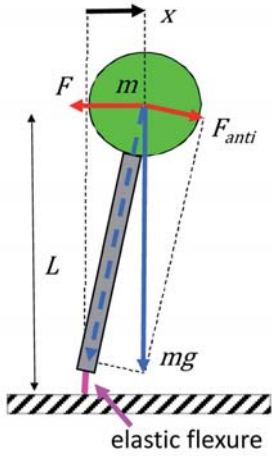
of oscillators in cascade. For a cascade consisting of N oscillators, the attenuation decreases as $1/f^{2N}$. Low-frequency resonant modes need to be damped, either passively or actively.

Horizontal: inverted pendulum

A widely applied low-frequency/small-sized horizontal oscillator consists of a mass on top of a stiff rod, which is attached to the ground with a thin flexural spring that just prevents it from falling over (Figure 5). The horizontal restoring force for a small deflection x equals:

$$F_{tot} = F_{flex} + F_{anti} = - \left(k_{flex} - \frac{mg}{L} \right) \cdot x \tag{1}$$

Here g is the gravitational acceleration, L is the length and k_{flex} is the elastic spring constant. The second term shows that gravity acts as an ‘anti-spring’: it contributes negatively



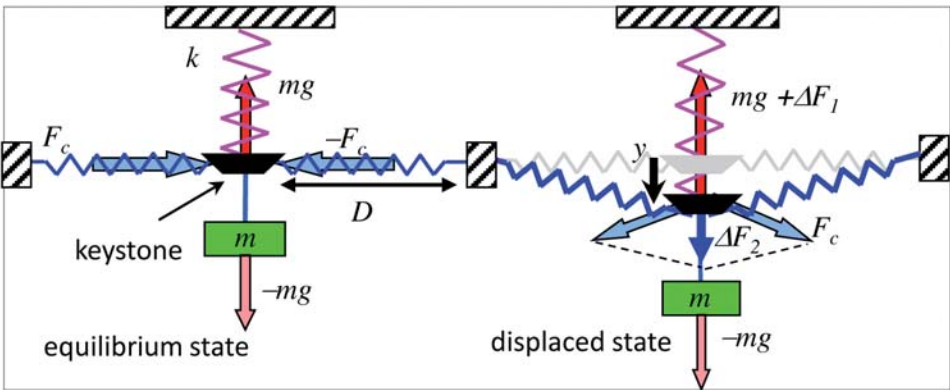
5

to the stiffness. The resonance frequency can be tuned arbitrarily close to zero, for instance by adjusting the mass close to $k_{flex} \cdot L/g$. If it exceeds this value the pendulum will become unstable and fall over. In practice $f_0 = 0.05$ Hz is feasible.

Note that a suspended pendulum would need a 100m-long wire to reach that frequency. The seismic attenuation systems for Virgo all contain three inverted pendulum legs, allowing isolation of the payload mass in three horizontal degrees of freedom (DoFs), i.e. two horizontal displacements and the rotation around the vertical axis, without inducing unwanted tilt motion.

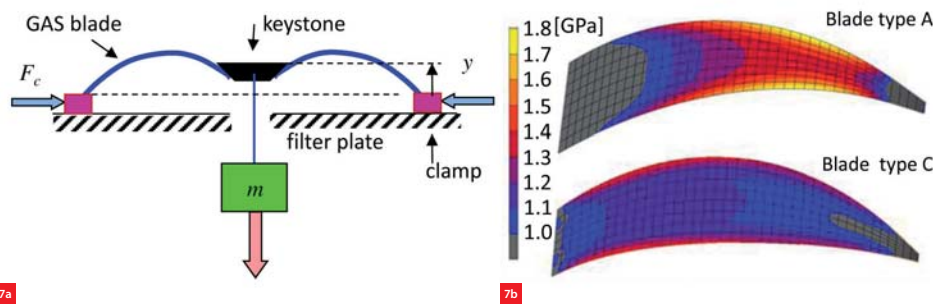
Vertical: geometric anti-spring (GAS) filter

Figure 6 shows the anti-spring principle for vertical oscillations. The oscillator mass is suspended from a



6a

6b



7 GAS filter, design and realisation.
 (a) Sketch of GAS filter with two blades.
 (b) Top surface stress profiles of different GAS-blade types, calculated by finite-element analysis.
 (c) GAS filter (Ø 650 mm) for 420 kg load, fitted with ten maraging steel blades of 2.7 mm thick, typically tuned at $f_0 = 0.25$ Hz.

vertical spring with spring constant k via a wire. The connecting 'keystone' is subjected to horizontal forces F_c from compressed springs at either side that cancel in the equilibrium state. At a small displacement y the vertical spring force changes by ΔF_1 . This is partially cancelled by the vertical components of the two compressive forces:

$$F_{tot} = \Delta F_1 + \Delta F_2 = - \left(k - \frac{2F_c}{D} \right) \cdot y \quad (2)$$

Here D is the length of the compressed springs. The second term acts as an anti-spring: the compression contributes negatively to the total stiffness. The resonance frequency can be tuned arbitrarily close to zero by adjusting the compression such that F_c approaches $k \cdot D / 2$. If it exceeds this critical value, the system becomes unstable.

In a geometric antispring (GAS) [2] the horizontal and vertical spring functions are combined in a single elastic element, a triangular, initially flat blade spring (Figure 7). Two or more of these GAS blades can be combined to establish a GAS filter. Detailed mathematical and numerical analysis is required to calculate the properties of the blade, such as its curvature, stress profile and highly non-linear force-displacement curves. They depend on the imposed clamping angles, the suspended mass, the blade shape and the applied compressive force. The latter can be adjusted by shifting the clamps in- or outward on the filter plate. The analysis enables the design of blades with optimal characteristics, and help to predict the optimal positions of clamp and blade tip.

To design a GAS filter as compact as possible, the blades are made from low-creep, ultra-high-strength materials, like maraging steel [3]. In practice, it can be tuned down to 0.15 Hz. At such a low resonant frequency the observed quality factor is typically as low as $Q = 3$. Its measured transfer function shows a nice $1/f^2$ roll-off down to 10^{-4} at 20 Hz. Referring to Figure 4, this suggests that it can be modeled (in the frequency domain) by a structurally damped oscillator.

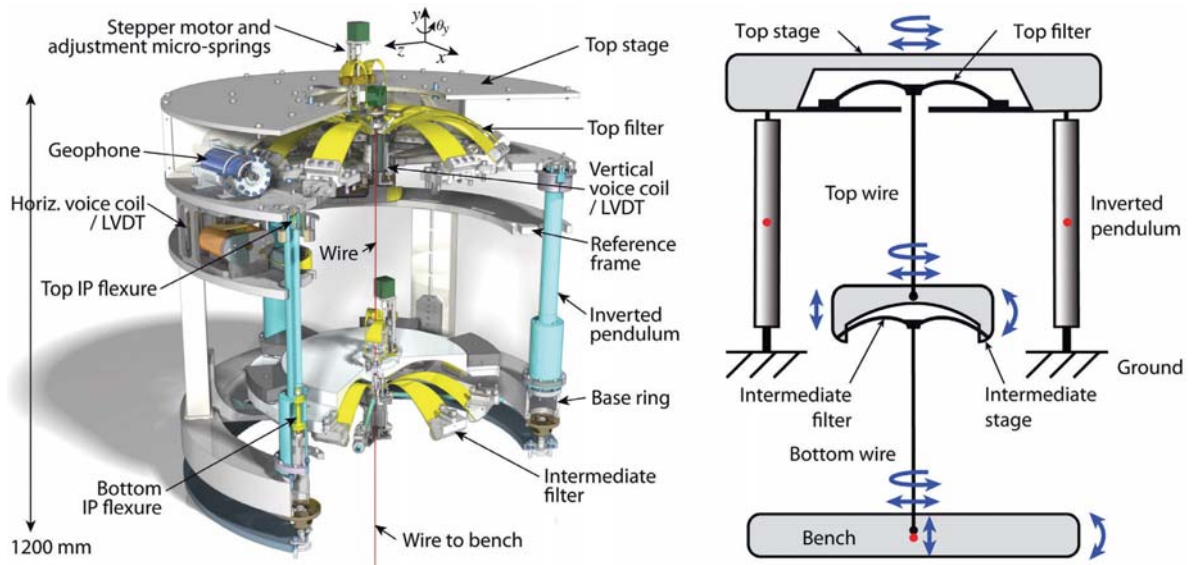
Rotational low-frequency oscillator

Both horizontal and vertical vibrational sources may induce rotations in the system. For instance, a horizontal vibration of the filter plate in Figure 7 causes the suspended mass not only to swing, but also to tilt. The tilt amplitude response is of the same type as shown in Figure 4, with f_0 being the rotational mode frequency. It can be minimised by choosing f_0 (again) as low as possible. This is achieved by making the wire as thin as possible, and by attaching it close to, or even below the center of mass of the payload. In the last case a rotational anti-spring is realised.

Compact 6-DoF isolator 'MultiSAS'

MultiSAS is a multi-stage 6-DoF isolator including three inverted pendulums and two pendulums for horizontal, and a chain of two GAS filters for vertical isolation, all inside a vacuum tank (Figure 8). Five of these systems will each isolate an auxiliary optical bench, used for the alignment optics of the interferometer (as indicated in Figure 2). The required residual displacements and angles (see Table 1) allow the interferometer to lock its optical cavities. MultiSAS has been designed to achieve these vibration levels within the limited space available in the existing facility.

The very strict rotational requirements necessitate the suspension of the 1 m x 1.4 m rectangular optical bench from a single wire at (or even just below) its center of mass, such that its tilt modes are around 0.2 Hz. Finite-element calculations show that passive isolation is expected to be effective up to about 50 Hz, close to the first high-frequency modes. If necessary, the quality factors of these modes can be suppressed by passive resonant dampers. Above 50 Hz the natural seismic fluctuations are assumed to be sufficiently small. An active feedback control system is used only to damp the low-frequency rigid-body eigenmodes and to maintain long-term position and orientation of the payload. This is accomplished by three horizontal voice coils actuating the top stage, a vertical voice coil on each GAS filter and both a vertical and horizontal voice coil on each bench corner.



8

The horizontal displacements and yaw of the top stage are measured with three LVDT displacement sensors (with respect to ground) and also inertially, with three velocity sensors (geophones). The bench position and orientation with respect to ground are measured with LVDTs at each corner. The GAS spring vertical displacements are also sensed with an LVDT. A state-of-the-art Trillium seismometer attached to the ground can be used for sensor correction of the top stage LVDT signal, making it an inertial sensor. Finally, the bench is equipped with geophones for diagnostic and control purposes. For more details see [4].

In August 2013, the first MultiSAS prototype has been built and is about to be installed in its vacuum enclosure. Its stages have been tested one by one for their open-loop transfer in air, using dummy payloads. The calculated vertical and horizontal ground-to-bench transfer functions are shown in Figure 9, together with the vertical measured transfer. Above 2 Hz they show the expected $1/f^4$ and $1/f^6$ characteristics of the respective vertical and horizontal filter chains. Above 10 Hz MultiSAS provides roughly 100 dB suppression of vertical vibrations and over 140 dB horizontally. Above 50 Hz the transfer functions begin to level off. Also internal resonances show up in the measured transfer function.

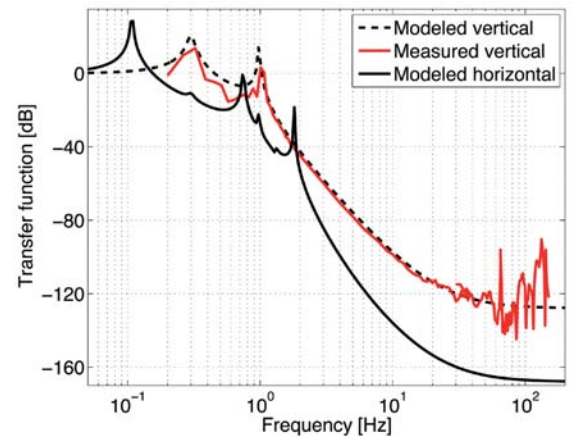
Table 1 Requirements for the suspended terminal benches, valid for all translational and rotational DoFs.

MultiSAS requirements	Translation	Rotation
Noise above 10 Hz	$2 \cdot 10^{-12}$ m/ $\sqrt{\text{Hz}}$	$3 \cdot 10^{-15}$ rad/ $\sqrt{\text{Hz}}$
Residual rms	1 μm	0.03 μrad

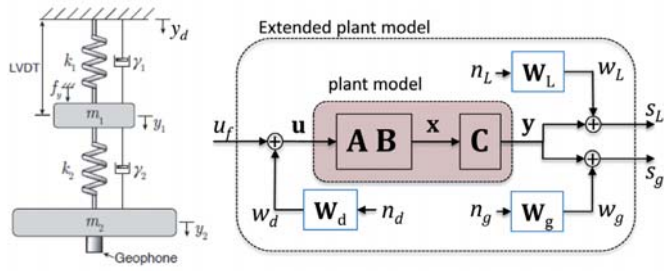
8 MultiSAS-design for Virgo encompassing two GAS filters in cascade, three inverted pendulum legs and two hard-steel suspension wires, all mounted in a vacuum tank. The 2mm-thick lower wire carries a 320kg optical bench. The arrows indicate the compliant DoFs of the rigid bodies (translations, tilt and yaw).

9 MultiSAS vibration isolation performance. Modeled vertical (dashed black curve) and horizontal (solid black curve) transfer functions and the measured vertical transfer function (solid red curve).

Control strategies for damping the low-frequency rigid-body mode peaks are under study. There are fifteen of these modes, corresponding to the number of compliant DoFs: three horizontal ones for the top stage, six for the intermediate filter and six for the bench. They could simply be damped by feeding back the velocity measured by each sensor to its collocated actuator, i.e. applying viscous damping. However, maybe this can be done better. The symmetry of the design allows to select mutually uncoupled subsets of these modes: (a) three yaw modes (rotations around the vertical y -axis), (b) five horizontal and tilt modes in the y - z plane, (c) same five in y - x plane, and (d) two vertical modes.



9



10a

10b

State-space model for vertical displacement

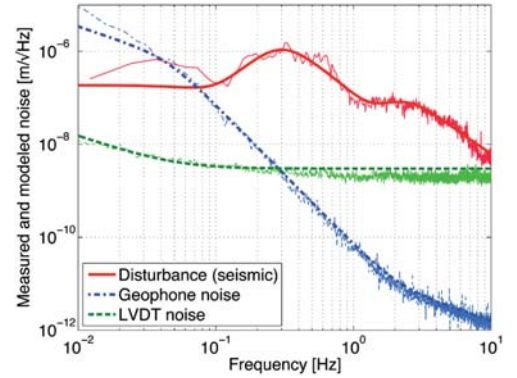
The vertical mode damping is based on the simplified mass-spring model shown in Figure 10a. It is controlled by the top-stage actuator coil force $f_y = k_1 \cdot u_f$. The sensing is two-fold: the sensor-corrected LVDT signal s_L measures the displacement y_1 of the intermediate mass, while the geophone (s_g) is sensing the bench velocity $v_2 = \dot{y}_2$. The colored ‘plant’ box in Figure 10b shows the state-space representation of the plant with corresponding dynamical equations:

$$\dot{\mathbf{x}}(t) = \mathbf{A} \mathbf{x}(t) + \mathbf{B} \mathbf{u}(t), \mathbf{y}(t) = \mathbf{C} \mathbf{x}(t) \tag{3}$$

with state vector $\mathbf{x} = [y_1, y_2, v_1, v_2]^T$, input vector $\mathbf{u} = [u_f + w_d]$ and 2D output vector \mathbf{y} . The matrices **A** and **B** contain the plant properties: stiffnesses, masses and damping. Matrix **C** selects the measured quantities from **x**. Figure 10 also shows an extended model, that accounts for sensor and seismic disturbance noise contributions (w_L, w_g, w_d). Their spectral distributions have been measured (Figure 11) and are each modeled by a shaping filter (**W**), fed with a zero-mean, unity-variance white-noise signal (*n*).

Optimal controller

The representation of the plant model in terms of linear filters (**A**, **B**, **C** and **W_i**) and white noise sources n_i ($i = d, L, g$) allows to create an optimised filter, the Kalman state observer **K_{obs}** [5]. This calculates the statistically most reliable estimate $\hat{\mathbf{x}}$ of the plant state **x** from the control signal u_f and the sensor signals (s_L, s_g), for the given spectral properties of sensor and disturbance noises (w_L, w_g, w_d). The control signal u_f is delivered by a linear quadratic regulator, an independently configured filter, which minimises a cost function J_{LQR} based on designer-chosen weighting criteria. In this case $J_{LQR} = \int [u_f^2 + R(\hat{x}_1^2 + \hat{x}_4^2)] dt$, where *R* is a tunable weighting factor. Note that \hat{x}_1 and \hat{x}_4 are the ‘observed’ intermediate filter displacement and bench velocity, respectively. A Kalman state observer combined with a linear quadratic regulator is called a Linear Quadratic Gaussian controller (LQG, see Figure 12).



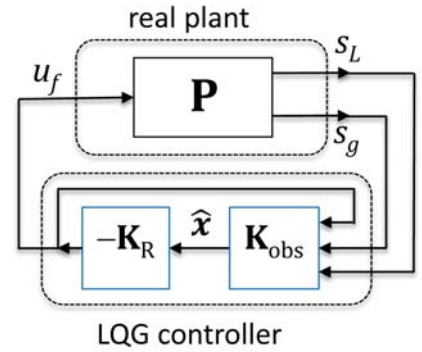
11

10 Vertical mode damping.

(a) Vertical mechanical model of MultisAS.
 (b) Noiseless state-space representation (plant model) including disturbance and sensor noise, using shape filters (extended plant model).

11 Measured spectra of the sensor and disturbance noise sources, together with the corresponding modeled shaping filter response to a zero-mean white-noise input.

12 MultisAS vertical control scheme with a MISO (multiple-in, single-out) regulator consisting of a Kalman state observer **K_{obs}** and a linear quadratic regulator (LQR) with gain matrix **K_R**.

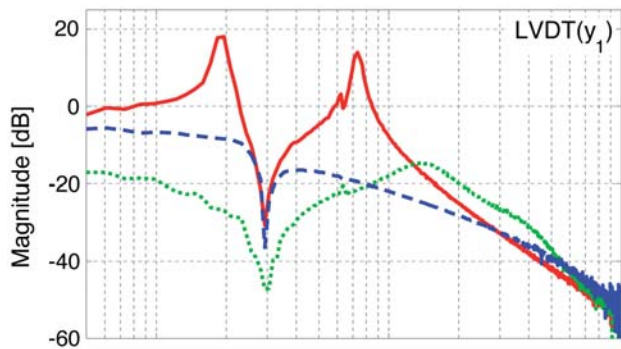


12

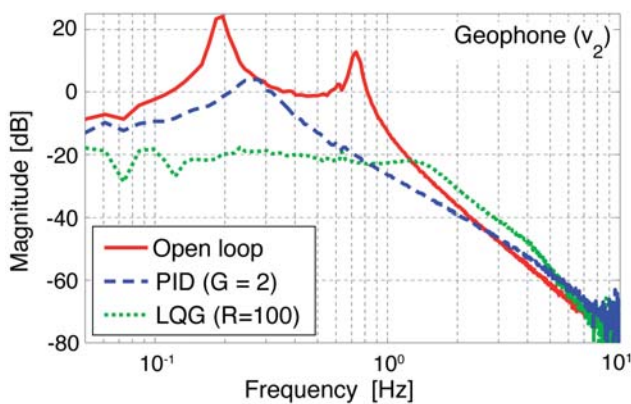
Control results

The red lines in Figure 13 are the measured open-loop transfer functions, obtained by exciting the voice coil such that the forced displacement is much larger than the seismic disturbance: $u_y \gg y_d$. The lowest of the two eigenmodes, at 0.2 Hz, corresponds to the common mode where both intermediate and bench masses move in phase. The second, around 0.75 Hz, is associated with the differential mode in which the two masses move in antiphase. There is agreement with modeled transfer functions. The bench velocity shows -60 dB magnitude at 5 Hz. This corresponds to a displacement attenuation of roughly 90 dB. Passive isolation at work!

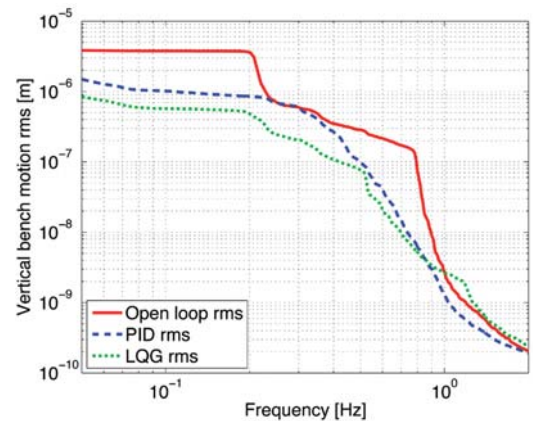
The blue lines show the in-loop transfer for a traditional PID controller with a bandwidth of 5 Hz, using only the LVDT signal for its feedback. The applied control filter is tuned to $C(s) = G \cdot (s + 0.5 + 0.05/s)$, where *G* is the gain. The resonances are damped effectively, but around the notch the sensor signal is too low; the bench motion is not damped in that region. The performance of the LQG controller (in green) is significantly better for the bench, in particular around the notch. Apparently the Kalman observer effectively exploits both sensor signals to deliver accurate system states to the LQR.



13a



13b



14

13 Vertical transfer functions in open and closed loop to test the performance of the LQG controller and a tuned PID controller.

(a) LVDT displacement (divided by the forced displacement).

(b) Geophone velocity (divided by the forced displacement).

14 Measured cumulative rms displacement of the bench, downward integrated.

The control was also tested with MultiSAS only subjected to environmental disturbances. Figure 14 shows the downward integrated residual displacement of the bench, both open loop and controlled (PID and LQG), as obtained from the geophone signal (v_2/ω_2). Below 0.1 Hz this signal is dominated by sensor noise (see Figure 11). At 0.1 Hz the PID control reduces the open-loop result by a factor 3. The LQG controller improves this by another factor 2, bringing the rms displacement down to 0.5 μm , well within the requirement of 1 μm (Table 1).

Conclusion

Nikhef has designed and tested a multi-stage seismic isolation system (MultiSAS) for the Advanced Virgo gravitational wave interferometer. Due to the application of anti-spring technologies and an optimal controller the attenuation of vertical vibrations is more than 100 dB at frequencies above 10 Hz, and the residual motion of the bench stays below 1 micrometer rms.

The application of horizontal, vertical and rotational anti-springs has pushed all rigid-body modes below 2 Hz. Above 5 Hz the attenuation is purely passive. The residual low-frequency motion is actively damped. The multiple-input,

single-output optimal controller for the vertical DoF is based on a linear quadratic regulator in combination with a Kalman state observer.

The results obtained thus far suggest that MultiSAS will comply with the requirements. The techniques discussed are also well applicable outside pure scientific instrumentation. Customised solutions based on these technologies are being made commercially available by Nikhef's spin-off company InnoSeis. ■

REFERENCES

- [1] S. Braccini et al., "Measurement of the seismic attenuation performance of the VIRGO Superattenuator", *Astroparticle Phys.*, 23, 557 (2005).
- [2] V. Sannibale et al., "Seismic attenuation performance of the first prototype of a geometric anti-spring filter", *Nucl. Instrum. Meth. A*, 587:652–660, 2002.
- [3] S. Braccini et al., "The maraging-steel blades of the Virgo super attenuator", *Measurement Sci. Technol.*, 11(5):467, 2000.
- [4] M.G. Beker, "Low-frequency sensitivity of next generation gravitational wave detectors", Ph.D. Thesis, 2013. www.nikhef.nl/pub/services/biblio/theses_pdf/thesis_m_g_beker.pdf
- [5] M. Grewal and A. Andrews, *Kalman filtering: Theory and practice*, second edition, John Wiley and Sons, Inc, New York, 2001.

COMPETITIVE FOR SERIAL PRODUCTION OF MICRO-PRECISION COMPONENTS

In micro-precision technology, spark-erosive or electrical discharge wire-cutting offers unique, largely unknown flexible production-oriented solutions. Ever-increasing quality requirements and changing geometric challenges in general can nevertheless only be successfully met by 'wire-cut specific design for manufacturing'. Inspired by professional forerunners in technology, state-of-the-art Wire-EDM is now able to accurately and cost-effectively produce ready-for-use, complex products with high added value in a single clamping.

JAN WIJERS

Design trends towards miniaturising and sustainably reducing weight have introduced more complex parts and subsystems with highly 'embedded' functionality to the industry. Traditional metal removal encounters barriers in highly detailed, small to medium-sized products made from modern technical materials. In micro-precision technology, EDM-wire-cutting offers a number of process-specific and largely unknown flexible production solutions. In general, prerequisite for successfully meeting the ever-increasing quality requirements and rapidly changing geometric challenges is 'wire-cut specific design for manufacturing'. Then, state-of-the-art Wire-EDM-ing is – in a competitive way, and inspired by professional forerunners in technology – able to accurately and cost-effectively produce ready-for-use, complex products with high added value in a single clamping.

Fundamental characterisation

From the very beginning, spark-erosion techniques (die-sinking, wire-cutting, drilling) and machines benefited from the latest innovations in their electric/electronic subsystems. The key issue in this non-conventional 'chipping' process is the intricate thermo-electric interaction – without any physical contact – through ultra-short electric pulses, triggered spatially and separated temporally, between the tool (wire electrode) and the

workpiece. Even in the 21st century there is still no clear insight into some basic aspects, providing a reason to restart research, e.g. into the plasma that occurs. The high-frequency pulses result in 'sparks' – over the gap flushed with a dual-function dielectric fluid (both insulating and conductive (after ionisation)). These discrete electrical discharges (tiny bolts of lightning) instantly heat up and effectively remove material by melting and evaporation. Therefore, there is still a minimal chance of thermal subsurface damage (heat-affected zone, HAZ) if the cutting parameters are not carefully selected for specific materials or if they are set incorrectly.

AUTHOR'S NOTE

Jan Wijers is a former Mechanical Division member of Philips Research ('NatLab'), serving as workshop manager, and has since become an internationally renowned EDM technologist. He contributed to the Dutch FME publication on EDM, 'Vonkersie, theorie en praktijk' (VM120) [1], acting as chairman of the Dutch Working Group on Physical-Chemical Machining Processes. He has been active as a lecturer and (up till now) a freelance technical writer for more than 25 years, covering a variety of conventional and non-conventional production technologies.

Wire-EDM

Crucial element in current high-performance, contactless wire-erosion machining is a standard pre-tensioned ultra-fine wire. Generally, in spark-erosive cutting, a part is made in a single operation by CNC-feeding the workpiece (anode) towards a slender, vertically travelling wire (cathode). In practice, the logistical and metallurgical effort of heat treatment can be avoided by starting from hardened stock. A strategic set of distinct passes leads up to the optimal result. Rough cutting of a through cavity is done using the full diameter, mostly followed by finishing with regard to form, size and recast-layer-free metallurgical structure in a trim regime, skimming the actual geometry sideways over an off-set path. The 'endless' metallic tool

(several kilometers in length) is by far the most precise tool in metalworking (approx. 1 μm , see Figure 1) and unwinds as a consumable from a supply spool, compensating for erosive wear. A relatively common ultra-fine wire is the crucial pre-tensioned element in current high-performance, contactless machining.

Wires were originally copper-dominated. Today, however, a wide variety of blank and stratified wires is on offer, based on high-strength brass, tungsten, molybdenum and steel, or special types of wire with process-specific properties ranging in diameter from 15 μm – one fifth of a human hair and almost invisible – to 0.350-0.380 mm. The higher tensile forces allowable on the newer wire types eliminate disturbing vibrations, resulting in improved surface quality and straightness.

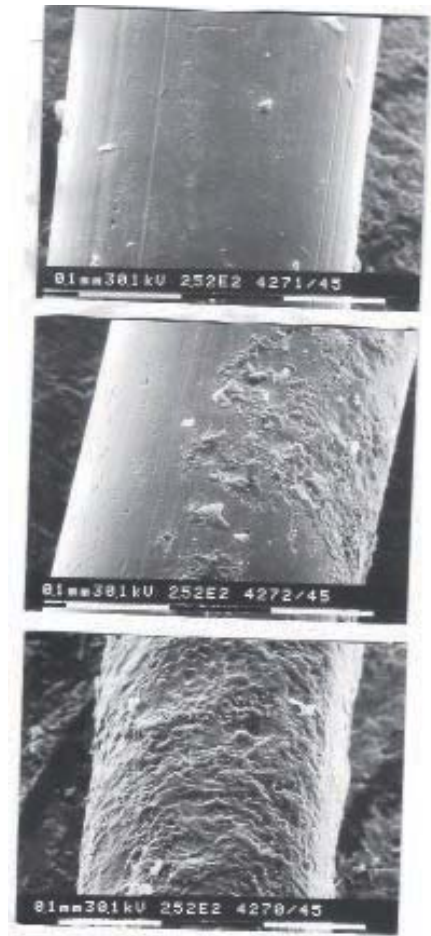
In high-speed cutting, brass and copper are losing the battle against the latest developments in special composite electrodes, which have a high-strength core encapsulated in EDM-specific multi-coatings. With this high-precision micro-tool, high-quality EDM-ing of intricate details can be achieved on an average machine on thin foils and sheet metal of thicknesses up to 250 μm and up to 600 μm on larger types. According to leading manufacturers cutting to mirror-like surface quality levels without the need for additional finishing is realistic on their top-line Wire-EDM machines fitted with advanced wire electrodes.

Digital control

Modern, powerful digital power supplies with several dedicated modes (cornering strategy, adaptation to sudden cross-section changes, anti-electrolysis, eco-settings) are capable of generating in ultra-rapid succession proper pulses in accordance with the many key parameters (amperage, voltage, pulse shape) and time settings (on/off frequency, discharge duration, pulse interval). The highly sensitive servo system is always in full control, even during challenging jobs. Corrections are made in-process in split seconds (down to ns) during the actual EDM cycle, if necessary by means of advanced pulse modulation and adaptation when sensors detect an abnormal erosion situation (open, shorting or arcing).

In EDM, mature micromachining technology and strategy, advanced electronics and sensors as well as a considerable level of intelligence are far more integrated into the CNC database of most high-tech machine tools and also into the NC code than in competitive processes. This integration is so advanced that machining cycles can be fine-tuned to existing portfolios by also storing company-specific user knowledge. The operator is able to optimise any particular job by selecting the most important features in the erosion cycle by hand, such as speed, geometric accuracy or surface

1 Microscopic views of (top to bottom) virgin wire, wire after centring, and used wire (WISE2000).



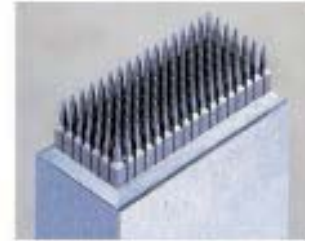
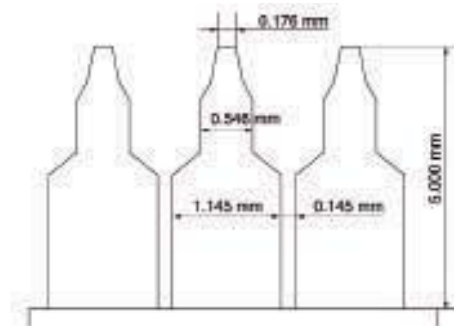
finish. In all these cases, it is nonetheless very helpful to assign a fully-fledged operator with adequate spatial insight and in-depth knowledge of both machine tool and wire-cutting process.

Advantages and drawbacks

Besides advantages, Wire-EDM also has a few drawbacks. Table 1 presents an overview.

Table 1. Advantages (+) and drawbacks (-) of Wire-EDM

+ Reliable, flexible and cost-effective cutting process with high uptime (> 5,000 hours/year).
+ Inherent high accuracy and surface finish (down to 0.05 μm R_a).
+ Competitive range of precision EDM wires ($\pm 1 \mu\text{m}$) available as standard.
+ Burr-free removal of materials independent of mechanical properties.
+ 3D geometrical cuts feasible, composed of straight line elements, including tapers (see Figure 2).
+ Extended, unattended machining autonomy (easy set-up, no need for external automation).
- Recyclable once-only wire wearing as a consumable (see Figure 1).
- Limited to electrically conductive materials.
- Sharp inside corners (minimum $\sim 0.05 \text{ mm}$ in radius) not feasible.
- Chance of HAZ effects.



2

Thresholds removed

Several inventions have helped overcome classical barriers and raise flexibility concerning geometry, dimensions, tolerances, finish and materials. Machining difficult, ultra-hard and wear-resistant metals, such as tungsten carbide, was the main goal of Russian inventors more than 65 years ago. Patented EDM drilling of natural diamond (insulator) for drawing dies already worked at Philips in the sixties, proving the rapid development, but the specific conduction threshold (~100 S/cm) hampered everyday spark-erosion of certain materials for quite a while.

In the meantime, W-EDM-ing PCD (Poly-Crystalline

- 2 Examples of cutting a mechanical part in one 90° indexing set-up.
- 3 Wire-EDM profiling of a special PCD-cutting tool on a System 3R index table.

Diamond, see Figure 3), high Ni-alloys (including Invar), biocompatible Cobalt-Chromium and complicated C-electrodes for die-sinking has become more or less normal.

Nowadays, innovations such as improved digital ultra-short pulse generators with extreme high amperages, peak pulse shapes and specific technology open up new possibilities for rather expensive exotic materials [2]. In response to the increasing interest in engineering ceramics, these innovations hold promises for profitability, especially in silicon (p-type), the most attractive substrate for microsystems, MEMS (even completely mechanical in the case of the French 'ChromoMems', not requiring battery power), sensors and wear-resistant parts. But these innovations are also useful in piezo-ceramics and special types of advanced EDM-able materials composed of a ceramic matrix, which includes traces of certain conductive borides, carbides or nitrides.

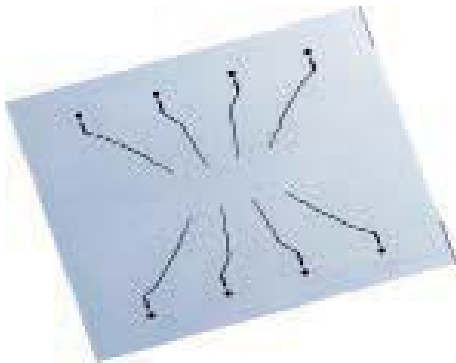
Using a moving wire as an expendable micro-tool makes even EDM milling of blind geometries feasible on dedicated CNC machines.

As only the volume of the kerf out of the start hole has to be machined (width (wire diameter + gap) x workpiece thickness x cutting path length), the race for top-speed cutting rates (currently > 500 mm²/min) has transformed into a far more practicable quest for the highest quality in one rapid process. To benefit from high-tech machine, tool, technology and strategy standards, the entire process chain has to be taken into account carefully, including the many different working conditions.

In general, brand-independent, dedicated Wire-EDM CAM software provides the best results with respect to the geometric and surface quality of the parts produced, even when nested. Pocketing – completely 'burning' the inner core or slug part – in a geometry-specific pattern of successive passes avoids damage to workpiece and machine.



3



4



5

It eliminates emergency stops, because no metallic parts can drop into the narrow gap between wire and actual part (preventing shorting or mechanical breakage).

Unique production applications

General tooling solutions – e.g. cutting, drawing, extrusion and injection mould and die tools (see Figure 4) for mass production – are traditionally the main wire-cutting application field. This product range has now been expanded by completely new creative design approaches specifically focused on Wire-EDM manufacturability. This generates real innovative potential for cutting-edge products perfectly matched to industrial needs, concerning 3D geometry and small-scale production as a replacement for conventional milling, sawing and stamping.

From a technical point of view alone, Wire-EDM – often used in the same breath as micro laser beam (μ -LBM) and water jet (μ -WJM) machining – has now reached serial production status, e.g. for enabling (without expensive tooling) rapid prototyping for market acceptance and functional tests, one-off products, pre-series lots and validated batches under real-world conditions. Key aspects and features depend to a large degree on the typical process characteristics (Table 1). Today, EDM-

- 4 Carbide lead frame die featuring 40 μ m wide slits (W-wire (tungsten): 20 μ m, start hole diameter 0.07 mm, three passes; Makino).
- 5 Microscope object holder with Wire-EDM-ed features (Queensgate).
- 6 Examples of medical Wire-EDM products.
 - (a) Instruments, prostheses and specials (Mitsubishi).
 - (b) Burr-free 'staples' made of titanium (Makino).
- 7 Serial Wire-EDM-ing of a stacked set of steel levers.
- 8 Mitsubishi serial production of horizontally and vertically nested parts.



6b

experts like CVT/Heinmade (company based in Hoogeloon, the Netherlands) actively explore the worldwide scope of applications in high-quality bores of any geometry, precision tools (see Figure 3), and free-form cutting of parts. Such parts range from helices, blades, gears and instruments (see Figure 5), to high-tech mechatronics and micro components in the medical (see Figure 6), automotive, aeronautic, semiconductor and similar industries (Figure 2).



7



8



profile-and-resharpen' CBN (Cubic Boron Nitride) or diamond grinding wheels – in the near future even fully automatic with a robot-assisted wheel changer (see Figure 9).

The introduction of so-called industrial film- or flex-joints and guidances has been ground-breaking in mostly play- and wear-free monolithic microsystems or precision stages with a characteristic pattern and close-to-nm-range position accuracy (see Figure 10). Assembling high-precision micro-parts manually is very challenging and expensive, especially with small, vulnerable components such as leaf-springs, featuring high aspect ratios. Combining them into one compact Wire-EDM-ed platform with some degrees of freedom solves most of these problems (see Figures 11 and 12). Early involvement in the engineering process is an absolute must in that case.

Evolution in machine configuration

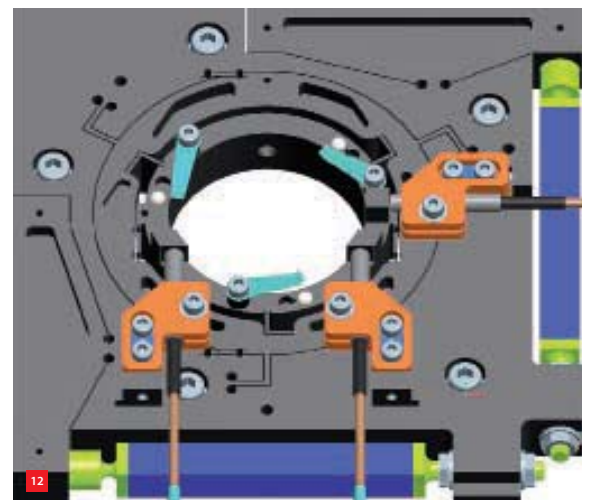
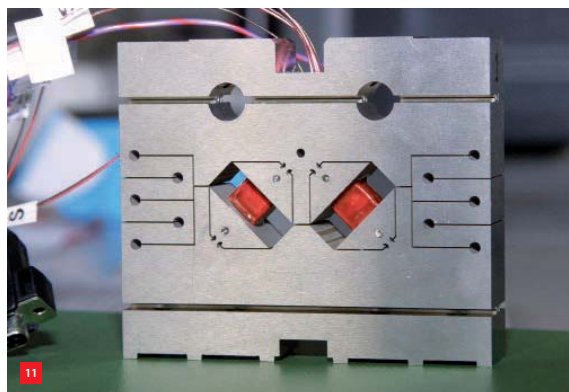
Wire-EDM machines feature three to five axes (X/Y/Z + U/V for tilting the wire while 3D-tapering) with optional rotating/indexing axes. Main axes are still mostly driven by ball screws, although direct-driven, dynamic linear motors are on the rise.

Automatic wire handling – including centring, aligning and edge-finding – is indispensable as it is directly linked to the specific, endless nature of the Wire-EDM tool. During start-up or after any unforeseen wire breakage, the intricate feed and guidance system threads even the thinnest cross sections – with ultra-precision, high repeatability and reliability close to 100%. This is achieved with an air or dielectric jet over the upper EDM head (housing wire guide, electrical contact and flushing nozzle) into the start hole inside the workpiece and out again through the lower head,

- 9 Fully automatic, easy truing strictly according to requirements, to be introduced on the EMO Hannover 2013 trade fair (ITS).
- 10 Monobloc platform for Mettler measuring cell with typical flex-joint pattern of start-holes and slits.
- 11 Kinematic design of integrated piezo active lens mount (Imotec).
- 12 Recently engineered SEM stage based on specific Wire-EDM design (Hittech).

Nesting parts horizontally or vertically (see Figure 7) is a well-known technique to generate sets of (dis)similar CAM profiles at a time. When producing series of nested pieces, temporarily 'bridging' micro-joints help to keep the in-line products connected to the blank until they are separated manually. Small batches can effectively be produced by vertically stacking a number of metal sheets or foils – out of (ultra)hard or conventional materials – and cutting all the identical, laminated elements in the package simultaneously in a single set-up (see Figure 8).

Core competences are, in particular, special mechanical features in modern high-strength materials. One of the latest additions to micro wire-cutting is profiling cylindrical electrodes to high requirements of dimension and geometry as rotating tools for die-sinking by way of so-called Wire-EDM grinding. Another welcome industrial expansion is truing single or multiple profiles and radii in 'hard-to-





with its twin-wire system for in-process switching to either a thicker (higher speed) or thinner cross section (finer details) or a different type of wire (cheap blank brass or more expensive, but faster multi-layer coated versions). Another leading Japanese brand, Makino, turned wire-cutting upside down in its ultra-precise Wire-EDM machine by converting to a horizontal wire position and hanging the workpiece underneath the Z-axis, resulting in simpler 3D contouring (see Figure 14).

13 Newest Mitsubishi MV1200S Wire-EDM with all TDS drives, improved auto-threading and extra index head

Most machine types use low-viscosity deionised water as an inflammable process medium with high machining rates. On the other hand, synthetic hydrocarbon dielectrics (such as Oel Held's IonoFil) allow highest precision (cutting slightly slower), an even better surface finish without any oxidation, microcracks or cobalt leaching on any hard metal, and also a smaller μm -gap.

14 Multiple clipper cut in vertical position.

to a take-up roller or chopper stage. Stable threading allows running fully autonomous cycles faster over extended periods without any human interference.

Recently, Mitsubishi introduced the world's first all-glass fibre optics lay-out for all intra-connections, raising the smooth, undisturbed digital data transfer to a 'speed-of-light' level between the patented tubular drive system (TDS) with precision measuring scales, generator, CNC and servo systems (see Figure 13).

Innovative topics, such as the latest nano-pulse power units (reportedly cutting 'cooler'), tablet controls, smartphone surveillance and brand-new premium wire types for cutting-edge technology will no doubt be introduced to the growing Wire-EDM market during the upcoming EMO Hannover 2013 international trade show (16-21 September) to enhance productivity and improve quality even further. ■

Almost all multi-wire EDMs – except the lines of ten-fold production specials on which Philips manufactures rotary shaving heads – have disappeared completely from the scene, as they were too cumbersome, expensive and of inconsistent quality, while also not offering auto-threading. More reliable, fast-cutting, high-quality single-wire-EDMs are taking over. The Swiss GFAC machine is rather unique

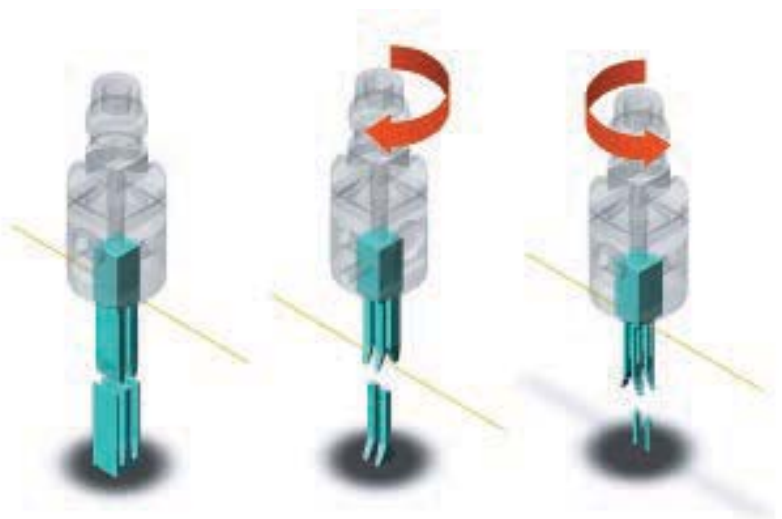
REFERENCES

- [1] J. Wijers et al., "VM 120 Vonkerosie, theorie en praktijk", FME-werkgroep Vonkerosie, 2008.
- [2] K. Liu, B. Lauwers and D. Reynaerts, 2010, "Crossing barriers in structuring ceramics", *Mikroniek*, Vol. 50 (1), pp. 28-34.

Clipper (medical part)



Workpiece material	Steel (SKD11)
Wire used	dia. 0.1 mm BS
Machining time	5 hr. 30 min.
Surface finish	Rz 1.8 μm
(Actual measured value)	



14

A ROBUST CONTROL APPROACH TO ELECTRO-MAGNETIC ACTUATORS

In the high-precision industry, electromagnetic actuators are widely used because of their simple structure, favourable force characteristics and low manufacturing costs. However, from a control point of view, they are non-linear systems. This article outlines system identification experiments as well as a possible robust approach for armature movement control.

ALEXANDRU FORRAI

Electromagnetic actuators have a simple structure – an electromagnet, a spring and a moving armature – as shown in Figure 1. They are used in active magnetic bearings (e.g. flywheels for energy storage), in valve actuators for fuel injection in the automotive industry, in electrical drives such as electromagnetic brakes, for electromagnetic levitation in high-speed transportation systems, in cleanroom applications, etc. In most of these applications, the armature's movement is controlled under feedback (closed-loop control).

The electromagnetic actuator is open-loop unstable, which means that between the two extreme positions – armature open/closed – there is no stable equilibrium position. In practice, the control engineer usually faces two different control set-ups:

- The armature is controlled around an operating point; see magnetic levitation and active magnetic bearings.
- The armature is controlled between the two extreme positions; see, for example, a fuel injector valve.

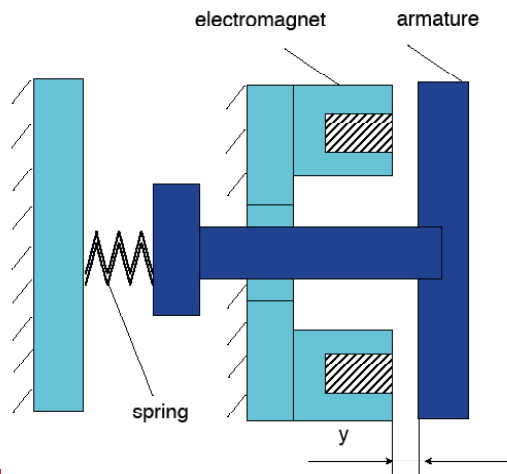
The first control set-up is easier, since the system can be linearised around an operating point and a linear controller can be designed. The second control set-up is more difficult as the system is nonlinear or at least linear parameter-varying, so the controller should be designed or at least analysed in a non-linear framework.

This article focuses on the second control set-up, where the armature is controlled between the two extreme positions (open/closed). The main goals are to derive a mathematical model of the actuator using system identification experiments and to use this model for controller design.

The mathematical model

The electromagnetic actuator can be described by the voltage equation (1) and the equation of movement (2).

$$u = Ri + \frac{d\psi}{dt} \quad (1)$$



1

AUTHOR'S NOTE

Alexandru Forrai obtained his M.Sc. in Electrical Engineering and a Ph.D. in Applied Computer Science both from the Technical University of Cluj-Napoca, Romania. In 2007, he started working as an R&D engineer at Mitsubishi Elevator Europe in Veenendaal, the Netherlands. His research interests are system identification and robust control as well as embedded systems and embedded safety loops. This article is based on a presentation at the Model-Driven Development Days 2013, which were held on 24-25 April in Eindhoven, the Netherlands.

a.forrai@emec.nl
www.mitsubishielectric.com

1 The electromagnetic actuator.

Here u stands for the applied voltage, i for the armature current, ψ for the electromagnetic flux and R is the electric resistance.

$$F_s - F_m = m \frac{d^2y}{dt^2} \quad (2)$$

Here F_s denotes the spring force, F_m the magnetic force, m the moving mass and y the armature position. The friction force during the armature movement can be neglected.

The main nonlinearity of the system derives from the fact that the electromagnetic force is a nonlinear function of armature current and armature position. It may be approximated by a nonlinear function as in Equation 3, where a_1 , a_2 , b_0 and b_1 are constants.

$$F_m(i, y) \approx \frac{a_0 i + a_1 i^2}{b_0 + b_1 y} \quad (3)$$

If the system is linearised around an operating point, then a transfer function of the plant is obtained, Equation 4, which describes an unstable plant.

$$P(s) = \frac{\Delta y(s)}{\Delta u(s)} = \frac{\beta_1}{(s + \beta_2)(s - \beta_2)} \quad (4)$$

where β_1 and β_2 are positive constants.

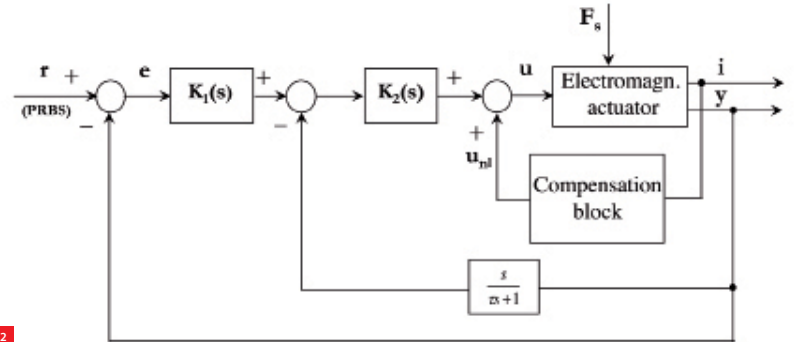
In some applications, the electromagnet is made from solid silicon iron, for manufacturing cost reasons, which leads to a higher influence of eddy currents. The influence of the eddy currents is not considered in the model above, but it will be taken into account during system identification, since the model is derived from experimental data.

System identification experiments

Whenever possible, a mathematical model – for control purposes – should be derived from experimental data, using, for example, system identification techniques [1] [2]. However, the reader could ask: what is a good model for control system design?

Basically, a good model for control design is a proper balance between model simplicity and model fidelity – a balance that is sometimes difficult to find in practice. It is also true that no mathematical model can precisely represent a real physical system; there is always uncertainty. The uncertainty arises from unpredictable inputs and unmodelled and unpredictable dynamics. Therefore, from the control viewpoint, the plant model should contain a nominal model and upper bound of the plant uncertainty [3] [4].

Based on this reasoning, we can easily pinpoint the main difference between classical and robust control. In case of classical control, the controller is designed for the nominal



2 Actuator stabilised under closed-loop control.

plant and validated for a set of plants. However, in the case of robust control, the controller is designed for the so-called augmented plant, which is the nominal plant extended with the plant uncertainty. Plant uncertainty is taken into account in the design phase of the controller.

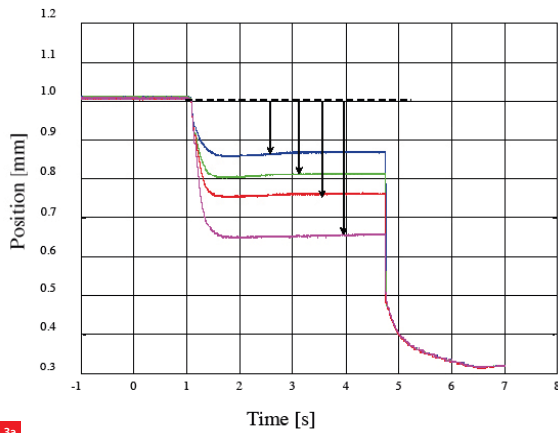
After the goal of model building has been defined, we are going to derive the mathematical model of the electromagnetic actuator from experimental data using system identification. There is a natural/logical flow to system identification. First, we have to design a system identification experiment: we have to decide which signals to measure, when to measure and how to measure. Next, we have to collect the data, choose a model set and a criterion of fit and then derive the model. Finally, we have to validate the model in the time and the frequency domain [1]. Since the system is open-loop unstable, we first have to stabilise the system, using the control structure presented in Figure 2 for instance.

The controllers $K_1(s)$ and $K_2(s)$ can be designed (see classical control theory) based on an approximate analytical mathematical model of the actuator. Furthermore, the compensation block provides the bias voltage, which is required around an equilibrium position to keep the armature levitated. In our case, the compensation block is defined according to Equation 5.

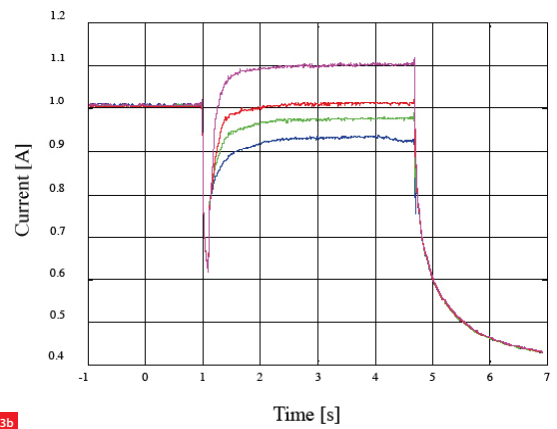
$$u_{nl} = Ri \quad (5)$$

where i is the armature current and R is the electric resistance.

This compensation has a nice interpretation from a passivity control point of view [5]. From an energy point of view, the injected energy – to hold the system around the equilibrium position – equals the Ohmic losses. This means that if the linear control system designed around an equilibrium position is stable, then the compensation block will not make the closed-loop system unstable.



3a



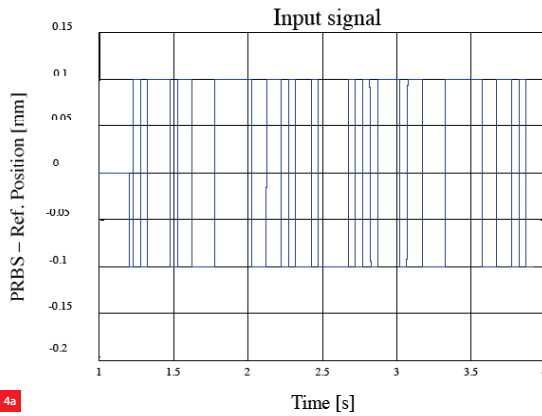
3b

3 Experimental results for the armature under feedback.

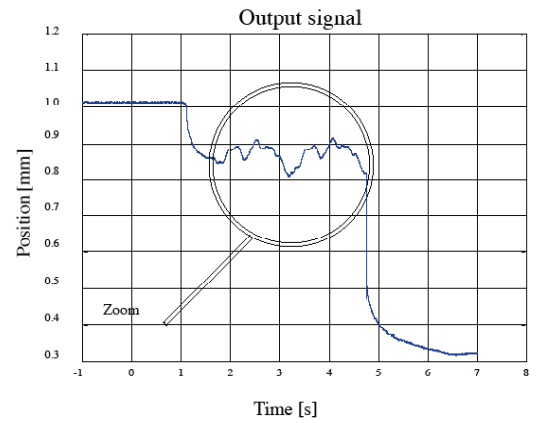
- (a) Position.
- (b) Current.

4 Signals during system identification.

- (a) Input.
- (b) Output.



4a



4b

System identification under closed-loop

First, the system is stabilised – under closed-loop – around different equilibrium points. Experimental results for armature position and armature current are shown in Figure 3.

Next, system identification experiments are performed around different equilibrium points, when the applied input signal is the pseudo-random binary signal (PRBS) [1] [6].

Let us consider that the plant transfer function is written as $P(s) = B(s)/A(s)$, where $A(s)$ and $B(s)$ are polynomials in s , with order n and m , with $n \geq m$. It is said that the system identification experiment is informative if the input signal is persistently exciting of order $n+m$, which means it contains at least n sinusoids [1].

This condition can be achieved by proper design of the pseudo-random binary signal. However, the basic problem in the case of system identification under closed-loop is that the collected data provides less information about the open-

loop system. The purpose of feedback is to make the closed-loop system less sensitive to changes than the open-loop system. Several methods that provide consistent estimates for open-loop data may fail when applied in a direct way to closed-loop identification [1].

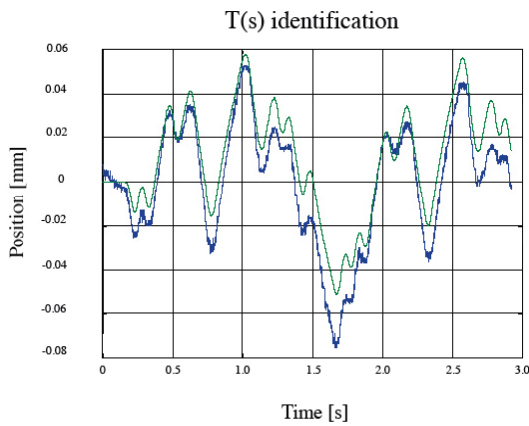
Next, we are going to identify the system in two different frequency ranges, when the considered model structure is the ARX (Auto Regressive eXogenous) model.

$$4 \text{ [rad / sec]} \leq \omega_{low} \leq 62 \text{ [rad / sec]}$$

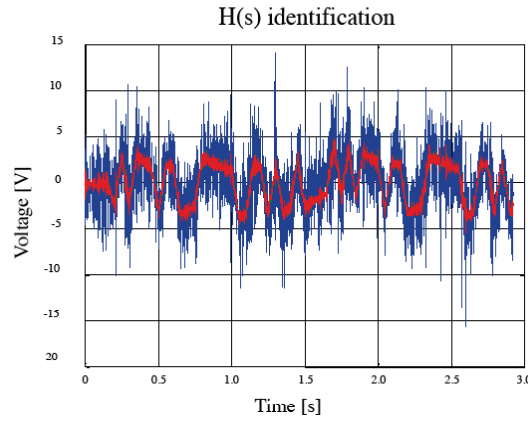
and

$$20 \text{ [rad / sec]} \leq \omega_{high} \leq 314 \text{ [rad / sec]} \tag{6}$$

Model-order reduction is performed based on a Gramian matrix – the Gramian is a measure (or metric) of how controllable or observable a state is, based on a state-space representation of a system) – using the balanced truncation technique, i.e. we delete the weakly observable, weakly controllable states [7].



5a



5b

During system identification the input signal is the pseudo-random binary signal, which is applied over the reference signal. Figure 4 shows the input and output signals during system identification experiments around an equilibrium point.

Since the identification is made under closed-loop, we first have to identify two transfer functions denoted here by $T(s)$ and $H(s)$ and then compute the plant transfer function $P(s)$ according to Equation 7.

$$P(s) = \frac{Y(s)}{U(s)} = \frac{T(s)}{H(s)(1 - T(s))} \quad (7)$$

Here, $T(s)$ stands for the transfer function between the reference input signal, r , and the control system output, y . The $H(s)$ transfer function is defined between the control error signal, e , and the control signal output, u , [1].

Next, the derived mathematical model is validated in the time and the frequency domain. Figure 5 shows how well the model fits the experimental data – in the case of $T(s)$ and $H(s)$ transfer functions – where the blue line denotes the experimental (measured) data [8].

System identification usually leads to a high-order mathematical model. This might be very useful in simulations, but is not suitable for controller design. Therefore, model-order reduction is performed, where the higher-order model is considered real plant $P(s)$ and the reduced-order model $P_n(s)$ as nominal plant [4] [6]. The difference between the two is viewed as plant uncertainty $\Delta_m(s)$ (see Equations 8 to 10). The upper bound of the plant uncertainty is described by the $W_T(s)$ transfer function, which is greater at any frequency than $\Delta_m(s)$, according to the infinity norm.

5 Time-domain validation of transfer functions.

- (a) $T(s)$.
- (b) $H(s)$.

$$P_n(s) = \frac{120}{(s - 1.4)(s + 300)} \quad (8)$$

$$\Delta_m = \frac{P - P_n}{P_n} \quad \text{with} \quad \|\Delta\|_\infty \leq 1 \quad (9)$$

$$P = (1 + \Delta W_T)P_n \quad (10)$$

Furthermore, the system identification experiments are repeated in two different frequency ranges, the reason being that the pseudo-random binary signal is persistently excited in a limited frequency band.

The upper bound for the plant uncertainty – around an equilibrium position – is shown in Equation 11.

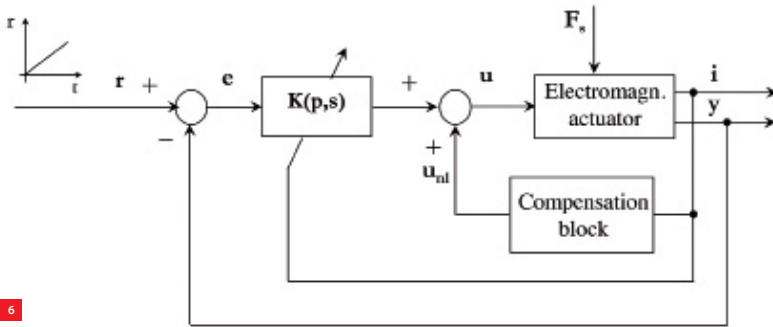
$$W_T(s) = 0.5 \frac{s^2 + 140s + 10^4}{10^4} \quad (11)$$

Linear parameter-varying mathematical model

Our goal is to control the armature movement between the two extreme positions: armature open/closed. This means that the system identification experiments should be repeated around different equilibrium points. The actuator may operate in different environments such as fluids, wide temperature ranges may occur or the spring force may exhibit variations due to manufacturing dispersion. Then the experiments should be repeated covering the full range of variations in the operating environment and the model (plant uncertainty) should reflect the influence of the operating environment.

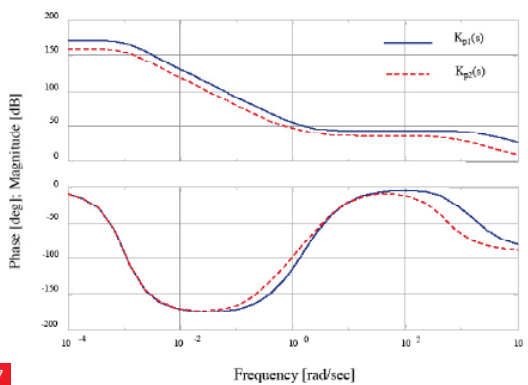
For this case, the experiments have been repeated around different equilibrium points. The experimental results show that the plant gain increases as the air gap increases.

Therefore, a simple linear parameter-varying (LPV) model (where p is the varying parameter) can be derived, which is shown in Equation 12.



6

6 The LPV control system.
7 Two linear controllers, which form the base of the LPV controller.



7

$$P_n^{LPV}(p, s) = \frac{p}{(s - 1.4)(s + 300)} \quad (12)$$

where the parameter p varies between the two limits p_{min} and p_{max} , according to Equation 13.

$$p \in [p_{min}, p_{max}] \quad (13)$$

$$p_{min} = 30; p_{max} = 120$$

The upper bound for the plant uncertainty – around all investigated equilibrium positions – holds according to Equation 11.

LPV robust controller design

The system identification experiments lead to an LPV model and an upper bound for the plant uncertainty. Based on these, an LPV controller can be designed using software tools like Robust Control Toolbox [9] or LMI Toolbox of Matlab [10]. To keep the treatment simple, we will design the controller using the Robust Control Toolbox and make some remarks related to the stability analysis of LPV systems.

The objective is to control the armature movement between the two extreme positions (see Figure 6), so we can require that our system asymptotically tracks a ramp signal. This means the controller should contain a double integrator term. This suggests choosing the performance weighting

function $W_s(s)$ as a second-order function as in Equation 14, where ω_1 and ω_2 are the design parameters.

$$W_s(s) = y \frac{s^2 + 2\tau\omega_2s + \omega_2^2}{s^2 + 2\tau\omega_1s + \omega_1^2} \quad (14)$$

Next, for each vertex, a robust controller is systematically designed, according to robust control theory. The controller denoted by $K_{p1}(s)$ is designed for the vertex $p = p_{min}$, and a controller denoted by $K_{p2}(s)$ is designed for the vertex $p = p_{max}$ (see Figure 7). The LPV controller is denoted by Equation 15 and its parameter p is a scheduled function on the armature current (but a scheduling function on armature position is also possible).

$$K(p, s) = \frac{p_{max} - p}{p_{max} - p_{min}} K_{p1}(s) + \frac{p - p_{min}}{p_{max} - p_{min}} K_{p2}(s) \quad (15)$$

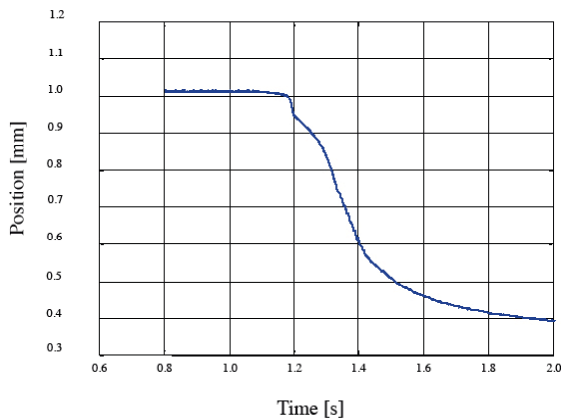
Furthermore, in the case of an LPV system, quadratic and biquadratic stability is verified considering the variation range and variation rate of parameter p [10] [11]. This is a very realistic approach since the signals in practice are bounded and have a limited variation range and rate. Since biquadratic stability holds, the LPV controller – which is a fourth-order one – is implemented in real time. Finally, experimental results are shown in Figure 8 (position and current), where the armature moves between the two extreme positions.

Conclusion

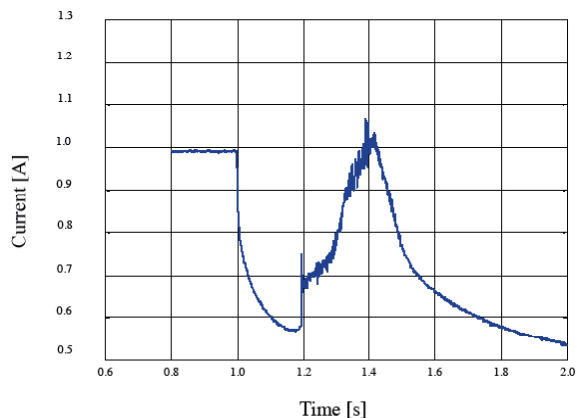
System identification experiments and robust linear parameter-varying (LPV) controller design in the case of a nonlinear electromagnetic actuator have been presented. Since the actuator is open-loop unstable, system identification has been performed under closed-loop. An LPV mathematical model and an upper bound of plant uncertainty have been derived. A robust LPV controller has been designed and tested based on an LPV model. ■

REFERENCES

- [1] Ljung, L., "System Identification – Theory for the User". New York: Prentice-Hall, 1987.
- [2] Adachi, S., "System Identification – Theory for the User". The Society of Instrument and Control Engineers, Japan, 1993 (in Japanese).
- [3] Doyle, J.C., Glover, K., Khargonekar, P.P., Francis, B., "State-space solutions to standard H_2 and H_∞ control problems". *IEEE Trans. Autom. Control*, Vol. 34 (8), 1989, pp. 831-847.
- [4] Doyle, J.C., Francis, B.A., Tannenbaum, A.R., "Feedback Control Theory". New York: McMillan, 1992.
- [5] Van der Schaft, A., "L₂-Gain and Passivity Techniques in Nonlinear Control". Springer Verlag, London, 2000.
- [6] Forrai A., "Embedded Control System Design – A Model Based Approach". Springer Verlag, Berlin, 2012.
- [7] Dullerud, G.E., Paganini, F., "A Course in Robust Control Theory – Convex Approach". New York: Springer, 2000.



8a



8b

8 Armature LPV control.
(a) Position.
(b) Current.

- [8] Forrai A., Ueda T., Yumura T., "Electromagnetic Actuator Control: a Linear Parameter-Varying (LPV) Approach". *IEEE Trans. Ind. Electr.*, Vol. 54 (3), 2007, pp. 1430-1441.
- [9] Chiang, R.Y., Safonov, M.G., "Robust Control Toolbox, User's Guide". The MathWorks, Inc., 1992.

- [10] Gahinet, P., Nemirovski, A., Laub, A.J., Chilali, M., "LMI Control Toolbox, User's Guide". The MathWorks, Inc., 1994.
- [11] Shamma, J.S., Athans, M.M., "Guaranteed Properties of Gain Scheduled Control for Linear Parameter-Varying Plants". *Automatica* 27 (3), 1991, pp. 559-564.

Measure and Succeed

Accurate measurements for humidity, dew point, carbon dioxide, pressure and moisture in oil

If the success of your operations depends on faultless measurements we have the solution for you: Vaisala HUMICAP®, DRYCAP®, CARBOCAP® and BAROCAP® sensors - the unrivaled industry quality benchmarks.

Choose from a wide range of fixed and handheld instruments for different applications, requirements and budgets. Tell us how you would like to measure your success. Our sensors will help deliver it.

www.vaisala.com/instruments
benelux.sale@s@vaisala.com

VAISALA

MAXIMISING STIFFNESS OVER A LONG RANGE OF MOTION

Flexure hinges inherently lose stiffness in supporting directions when deflected. This article presents a method for optimising the geometry of flexure hinges, aimed at maximising supporting stiffnesses. In addition, the new ∞ -flexure hinge design is presented. The considered hinges are subjected to a load and deflected a bidirectional angle of 20° . The optimisations show that the support stiffness is increased by a factor of 4.5 with respect to the conventional cross flexure hinge.

DANNIS BROUWER, HEDZER WIERSMA, STEVEN BOER AND RONALD AARTS

1 The geometric interpretation of the loadcase, which is based on the mechanism of [5-6].

AUTHORS' NOTE

At the time of the research described in this article, Dannis Brouwer was assistant professor at the University of Twente, Enschede, the Netherlands, in the Mechanical Automation and Mechatronics group, and senior applied research engineer at Demcon advanced mechatronics, now based in Enschede. Hedzer Wiersma contributed to this work as part of his master assignment. Steven Boer contributed to this work as part of his Ph.D. assignment. Ronald Aarts is associate professor at the University of Twente in the Mechanical Automation and Mechatronics group. This research was financially supported through the Dutch association Point-One, project MOV-ET PNE08006, by the Dutch Ministry of Economic Affairs.

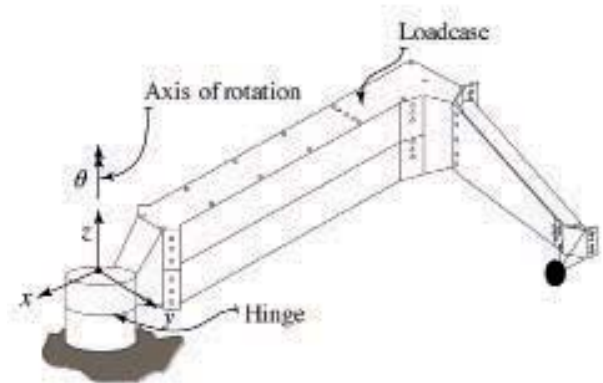
d.m.brouwer@utwente.nl
www.utwente.nl/ctw/wa

In high-precision manipulator mechanisms, flexure elements are often utilised for their deterministic static and dynamic behaviour [1-4]. Folkersma et al. [5-6] present a 2-DoF (degree of freedom) large-stroke elastic mechanism with eleven cross flexure hinges [7]. When the mechanism is in a deflected state, a significant decrease of the natural frequencies is observed. This will lead to a deteriorating dynamic performance of the mechanism. Hence, the challenge of designing a high-performance large-stroke compliant mechanism is to retain the supporting stiffnesses of the flexure hinges for large deflections.

This article aims at optimising the geometry of a number of spatial flexure hinge types subjected to a certain loadcase where the natural frequencies are evaluated. This loadcase scales the importance of the supporting rotational and translational stiffnesses such that they are made comparable. First, the optimisation method is presented. The efficient multibody dynamics code SPACAR is used [8], which offers a suitable non-linear flexible beam model. Subsequently, this model is used for optimising the various flexure hinges.

Method

First, a suitable loadcase is defined by an inertia tensor and a mass located in the instant centre of rotation of the hinges. In the optimisation, the inertia tensor can be rotated



1

Table 1. Principal moments of inertia of the loadcase.

Parameter	Quantity	Unit
J_{xx}	0.00376	kg·m ²
J_{yy}	0.0353	kg·m ²
J_{zz}	0.0382	kg·m ²
m	0.574	kg

an angle ϕ about the z_r -axis to optimally orient the load with respect to the hinge. From the mechanism presented by Folkersma et al. [5-6], a suitable loadcase is derived to which the flexure hinges will be subjected, see Figure 1. Table 1 shows the values of the loadcase inertia tensor.

Secondly, a set of parameters is chosen that defines the geometry of the considered flexure hinge. Subsequently, the flexure hinge, subjected to the specific loadcase, is optimised with respect to the first unwanted eigenfrequency. A hinge ideally releases one rotation and constrains all other directions. Therefore, the modeshape corresponding to the second eigenfrequency f_2 will set motion in the least stiff direction with respect to the chosen loadcase. Hence, f_2 is the first unwanted eigenfrequency which should be maximised.

In order to prevent the structure from failing, the Von Mises stress will be constrained, in this case to 600 MPa. The Young's and shearing modulus of steel (Stavax) are used, 210 GPa and 80 GPa, respectively. The maximum angle of deflection in the optimisation is $\pm 20^\circ$ and the maximum hinge height H is 85 mm. The actuation moment is constrained to 1.5 Nm, which ensures that the flexure hinge is compliant in the actuation direction. With these constraints, an optimisation routine converges to an optimal geometry, which reduces the loss in supporting stiffnesses to a minimum.

Optimisation

The parameter vector \mathbf{p} is defined for each hinge type and describes the geometry of the flexure hinge and the loadcase orientation. The optimisation is governed by a constraint function $\mathcal{C}(\mathbf{p})$ and cost function $\mathcal{F}(\mathbf{p})$, which are dependent on the parameter vector \mathbf{p} . Maximising f_2 is achieved by minimising its inverse, resulting in the following cost function to be minimised by an optimisation algorithm:

$$\mathcal{F}(\mathbf{p}) = \min_{\theta} f_2(\mathbf{p}, \theta)^{-1}, \forall \theta \in [-\theta_{\max} \dots \theta_{\max}] \quad (1)$$

Here θ is the angle of deflection between $\pm \theta_{\max}$. To prevent unbounded growth of the parameters during the optimisation and to ensure that the algorithm returns a manufacturable and sustainable flexure hinge, constraints are applied. Constraints on the maximum actuation moment $M(\mathbf{p}, \theta) < M_{\max}$, which achieves the angle of deflection $\pm \theta_{\max}$, and the maximum occurring Von Mises stress $\sigma(\mathbf{p}, \theta) < \sigma_{\max}$ define a non-linear constraint function:

$$\mathcal{C}(\mathbf{p}) = \max_{\theta} \left\{ \begin{array}{l} \max \sigma(\mathbf{p}, \theta) - \sigma_{\max} \\ M(\mathbf{p}, \theta) - M_{\max} \end{array} \right\}, \forall \theta \in [-\theta_{\max} \dots \theta_{\max}] \quad (2)$$

Here a feasible parameter vector must satisfy $\mathcal{C}(\mathbf{p}) \leq 0$. The optimal parameter vector \mathbf{p}_{opt} that minimises the cost function, subjected to the non-linear constraints, is given by:

$$\mathbf{p}_{opt} = \arg \min \mathcal{F}(\mathbf{p}) \text{ such that } \mathcal{C}(\mathbf{p}) \leq 0 \quad (3)$$

Derivative-free optimisation algorithms, which can include non-linear constraints, are well-suited to find the optimal

parameter vector of Equation 3. A suitable optimisation algorithm is described by Nelder-Mead [9]. A modified version of this algorithm is implemented, such that parameter vectors that violate the constraint function are not admissible.

Modeling

The flexible multibody modeling approach implemented in the SPACAR software [8] is used, which is well-suited to create and analyse the models for the optimisation of flexure hinges. Leaf-spring flexures have a thickness that is at least an order of magnitude smaller than their height and length, and modeling them as a plate seems appropriate. However, in order to keep the models simple with a limited number of DoFs, beam elements are used to model the flexures. Two aspects that are taken into account in the beam elements are transverse shear and torsion-extension coupling. Also, the mass moments of inertia of the beam cross section are considered. In addition, the torsional stiffness of the beams is modified to include torsional stiffening due to constraint warping [10-11].

The flexible multibody model used for the optimisation algorithm is expected to find the correct optimum. A validation model of the optimised solution is made in ANSYS, by which the eigenfrequencies, Von Mises stress and actuation moments are verified. An eight-node non-linear thin-shell element, Shell-281, is used. This element has bending and membrane capabilities and is well suited for linear, large rotation, and large-strain non-linear applications. Stress stiffening and large deflection features are included.

Results

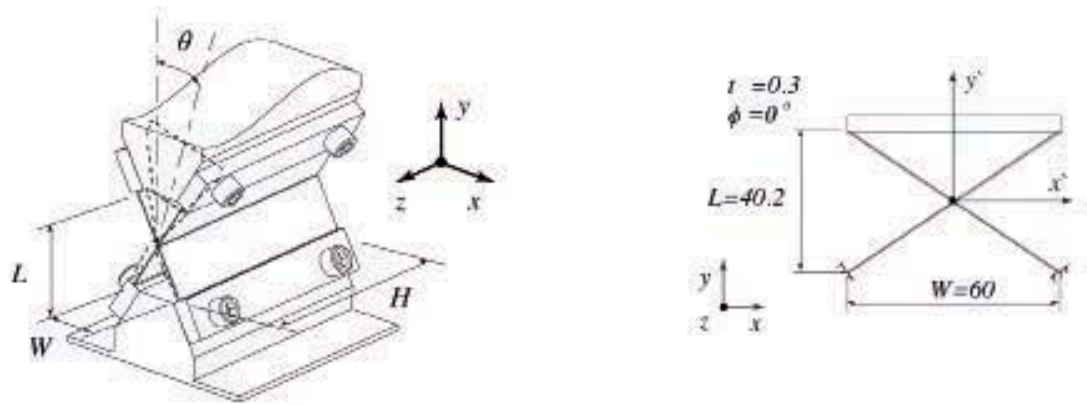
In the next subsections several flexure hinges are optimised according to the presented method.

Solid-flexure cross hinge

The solid-flexure cross hinge consists of a pair of crossing flexures. The flexures are joined at the intersection point, see Figure 2. This hinge is parameterised by parameter vector \mathbf{p} :

$$\mathbf{p} = \{L \quad W \quad t \quad \phi\} \quad (4)$$

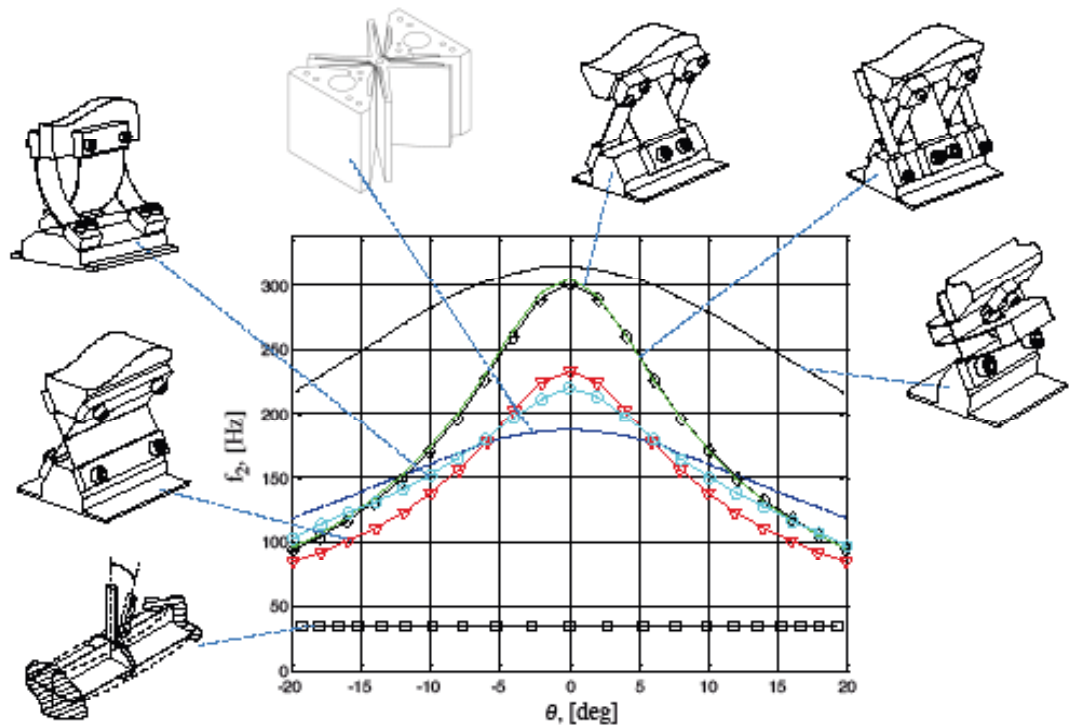
Here t is the leaf spring thickness and ϕ is the angle of the principal inertia coordinate system with the hinge coordinate system. The other parameters are shown in Figure 2. The optimised solid-flexure cross hinge geometry is presented in Figure 3. The optimal geometry is governed by the stress concentration, occurring at the intersection point of the flexures. Figure 4 shows the second eigenfrequency f_2 as a function of the angle of deflection θ .



2

3

- 2 Parametrisation of the solid-flexure cross hinge and illustration of the angle of deflection θ .
- 3 Optimal geometry of the solid-flexure cross hinge with the principal axes of inertia x' and y' , dimensions in [mm].
- 4 Second eigenfrequency as a function of the angle of deflection for the optimal solutions, determined with the finite-element method. From bottom left to right: cross-revolute hinge, solid-flexure cross hinge, curved-hinge flexure, butterfly hinge, three-flexure cross hinge, five-flexure cross hinge, and ∞ -flexure hinge.



4

Initially, at $\theta = 0^\circ$ the eigenfrequency is 230 Hz. This value drops 63% due to loss in supporting stiffnesses in the flexures, to 85.3 Hz.

Three-flexure cross hinge

The three-flexure cross hinge consists of three crossing flexures, which –contrary to the solid-flexure cross hinge – are not joined at their intersection point, see Figure 5. This hinge is parameterised by parameter vector p :

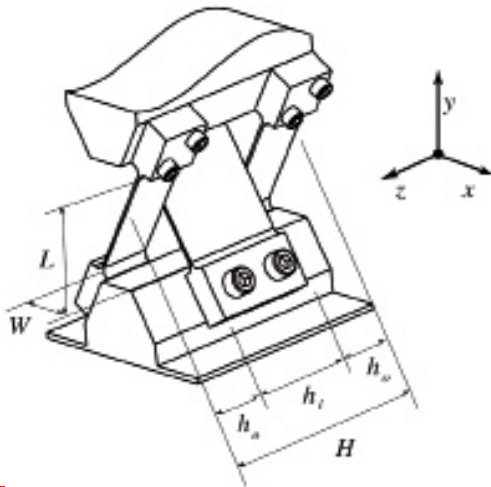
$$p = \{L \ W \ h_0 \ t \ \phi\}$$

The optimised three-flexure cross hinge geometry is presented in Figure 6. In Figure 4 the second eigenfrequency f_2 is graphed as a function of the angle of

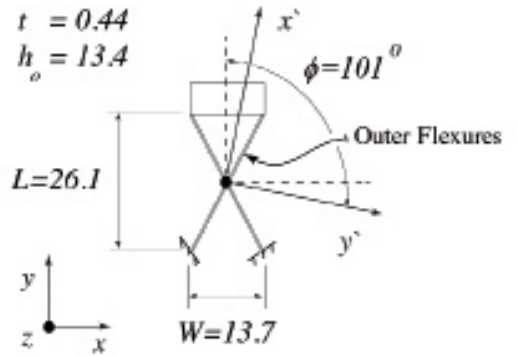
deflection θ . Initially, at $\theta = 0^\circ$, the second eigenfrequency is 304.6 Hz. This value drops 68.8% due to loss in supporting stiffnesses in the flexures, to 95.0 Hz. Increasing the number of flexures up till five will result in a negligible increase in second eigenfrequency as shown in Figure 4 [11]. Hence, adding two flexures does not improve the performance of the hinge for this loadcase.

Butterfly-flexure hinge

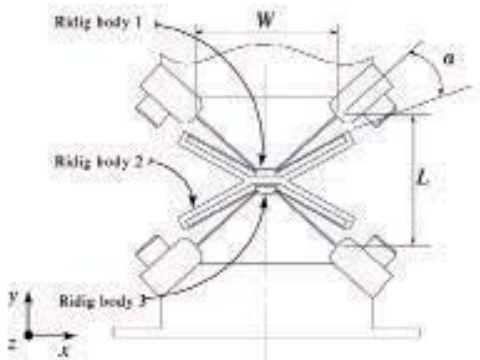
(5) The butterfly-flexure hinge [12] geometry is illustrated in Figure 7. The height of the cross section along the z -axis is H , see Table 1. Due to the serial connection, the angle of deflection of each flexure is $1/4$ of the total angle of deflection θ_{max} . Therefore, the drop in supporting stiffness will be limited for each flexure. The butterfly-flexure hinge



5

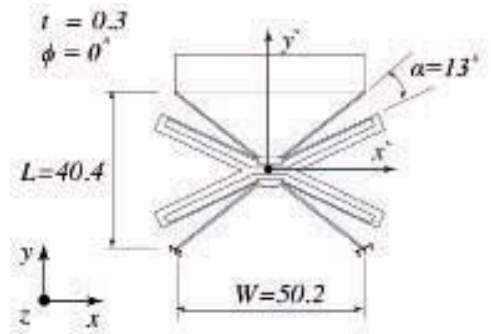


6



7

- 5 Parametrisation of the three-flexure cross hinge.
- 6 Optimal geometry of the three-flexure cross hinge, with the principal axes given in the pivot of the hinge, dimensions in [mm].
- 7 Parametrisation of the butterfly-flexure hinge.
- 8 Optimal geometry of the butterfly-flexure hinge, with the principal axes given in the pivot of the hinge, dimensions in [mm].



8

has a low-frequent internal eigenmode due to rigid body 2. In order to suppress this internal eigenmode, the angle of rotation of rigid body 2 should be kinematically coupled with the angle of deflection θ . Due to symmetry of the hinge, the angle of deflection θ is related to the angle of deflection of rigid body 2, θ_{R2} :

$$\theta_{R2} = \theta/2 \quad (6)$$

An additional mechanism is needed to constrain the relation of Equation 6. Such a mechanism was designed by Henein [12]. The internal mode is ignored in the optimisation. The butterfly-flexure hinge is parameterised by the parameter vector \mathbf{p} :

$$\mathbf{p} = \{L \ W \ t \ \alpha \ \phi\} \quad (7)$$

The optimised butterfly-flexure hinge geometry is presented in Figure 8. Parameter α shows to be equal to the minimum value of 13° . Therefore, it appears to be desirable to minimise this angle.

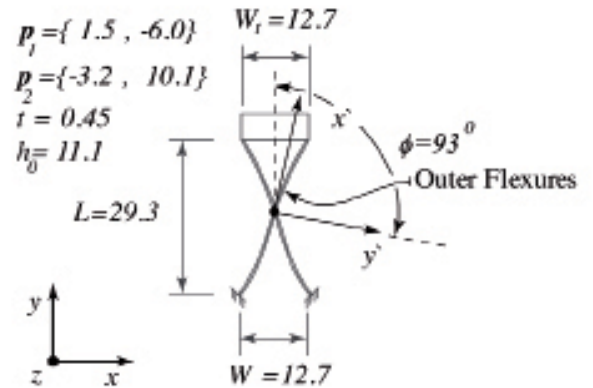
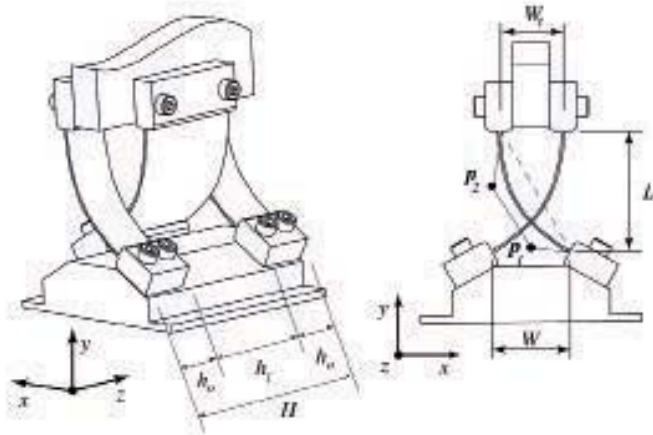
In Figure 4 the second eigenfrequency f_2 is given as a function of the angle of deflection θ . Initially, at $\theta = 0^\circ$, the second eigenfrequency is 187.2 Hz. This value drops 36.4% due to loss in supporting stiffnesses in the flexures, to 119.1 Hz. Initially, the performance is not high; nevertheless the drop in supporting stiffness is limited over the range of motion.

Curved-hinge flexure

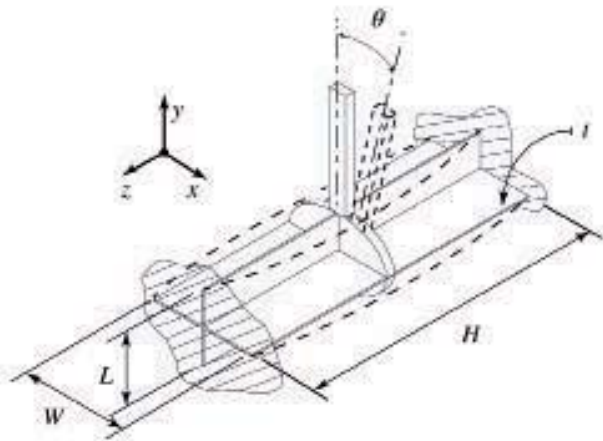
The curved-hinge flexure [13] consists of three crossing pre-curved flexures, see Figure 9. This hinge geometry allows the stiffness distribution to be tweaked over the range of motion. For instance, the stiffness in z -direction of the hinge is highest when one of the deflected curved flexures becomes straight. The curved-hinge flexure is parameterised by the parameter vector \mathbf{p} :

$$\mathbf{p} = \{L \ W \ W_t \ t \ \mathbf{p}_1 \ \mathbf{p}_2 \ h_o \ \phi\} \quad (8)$$

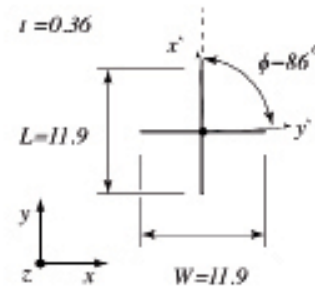
The planar points \mathbf{p}_1 and \mathbf{p}_2 define the Bézier curve.



9



10



12

The optimised curved-hinge flexure geometry is presented in Figure 10. A non-symmetric orientation of the loadcase with respect to coordinate system O_{xyz} is obtained. The optimisation has converged to a geometry where the hinge width at the bottom and top are equated and the flexure curvature is nearly straight. In Figure 4 the second eigenfrequency f_2 is given as a function of the angle of deflection θ . Initially, at $\theta = 0^\circ$, the second eigenfrequency is 220 Hz. This value drops 55.4%, due to loss in supporting stiffnesses in the flexures, to 98 Hz. Comparing the optimal curved-hinge flexure geometry with the optimal three-flexure cross hinge, see Figure 6, many similarities can be observed. Hence, the curved-hinge flexure tends to converge to the optimal three-flexure cross hinge geometry, making it a curved three-flexure cross hinge. Therefore, the optimisation does not benefit from the geometric freedom which is offered by the curved-hinge flexure.

Cross-revolute hinge

The cross-revolute hinge consists of a prismatic beam where the cross section is shaped like a cross with a small wall thickness, which is clamped at both ends, see Figure 11. This hinge is parameterised by the parameter vector \mathbf{p} :

9 Isometric and front view of the parameterised curved-hinge flexure.

10 Optimal geometry of the curved-hinge flexure, dimensions in [mm].

11 Isometric view and parameterisation of the cross-revolute hinge.

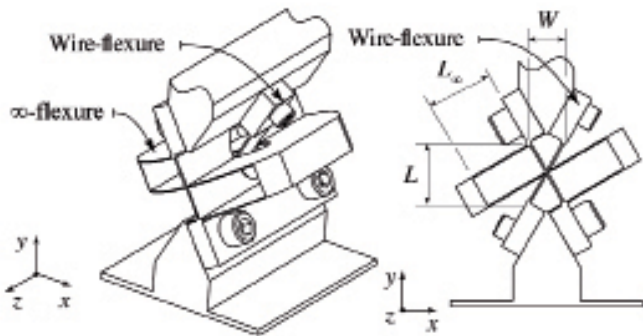
12 Top view of the optimised cross-revolute hinge geometry, dimensions in [mm].

$$\mathbf{p} = \{L \ W \ t \ \phi\} \quad (9)$$

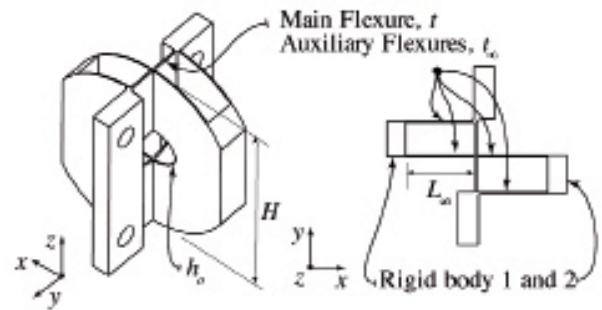
The cross section of the optimised cross-revolute hinge geometry is presented in Figure 12. In Figure 4 the second eigenfrequency f_2 is given as a function of the angle of deflection θ . Initially, at $\theta = 0^\circ$, the second eigenfrequency is 35 Hz. This value hardly decreases due to loss in supporting stiffnesses. Although these supporting stiffnesses are not high, they remain constant over the range of motion, which can be advantageous for specific applications.

∞ -flexure hinge (∞ -FH)

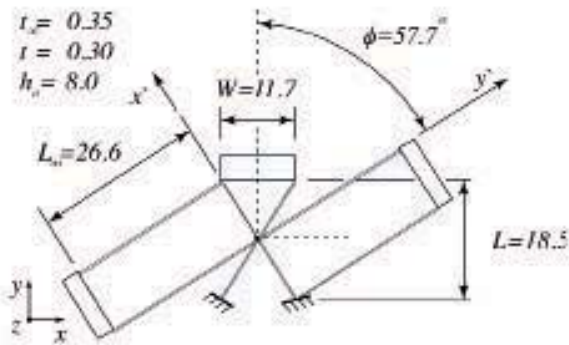
Based on the insight obtained from the analysis of the previous hinges, a new so-called ∞ -flexure hinge is designed, aiming at a high torsional stiffness over the range of motion, see Figure 13. This hinge consists of an ∞ -flexure, see Figure 14, and a wire flexure. The ∞ -flexure is composed of a main leaf-spring flexure and perpendicular to this, four auxiliary flexures are placed, which are rounded in the x - z plane. These auxiliary flexures are connected by two rigid bodies. Loading the ∞ -flexure in torsion will load the auxiliary flexures in the stiff in-plane direction. Since the auxiliary flexures are connected in



13



14



15

- 13 Isometric and front view of the parameterised ∞ -FH (part 1).
- 14 Isometric and front view of the parameterised ∞ -FH (part 2).
- 15 Optimal geometry of the ∞ -FH, with the principal axes of inertia, dimensions in [mm].

release just the desired rotational DoF about the z -axis, the wire flexure is added to constrain the translational DoF of the ∞ -flexure. In order to place the wire flexure, a hole is made at the centre of the ∞ -flexure. This hinge is parameterised by the parameter vector p :

$$p = \{L \ W \ h_0 \ L_\infty \ t \ t_\infty \ \phi\} \quad (10)$$

The optimised geometry of the ∞ -FH is presented in Figure 15. It can be seen that the x' -axis is exactly aligned with the main flexure and consequently the y' -axis is oriented perpendicular to the main flexure. In Figure 4 the second eigenfrequency f_2 is given as a function of the angle of deflection θ . Initially, at $\theta = 0^\circ$, the second eigenfrequency is 315 Hz. This value drops only 31% due to loss in supporting stiffnesses, to 217 Hz. This high performance is accomplished by the high torsional stiffness of the ∞ -flexure.

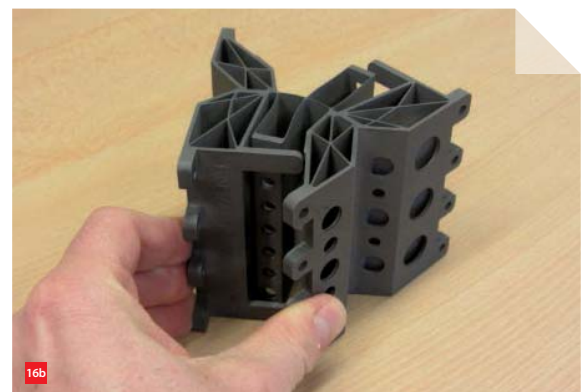
The ∞ -flexure hinge has been designed such that it can be manufactured by wire-EDM (Electrical Discharge Machining). Alternatively, for demonstration purposes it has been additively manufactured using selective laser melting of Ti6Al4V, see Figure 16 [14].

series, the deflection of each of these flexures is 1/4 of the total angle of deflection, θ_{max} . Due to this, the decrease of the in-plane stiffness is limited for these flexures. Through the coupling of the auxiliary flexures with the main flexure in parallel, the obtained configuration becomes torsionally stiff for a large angle of deflection. Therefore, the resulting ∞ -flexure contains two compliant directions; the translation in x -direction and the rotation about the z -axis. In order to

- 16 Additively manufactured ∞ -flexure hinge, made using selective laser melting of Ti6Al4V. In view of additive material cost rigid parts have been hollowed. (a) Undeformed state. (b) Maximum deflection of 20° .



16a



16b

Finite-element validation

Table 2 gives an overview of the maximum Von Mises stress and actuation moment, determined with SPACAR and ANSYS for the optimal geometries. Some differences are observed. These discrepancies can be caused by anticlastic curving and boundary effects of the flexures. Nevertheless, these discrepancies are within acceptable limits. Considering the computation time, a SPACAR model is typically twenty times faster than an FE (finite-element) model, for which reason the SPACAR model is much better suited for use during design optimisation.

Discussion

Table 3 summarises the optimal parameter vectors of the considered flexure hinges. Here f_d is the percentage of the observed decrease in the second eigenfrequency comparing the undeflected and most deflected states. The flexure hinge that gives the highest second eigenfrequencies over the full range of motion is the ∞ -FH. For all the considered hinges, the modeshape corresponding to the second eigenfrequency deforms the flexures in torsional direction. The ∞ -FH is designed to constrain this direction even when deflected, which appears to give a significant increase in supporting

stiffness compared to the other hinges. A journal article has been submitted [15].

Conclusion

The method for optimising flexure hinges shows to be capable of finding optimal geometries for flexure hinges, such that high supporting stiffnesses are obtained in the desired directions. With the ∞ -flexure a significant increase in torsional stiffness over the range of motion is realised, which results in the highest second eigenfrequencies over the range of motion of the considered hinges. This research has highly benefited from the use of a computational efficient and accurate non-linear finite-element model, which made it possible to evaluate a large number of designs within a reasonable time. ■

Table 2. FE validation of the Von Mises stress, σ_{max} , and actuation moment, M_{act} , for the optimal geometries.

	σ_{max} [MPa]		M_{act} [Nm]	
	SPACAR	ANSYS	SPACAR	ANSYS
Solid-flexure cross hinge	600	673	1.5	1.88
Three-flexure cross hinge	600	680	1.5	1.65
Butterfly-flexure hinge	493	473	1.5	1.65
Curved-hinge flexure	600	668	1.5	1.62
Cross-revolute hinge	600	690	0.7	0.83
∞ -FH	600	681	1.5	1.6

Table 3. Optimal parameter vectors overview.

Parameter	Flexure hinge					
	Solid-flexure cross hinge	Three-flexure cross hinge	Butterfly-flexure hinge	Curved-hinge flexure	Cross-revolute hinge	∞ -FH
L [mm]	40.2	26.1	40.4	29.3	11.9	18.5
W [mm]	60.0	13.7	50.2	12.7	11.9	11.7
t [mm]	0.30	0.44	0.30	0.45	0.36	0.30
t_{∞} [mm]	–	–	–	–	–	0.35
ϕ [deg]	0	101	0	93	86	57.7
h_o [mm]	–	13.4	–	11.1	–	8.0
h_i [mm]	–	58.2	–	62.8	–	–
L_{∞} [mm]	–	–	–	–	–	26.6
α [deg]	–	–	13	–	–	–
min f_2 [Hz]	85	95	119	98	35	217
f_d [%]	63.0	68.8	36.4	55.4	1.7	31.2

REFERENCES

- [1] Koster, M.P., 1996, "Constructieprincipes voor het nauwkeurig bewegen en positioneren", Uitgeverij Universiteit Twente, Enschede, NL.
- [2] Smith, S., 2000, "Flexures: Elements of Elastic Mechanisms", Taylor & Francis, London, UK.
- [3] Howell, L.L., 2001, "Compliant Mechanisms", Wiley, New York, USA.
- [4] Soemers, H.J.M.R., 2010, "Design Principles for Precision Mechanisms", T-Pointprint, Enschede, NL.
- [5] Folkersma, K.G.P., Boer, S.E., Brouwer, D.M., Herder, J.L., and Soemers, H.M.J.R., 2012, "A 2-dof Large Stroke Flexure Based Position Mechanism", DETC2012-70377, *International Design Engineering Technical Conferences & Computers and Information in Engineering Conference*, Chicago, USA.
- [6] Folkersma, K.G.P., Boer, S.E., Brouwer, D.M., Herder, J.L., and Soemers, H.M.J.R., 2011, "A large stroke planar 2-DOF flexure-based positioning stage for vacuum environments", *Mikroniek*, 51(6), pp.12-17.
- [7] Haringx, J.A., 1949, "The Cross-Spring Pivot as a Constructional Element", *Applied Scientific Research, Sect. A*, A1, pp. 313-332.
- [8] Jonker, J.B., and Meijaard, J.P., 1990, "Spacar – Computer Program for Dynamic Analysis of Flexible Spatial Mechanisms and Manipulators", in *Multibody Systems Handbook*, W. Schiehlen (ed.), Springer-Verlag, Berlin, DE, pp. 123-143.
- [9] Nelder, J.A., and Mead, R., 1965, "A Simplex Method for Function Minimization", *The Computer Journal*, 7 (4), pp. 308-313.
- [10] Eijk, J. van, 1985, "On the Design of Plate Spring Mechanism", Ph.D. thesis, Delft University of Technology, Delft, NL.
- [11] Wiersma, D.H., Boer, S.E., Aarts, R.G.K.M., and Brouwer, D.M., 2012, "Performance Optimization of Large Stroke Spatial Flexure Hinges". DETC2012-70502, *International Design Engineering Technical Conferences & Computers and Information in Engineering Conference*, Chicago, USA.
- [12] Henein, S., Spanoudakis, P., Droz, S., Myklebust, L.I., and Onillon, E., 2003, "Flexure Pivot for Aerospace Mechanisms", ESA SP-524, in: *Proceedings of the 10th ESMATS / ESA*, San Sebastian, ES.
- [13] Brouwer, D.M., Meijaard, J.P., and Jonker, J.B., 2009, "Elastic Element Showing Low Stiffness Loss at Large Deflection", *Proceedings of the 24th annual meeting of the American Society of Precision Engineering*, Monterey, USA, pp. 30-33. www.layerwise.com
- [15] Wiersma, D.H., Boer, S.E., Aarts, R.G.K.M., and Brouwer, D.M., Submitted 2012, "Design and Performance Optimization of Large Stroke Spatial Flexures", *Journal of Computational and Nonlinear Dynamics*.

IN SEARCH OF THE INVOLUTE

Computer software meant a true revolution for measuring gearwheels. Before the computer era, only manual measuring tools could give some indication of the precision with which a gear tooth had been shaped. But the real form of the involute flank remained a mystery. Until the emergence of sophisticated computer programs, that is, as these made it possible to translate a cloud of measuring points into the deviation of a tooth profile from the involute form prescribed.

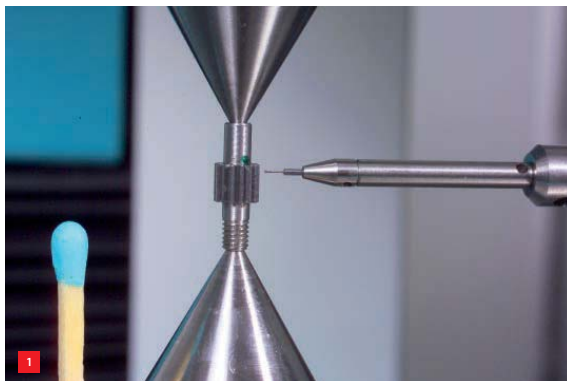
FRANS ZUURVEEN

An interesting aspect of measuring gearwheels is the miniaturisation of these industrial products. The manufacturing of gearwheels with modules down to 0.1 (the unit, mm, usually is not mentioned) is a real precision-technological challenge. However, this is not what this article is about; this article will go into the details of measuring them (see Figure 1), which in itself poses just as many problems.

Many measuring equipment suppliers have instruments for measuring gearwheels in their delivery programme. Such instruments can be designed especially to measure gears (see Figure 2). On the other hand, versatile coordinate measuring instruments may be able to measure gearwheels thanks to software with gear measurement facilities (see Figure 3).

AUTHOR'S NOTE

Frans Zuurveen is a freelance text writer who lives in Vlissingen, the Netherlands.



1

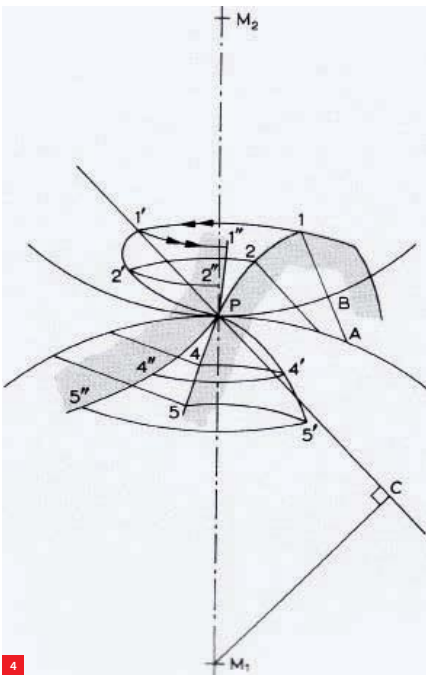
- 1 Measuring a miniature gearwheel module 0.3, stylus diameter 0.3 mm. (Photo courtesy of Wenzel)
- 2 The Wenzel WGT 280 gearwheel measuring instrument.
- 3 The Werth ScopeCheck V coordinate measuring machine.



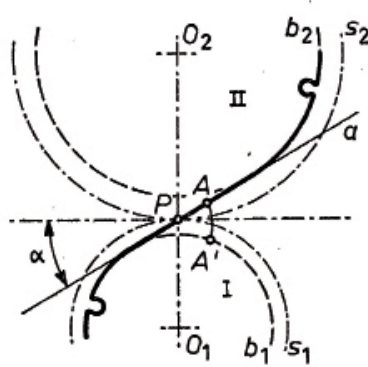
2



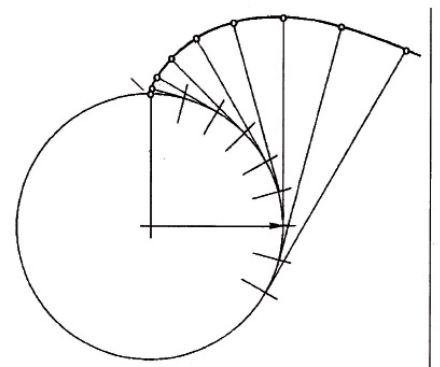
3



4



5a



5b

- 4 Reulaux's construction. Wheel 1 has centre M_1 , wheel 2 has centre M_2 . Perpendicular line 1-A has to pass through pole P when point 1 touches the mating profile of wheel 2. Turning wheel 1 to the left until 1-A crosses P gives 1'-P. Turning 2 back across arc PB (PB equals PA) causes 1'-P to enter position 1''-B. Point 1'' now is a point of the mating tooth profile. The same goes for 2'', 4'' and 5''.
- 5 The involute.
 (a) A straight line of action provides an involute. a is the pressure angle. b_1, b_2 are base circles. s_1, s_2 are pitch circles.
 (b) Its construction by unrolling an imaginary rope.

Most mechanical designers know that one of the advantages of an involute gearwheel transmission is the absence of heavy demands to the accuracy of the distance between the two wheel centres. Moving a gearwheel slightly inwards or outwards – within certain limits – does not affect the quality of the transmission at all.

Another well-known fact is that a gearwheel is characterised by its module m , defined as p/π , with p the pitch of the teeth. The unit m was introduced to simply calculate the pitch diameter as the product $m \cdot z$, with z the number of teeth.

Despite these well-worn truths, it would be a good idea to go over some theory of involute gearwheel systems. This will make the ins and outs of gearwheel measuring procedures easier to understand. We only deal with spur gears – other gearwheel transmissions are based on the same fundamentals.

The origin of the involute

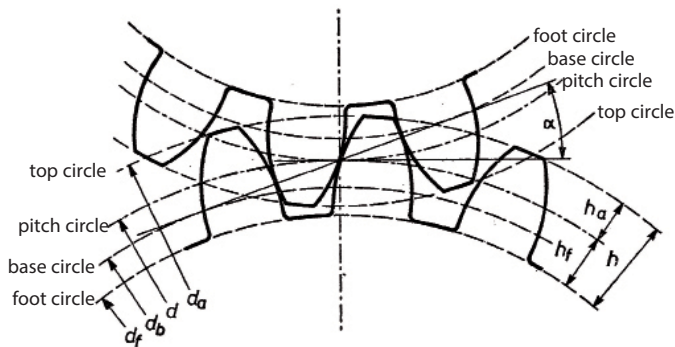
The main problem of designing a gear tooth profile is keeping the transmission ratio $i = z_1/z_2$ constant within one tooth rotation angle, with z_1 and z_2 the teeth quantities of the two gearwheels. In 1876, Franz Reulaux demonstrated in his book “The Kinematics of Machinery” that, when selecting any kind of profile for a tooth, a profile can always be determined for the mating profile, keeping i constant (see Figure 4).

When the two gearwheels are revolving, the contact point of the two mating tooth profiles moves along the line of action, also called pressure line. Common forms of this line of action are a straight line (see Figure 5a) or a circular line. In the latter case, this provides a tooth flank profile in the form of a cycloid: the curve describing one point of a circle when rolling along a second circle. Gearwheels with this kind of tooth profile are called cycloidal gears. They are mainly applied in the watch and clockwork industry.

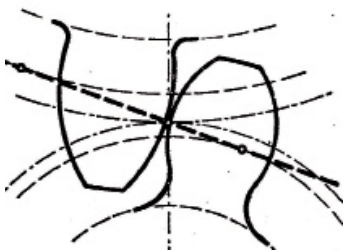
A straight line of action brings us to the involute (see Figure 5b). Figure 5a shows that this curve, originating from rolling a straight line along a circle, is the consequence of a straight line of action. The circle along which the straight line rolls is called the base circle. Figure 5a also illustrates that the cooperation of two involute gearwheels can simply be regarded as an imaginary rope rolling along the two base circles and making them revolve. Point P, the intersection of the line of action and the line connecting the two centres, defines the pitch circle (see Figure 6a). The angle between the line of action and the line perpendicular to the line connecting the centres (α in Figure 5a) is called the pressure angle. In most cases, this angle equals 20°.

The advantages of the involute

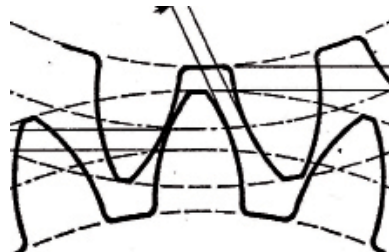
The first advantage is that two gearwheels with involute flank profiles with the same module always work together properly, regardless of their number of teeth. Secondly, some variation in the distance of the two centres is permitted, as already noted. The third advantage is that the force between the two cooperating teeth always goes in the same direction, i.e. through point P (Figures 4 and 5a) and pointing along the line of action – apart from the friction force. Only when the two flank profiles meet in point P the friction force is zero, which corresponds with pure rolling. In the other points of flank contact, slip occurs, more so at a greater distance from P on the line of action.



6a



6b



6c

- 6 Gearwheel geometry.
 (a) The naming of circles in two cooperating gearwheels. h is the tooth height, h_a top height, h_f foot height.
 (b) Too few teeth results in undercutting: the cutting tool removes a part of the tooth foot.
 (c) Teeth correction by moving the cutting tool outwards (addendum modification).
 7 A conventional gear tooth screw gauge.



7

An unwanted effect occurs when the number of teeth is too small. This effect is called undercutting (see Figure 6b). In this case, a part of the tooth foot is removed by the cutting tool, which, in general, is a gear rack that moves up and down when rolling along with the workpiece. The solution to this undercutting problem is to carry out a corrective action called 'addendum modification'. Here, the cutting tool is positioned slightly outwards, which makes the teeth 'slender' (see Figure 6c). This is applied to the gearwheel with the lowest number of teeth, of course. The mating wheel then has to undergo an opposite correction by moving the tool the same distance inwards.

Conventional gearwheel measuring

Mechanical gearwheel testing tools are indispensable aids in workshops, e.g. the gear tooth screw gauge shown in Figure 7. While such a device does not provide any information about the involute itself, it is useful when comparing measuring results with the ones acquired by measuring a precision-made master wheel.

Run-out deviations of gearwheels can easily be measured with a dial gauge with spherical stylus by introducing the stylus in between two teeth. Other means for controlling gears are profile projectors and coordinate measuring machines for checking tooth heights and roundness deviations, etc.

More information about the accuracy of the involute profile could be obtained by functionally testing two cooperating wheels. Driving the first wheel with a uniform angular speed, the uniformity of the rotation of the second wheel could be compared with the rotation of two precision-made master wheels (double-flank testing). Nowadays, measuring equipment manufacturers no longer have that kind of functional test equipment in their programme because master wheels are very expensive and because much better measuring equipment is available.

Measuring the involute

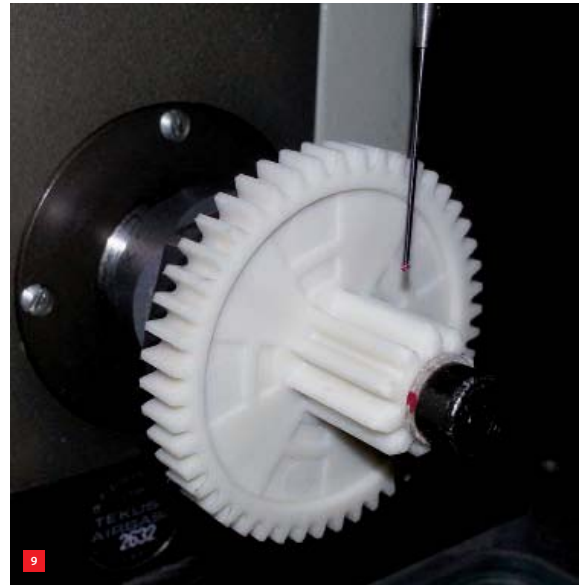
Relatively recently, the advent of advanced computer programs and the availability of extremely small spherical sensors made it possible to determine deviations from the prescribed involute for small gearwheels. For this article, we used information from two renowned measuring equipment manufacturers: Wenzel Group and Werth Messtechnik.

Wenzel and Werth differ somewhat in their approach to the issue of small-module gearwheel measurement. Wenzel has dedicated gear measurement instruments in its portfolio (see Figure 8). Werth does not have such dedicated instruments in its programme because most of the Werth Multisensor coordinate measuring instruments can measure gearwheels thanks to the WinWerth software GearMeasure module and the availability of dedicated sensors (see Figure 9).

When we asked gearwheel measurement specialists at Werth and Wenzel why customers should choose their equipment for solving small-gearwheel measurement problems, we got the following answers.

Wenzel

"Besides 3D coordinate measuring instruments, Wenzel also has pure gearwheel measuring instruments in its



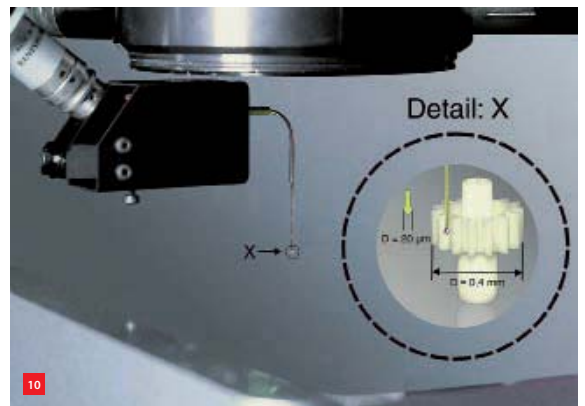
delivery programme. These measurement machines – series WGT – are 4-axis instruments: three linear degrees of freedom and one rotational, realised by an accurate turntable. This means that such an instrument is dedicated to measuring individual characteristics of involute profiles of internal and external spur and helical gears.

Another plus point of Wenzel's gearwheel measurement instrumentation is the decades of experience the company has in the technology of air bearings on a granite base that we use in our CMMs. This technology is also being applied in our WGT machines. That's why these high-precision and robust machines do not wear and have a long lifespan. WGT machines are specified to measure gearwheels down to module 0.5, or optionally even down to 0.2. The modular measurement software provides broad functionality for the measurement of gears, shafts and other rotationally symmetrical parts. Besides the evaluation of gear parameters, this also allows the analysis of other geometrical features."

Werth

"The most important reason to use Werth coordinate measuring machines for measuring gearwheels is the high level of flexibility they provide thanks to a large sensor variety. The Werth Multisensor Technology makes it possible to measure almost every workpiece, including small gearwheels, very time-efficiently. For example, customers use the Werth ScopeCheck V measuring instrument (Figure 3) to measure shafts. Here, the instrument not only measures diameters, lengths, flatness and roundness, but also parameters from integrated involute toothings.

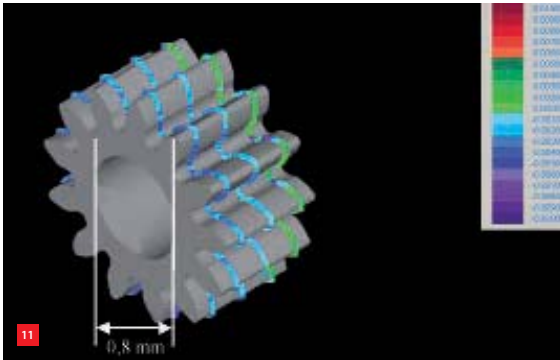
- 8 Working with the dedicated Wenzel WGT 1200 gear measuring machine.
- 9 Measuring a small gearwheel with a Werth multisensor measuring machine.
- 10 Inspecting a small gearwheel with the Werth glass fibre probe with a sphere diameter of only 20 µm.



Another aspect is the uniqueness Werth can offer because of the Werth WFP patented glass fibre scanning probe in its delivery programme. With this probe, which has a minimal diameter of 20 µm, very small gearwheels can be inspected (see Figure 10). This means that gearwheels down to module 0.1 can be measured."

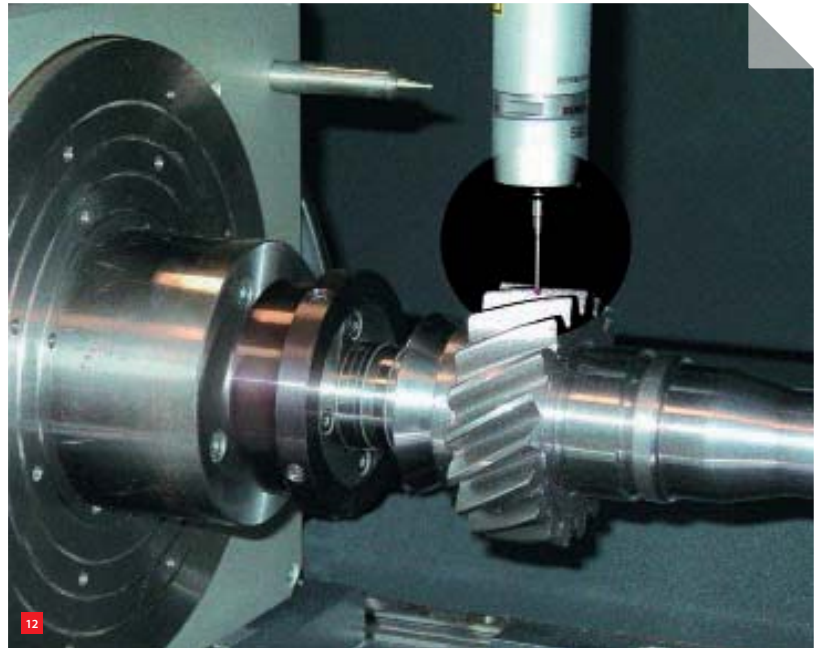
Measurement results

Of course, in our digital world, we are accustomed to beautiful visual presentations of data. Nevertheless, viewing Figure 11 with colour-coded deviations presented by the WinWerth 3D CAD module when measuring an extremely small gearwheel commands admiration. The deviations of the ideal involute are shown in various colours, making clear that this gearwheel has been manufactured with micrometer precision.



11 Measuring a small gearwheel with the 3D CAD module of the WinWerth computer program. The deviations of the ideal involute are shown in various colours (levels in mm).

12 Measuring a gearwheel on a Werth 3D-CNC Multisensor CMM VideoCheck-IP 400 (measuring range 400 x 200 x 250 mm³) with a Renishaw sphere stylus probe 2 mm in diameter.



When working with gearwheel measuring software, the operator feeds the gear design data into the computer: number of teeth, module and, if relevant, the addendum modification factor. From this data, the computer calculates the nominal involute profile. Scanning of the workpiece starts next, with selection of the appropriate stylus at the same time (see Figure 12). A Renishaw stylus has a minimal diameter of 0.3 mm, while a Werth glass fibre stylus measures 20 µm, as stated before.

The measurement results can prove the accuracy with which the involute flank form has been realised, showing the involute deviations for both the left and the right flanks. In addition to profile deviations, tooth widths, pitch, roundness, etc., can be measured.

To conclude

This article outlines the arguments for preferring the involute as the flank form curve for gearwheel teeth. Making such teeth for extremely small gearwheels may be an enormous challenge, but measuring them is a real challenge too. That's why the task of finding deviations of the ideal involute profiles for small gearwheels might be considered a search for geometrical truth. Ultimately, there's a happy ending to this search because sophisticated measurement instruments with advanced computer programs make it possible to record involute deviations with sub-micrometer precision. ■

SOURCES

- <https://en.wikipedia.org/wiki/gear>
- Winkler Prins, "Technische Encyclopedie", part 6, Elsevier, 1975.
- F. Reulaux, "The Kinematics of Machinery", Dover Publications, 1963.
- F.C.W. Slooff, "Kinematica", in A. Davidson (Ed.), *Handboek van de Fijnmechanische Techniek, deel 1, Algemene grondslagen*, 1966.
- J.W. van Beek, "Schut's atlas der geometrische meettechniek", 1994.

Miniature Drive Systems

<ul style="list-style-type: none"> • DC-Motors • Brushless DC-Motors • Linear DC-Servomotors 	<ul style="list-style-type: none"> • Stepper Motors • Piezomotors • Ball Screws 	<ul style="list-style-type: none"> • Precision Gearheads • Motion Control • Encoders
---	--	---

MINIMOTOR Benelux · www.faulhaber.com

INDISPENSABLE TIME SAVER OR EROSION OF KNOWLEDGE AND EXPERTISE?

Since the first CAD/CAM software packages were introduced in the 1970s, engineering software has enjoyed a steady rise. This trend is illustrated by three examples from the academic literature on predicting the dynamic behaviour of mechanisms. Over the past decade, the development of systems that are faster and more precise has seen interest in this discipline increase. Having sound knowledge and expertise of this field is, therefore, a key skill of the modern engineer.

AUTHORS' NOTE
Sjors Hienekamp and Raymond van der Wee are both Mechanical Engineering students at Avans University of Applied Sciences in 's-Hertogenbosch, the Netherlands. They wrote this article as part of their 'Machines in Motion' minor (see box).

SJORS HIENEKAMP AND RAYMOND VAN DER WEE

Matrix calculation

In 2000, researchers at the Serbian Academy of Sciences and Arts reported on a study into internal redundancy [1]. According to the researchers, this was the best way to improve the dynamic behaviour of robots. Internal redundancy means that the position of one or more links in a mechanism has no effect on the final position and orientation of the output. These seemingly useless links do, however, play a very important role in terms of increasing the total stiffness of the mechanism and the distribution of the various loads. To highlight this internal redundancy, the researchers used a purely mathematical method. The

various stiffnesses in the system can be linked by means of matrices. Figure 1 shows a simple example of such a matrix (not related to [1]). Certain values within the matrix can be manipulated to achieve an optimal configuration.

Simulation based on theoretical comparisons

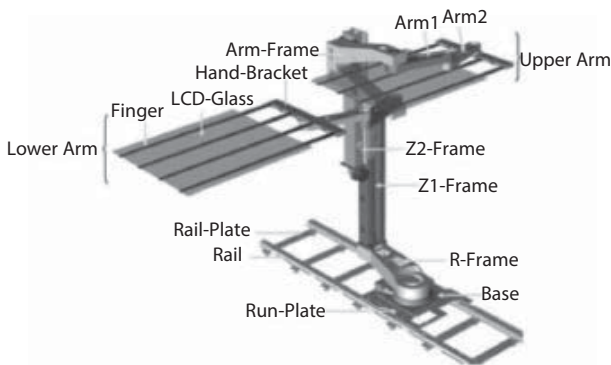
Samsung's Robot Technology Lab in Korea took a different approach [2]. Around 2005, the technology for manufacturing LCD screens underwent an enormous boost, as a result of which ever larger screens could be manufactured. As this involved very delicate glass plates, a robot for handling such screens had to be developed with a keen eye for dynamic behaviour (see Figure 2). The method used by the scientists at Samsung was based partly on mathematical and partly on physical comparisons. These comparisons were put into a simulation program, which simulated various operating conditions and introduced vibrations into the system. The output from the simulation program revealed the robot's weak points (see Figure 3). By structurally improving these spots, the robot can be optimised.

SAM: Synthesis and Analysis of Mechanisms

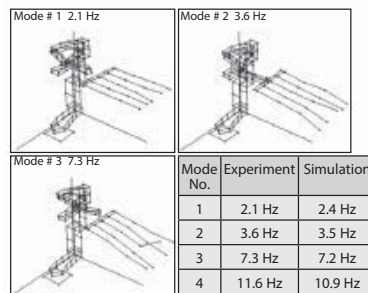
Due to the increasing cost of energy, the topic of 'green' machines has become more and more important over the last few years. For this reason, a software program has been

$$K = \begin{bmatrix} \frac{EA}{L} & 0 & 0 & 0 & 0 & 0 \\ 0 & \frac{12EI_z}{L^3} & 0 & 0 & 0 & -\frac{6EI_z}{L^2} \\ 0 & 0 & \frac{12EI_y}{L^3} & 0 & \frac{6EI_y}{L^2} & 0 \\ 0 & 0 & 0 & \frac{GJ}{L} & 0 & 0 \\ 0 & 0 & \frac{6EI_y}{L^2} & 0 & \frac{4EI_y}{L} & 0 \\ 0 & -\frac{6EI_z}{L^2} & 0 & 0 & 0 & \frac{4EI_y}{L} \end{bmatrix}$$

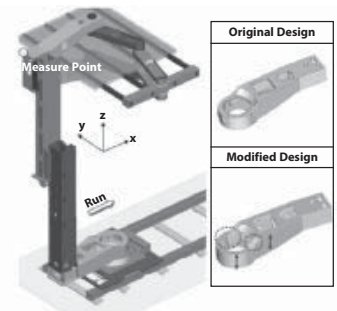
1 Relatively simple stiffness matrix for determining the optimal configuration of a mechanism.



2



3a



3b

developed with which energy and performance losses in highly dynamic machines can be minimised. This program (Synthesis and Analysis of Mechanisms, SAM, see Figure 4) is based on the fact that with lighter constructions, less acceleration and the addition of passive compensation parts, motors require less energy for movement [3]. This program can analyse the change in drive power/torques for a required drive capacity. The construction blueprint including animation is on screen within minutes. SAM's optimisation module allows the designer to alter various variables.

Modelling mass-damper systems

The above two modelling examples demonstrate the increasingly prominent role of software-based calculation.

Dynamic modelling (Figure 5) based on the theory of mass-damper systems provides a complete theoretical analysis, just like matrix calculation. This tests the engineer's mechanical insight and knowledge of the theory of the strength of materials and dynamics. Although it is almost a traditional form of modelling, it can be a fantastic way of quickly gaining insight into the dynamic behaviour of a mechanism. Once the output is known, the engineer can easily determine which parts contribute most to dynamic instability and position inaccuracy of the mechanism. This can prevent unnecessary time and energy being invested in modifying the parts that contribute little or nothing to more efficient dynamic behaviour. What's more, the outcome of this method provides leads for deciding on the best kind of (servo) motor and transmission.

- 2 LCD screen transfer robot, telescopic type.
- 3 Analysis from Samsung's Robot Technology Lab. The wire-frame model of the robot shows a platform with five arms. These arms, especially their displacements at the extremities, are crucial for correctly supporting the LCD screens.
 - (a) Comparison of vibration mode frequencies as determined by experiment and simulation.
 - (b) Design study using dynamics simulation for reducing the vibrations.

Minor Machines in Motion

The four-year course in Mechanical Engineering at Avans University of Applied Sciences (Avans Hogeschool) in 's-Hertogenbosch includes a six-month specialisation, called minor, in the final year. One of the minors, 'Machines in Motion', covers the design of fast and precise machines for the so-called 'high tech, low volume' market. In terms of mechanics, design and tolerances are subject to stringent requirements, and motion control – or motors in servo systems – is just as important.

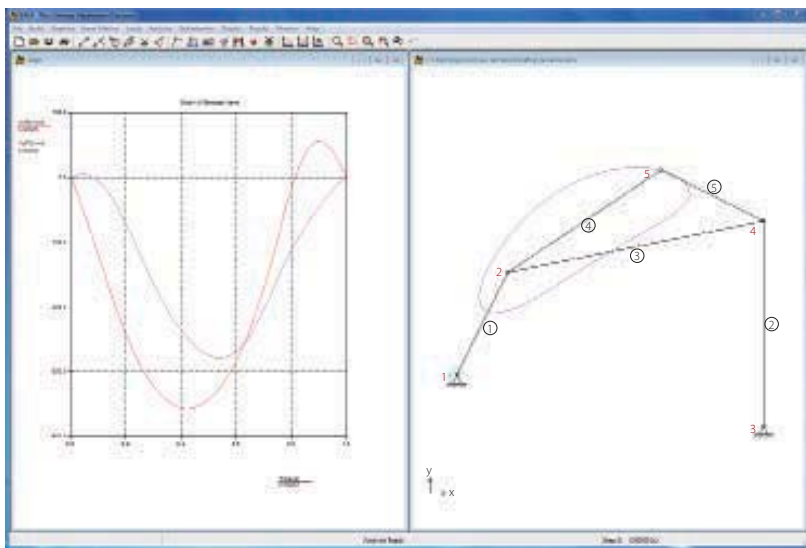
The minor teaches students to work together with colleagues from other fields of study (e.g. electronics, and control) and often with suppliers too. They gain an insight into the relationship between machine design and the production process that the machine in question is going to run. Naturally, creativity is a prerequisite for finding good solutions to complex design problems. The minor includes a project, generally suggested by a company, which covers the whole process from the initiation stage right through to manufacturing a prototype, from drafting a list of requirements and wishes, to preparing and overseeing manufacture and testing.

The students also study theoretical subjects, do practical training, go on company visits and attend guest lectures given by companies on topics that are important for designing fast and precise machines. Every year, about thirty students take the 'Machines in Motion' minor at Avans Hogeschool, which results in about ten articles. Articles relevant to precision engineers can be selected for publication in Mikroniek.

PF.KIVITS@AVANS.NL (ERIC KIVITS, COORDINATOR) WWW.AVANS.NL WWW.LINKEDIN.COM/GROUPS/MACHINES-IN-MOTION-4793196/

Rise of engineering software

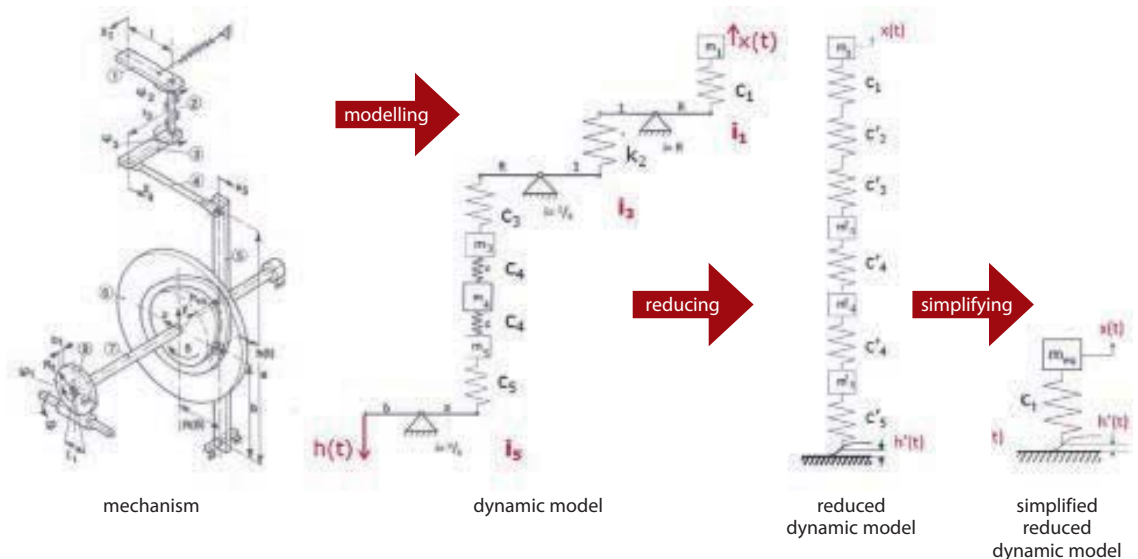
The development of specialist engineering software has been ongoing for quite some time now [4]. CAD/CAM appeared well before 2000, when the first article discussed here was published. Since the 1980s, such 3D CAD programs have become commonplace in the design departments of technical companies. In the past, all drawings were done by hand, which was incredibly time-consuming. Nowadays, however, generating 3D drawing is a ‘piece of cake’.



4

4 The standard SAM opening screen, illustrating the type of problems SAM can deal with. The schematic on the right shows a bar mechanism onto which the trajectory of point 5 is projected. The graph on the left represents the relative displacements in x- and y-direction.

5 The consecutive steps of dynamic modelling, in which mechanisms are represented by masses, springs and transmissions, supplemented with drives and controls.



5

That said, this time-consuming work was mainly done by semi-skilled staff. The design itself had to – and still has to – come from highly-trained engineers, who consider every aspect of it thoroughly, and have to – and are able to – carry out various calculations. The traditional way of working is increasingly being lost to all kinds of software programs that, although saving a lot of time (and hence money), may be eroding the knowledge and expertise of engineers as a result.

Sound theoretical foundation

The danger, therefore, is that highly-trained technical staff increasingly use fewer hands-on engineering skills because of the rise of engineering software, as a result of which theoretical foundations may become eroded. It is the job of education to anticipate this trend and to provide future senior technical staff with a sound theoretical foundation. The mass-damper method discussed is taught at Avans Hogeschool, and as such is an integral part of the knowledge and expertise of the senior technical staff of the future. ■

REFERENCES

[1] M. Vukobratovic, V. Potkonjak and V. Matijevic, "Internal redundancy – the way to improve robot dynamics and control performances". *J. Intel. Rob. Syst.*, no. 27 (2000), pp. 31-66.
 [2] J.H. Seo, H.J. Yim, J.C. Hwang, Y.W. Choi and D. Il Kim, "Dynamic load analysis and design methodology of LCD transfer robot". *J. Mech. Sci. Technol.*, no. 22 (2008), pp. 722-730.
 [3] H. Schrama, "Optimalisatie van mechanismen leidt tot lichtere aandrijvingen en minder energieverbruik" [Optimisation of mechanisms leads to lighter drives and less energy consumption], *Constructeur*, no. 4 (2012), pp. 28-31.
 [4] cadcamfunda.com/history_of_cadcam.

UPCOMING EVENTS

1 October 2013, Rijssen (NL)

Electrical Discharge Machining seminar

EDM market leader Ter Hoek Vonkerosie organises a seminar on the potential of EDM, illustrated by the case of a micro cutting die. Chairman of the day will be Prof. Bert Lauwers of K.U.Leuven University (Belgium). Presentations will be given by IMS, Ceratizit, Ter Hoek Vonkerosie, Agie Charmilles and Mitutoyo. See also the News section in this issue.

WWW.TERHOEKVONKEROSIE.NL

7 October 2013, Eindhoven (NL)

DSPE Symposium Optics & Optomechatronics

Symposium in the Conference Center of the High Tech Campus Eindhoven, organised by the newly established DSPE Special Interest Group Optics & Optomechatronics. See also the DSPE section in this issue.



WWW.DSPE.NL

7 November 2013, Den Bosch (NL)

Bits&Chips 2013 Embedded Systems

For the 12th edition, Bits&Chips publisher Techwatch has joined forces with INCAS³, a research institute developing high-tech sensor systems, to organise the Embedded Systems conference. The topics of this year's conference are big science, co-development, distributed sensing, electric vehicles, healthcare and 'smart cities'.



WWW.EMBEDDED-SYSTEMEN.NL

21 November 2013, Utrecht (NL)

Dutch Industrial Suppliers Awards 2013

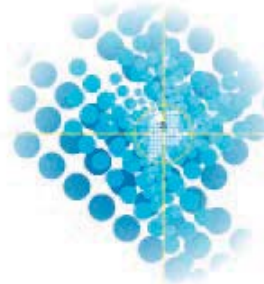
Event organised by Link Magazine, with awards for best knowledge supplier, best logistics supplier and best customer.

WWW.LINKMAGAZINE.NL

3-4 December 2013, Veldhoven (NL)

Precision Fair 2013

Thirteenth edition of the Benelux premier trade fair and conference on precision engineering. Some 260 specialised companies and knowledge institutions will be exhibiting in a wide array of fields, including optics, photonics, calibration, linear technology, materials, measuring equipment, micro-assembly, micro-connection, motion control, surface treatment, packaging, piezo technology, precision tools, precision processing, sensor technology, software and vision systems. The conference features over 50 lectures on measurement, micro-processing, motion control and engineering. The Precision Fair is organised by Mikrocentrum.



Precision Fair 2013

WWW.PRECISIEBEURS.NL

11-12 December 2013, Ede (NL)

Netherlands MicroNanoConference '13

Conference on academic and industrial collaboration in research and application of microsystems and nanotechnology. The ninth edition of this conference is organised by NanoNext.NL and MinacNed.

WWW.MICRONANOCONFERENCE.NL

26-27 February 2014, Veldhoven (NL)

RapidPro 2014

The annual event for the total additive manufacturing, rapid prototyping and rapid tooling chain.

WWW.RAPIDPRO.NL

7-8 May 2014, Den Bosch (NL)

High-Tech Systems 2014

The second edition of this event focuses on the high-tech systems industry in all European areas with significant high-tech roadmaps. It entails sectors and topics like advanced system engineering and architecture, precision engineering, mechatronics, high-tech components system design as well as advanced original equipment manufacturing (OEM).



WWW.HIGHTECHSYSTEMS.EU

22-23 May 2014, Aachen (DE)

28th Aachen Machine Tool Colloquium

The Aachen Machine Tool Colloquium (Aachener Werkzeugmaschinen-Kolloquium, AWK) has established itself as an important platform for exchanging future perspectives for production technology. The general topic of AWK 2013 is 'Industry 4.0 – The Aachen Approach', focusing on the potential as well as risks of implementing a cross-linked, intelligent production and demonstrating the technical realisation by means of case studies.

WWW.AWK-AACHEN.DE

A STABLE MICROSCOPE IMAGE IN ANY BUILDING: HUMMINGBIRD 2.0

Low-frequency building vibrations can cause unacceptable image quality loss in microsurgery microscopes. The Hummingbird platform, developed earlier by MECAL, now also can serve as a vibration filter between a ceiling and a microscope. Based on a patented solution, the Hummingbird platform isolates equipment from low-frequency vibrations better than any other state-of-the-art vibration damper. As a result, the microscope user can always enjoy a stable image in any building.

RONALD RIJKERS, JOOP DE SMIT, JOS VAN GRINSVEN AND OLGA SEMEYKO

AUTHORS' NOTE

Ronald Rijkers, Joop de Smit, Jos van Grinsven and Olga Semeyko all work for MECAL Semiconductor Product Development in Eindhoven, the Netherlands. Their team has developed and realised the Hummingbird platform for the academic hospital Maastricht, azM, and is currently working on new projects based on the Hummingbird technology.

info@mecal.eu
www.mecal.eu

High, thin-walled buildings in glass and steel replace low and robust concrete constructions. Such modern buildings comply with all the regulations but are more sensitive to low-frequent vibrations caused by wind and traffic. These vibrations can compromise performance of sensitive equipment installed in the building. In case of microscopes used in microsurgery, this results in reduced image quality.

Introduction

All things in life, from tectonic plates to atoms, exhibit vibrations. Some vibrations can be seen by the human eye and some can only be seen with very sensitive measurement equipment. At the academic hospital azM in Maastricht, the Netherlands, low-frequent vibrations were affecting a sensitive ceiling-mounted surgical microscope. Although the amplitude of the vibrations was about 100 times smaller than the thickness of a human hair (0.05 mm), they were visible because of the large magnification factors used in microsurgery.

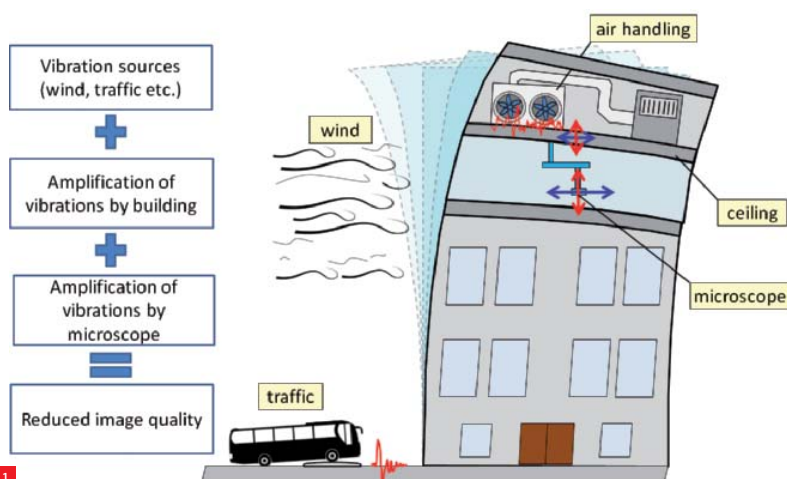
Commissioned by the project office “Bouw bureau azM/ RO groep” in Maastricht, MECAL investigated the case and successfully implemented a Hummingbird platform to isolate the microscope from vibrations in all directions, even at the lowest frequencies.

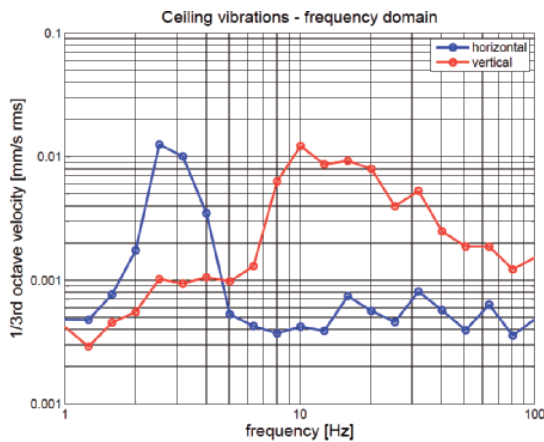
Investigation

In order to find the cause of the problem, vibration measurements were carried out by MECAL and by the consultancy firm Cauberg Huygen at the location of azM. These measurements showed the sources of vibration, as depicted in Figure 1:

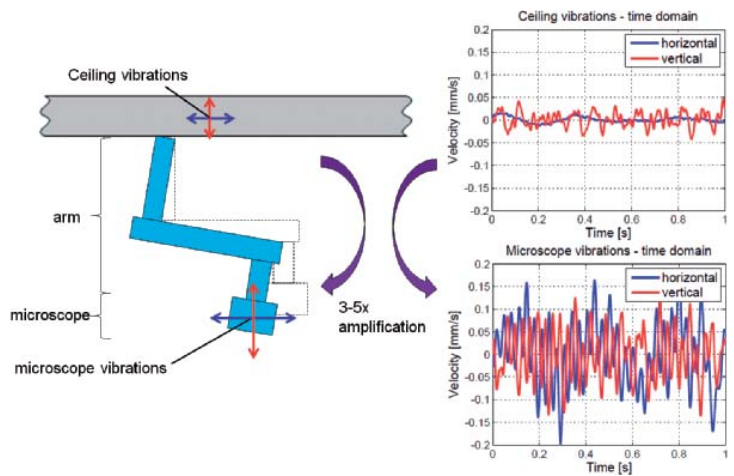
- Traffic
Whenever a bus drove over a speed bump nearby the building, vibrations were seen on the microscope image.

1 Vibration sources.





2



3

- Wind
After extensive measuring, it was found that microscope vibrations increased with increasing wind speeds.
- Air handling units
The air handling units on the floor directly above the microscope were also disturbing the image quality.

The combination of these vibration sources resulted in vibration of the ceiling to which the surgery microscope was mounted. The measured vibrations at the ceiling are shown in Figure 2; results are displayed in velocity units. It is important to note that image quality is directly dependent on the displacement of the microscope, rather than the velocity. For the same velocity, displacement of a low-frequency vibration is higher than displacement of a high-frequency vibration. Therefore, the low-frequency vibrations have more effect on image quality.

The measurements showed significant vibrations in both horizontal and vertical directions. Horizontal vibrations were mostly seen at low frequencies, due to the building's resonance frequency at 2-4 Hz (horizontal movement of the building in Figure 1). Vertical vibrations were mostly seen at higher frequencies between 10 and 30 Hz, caused by the vibrations of air handling units, in combination with the resonance frequencies of the ceiling.

Not only the building vibrations, but also the vibrations of the microscope have been measured. It was found that the vibration amplitudes of the microscope were 3-5 times larger than those measured at the ceiling (Figure 3). To find the cause of this amplification effect, MECAL determined the natural vibration modes (mass and stiffness properties) of the microscope arm with modal analysis techniques (Figure 4). This measurement showed that the resonance frequencies of the microscope can be found in the

- 2 Fourth-floor ceiling vibration measurement.
- 3 Vibration amplification by the microscope arm.

frequency range 2-4 Hz and 10-30 Hz, coinciding with the resonance frequencies of the building. This explained the amplification of vibrations of the building in the microscope.

The resonance frequencies of any construction are determined by its mass and stiffness properties; the resonance frequencies increase with increasing stiffness and decrease with increasing mass. In case of the surgery microscope typically the joints, the pendulum-like shape and the dimensions of the microscope are optimised to enable easy manipulation and adjustment of its position during use. This limits the stiffness, resulting in low resonance frequencies. Furthermore, because of the shape of the microscope, the vibrations at the microscope tip are seen both in horizontal and vertical directions.

The measurements showed significant motion of the microscope tip, which was visible on the images produced by the microscope at high magnification. Based on this, the following two main requirement specifications were proposed:

- S1) Dominant microscope vibrations between 2-30 Hz must be decreased by at least a factor of 10, in both horizontal and vertical direction.
- S2) Microscope mobility and robustness may not be altered; the user should be able to use the microscope in the same way as they would the original microscope.

Concepts

Based on the requirements, a robust platform is needed that provides vibration isolation in six degrees of freedom, i.e. in horizontal and vertical displacements and all rotations. Various technologies were evaluated in order to determine the optimal design.

Passive vibration isolation

The first concept for vibration reduction that was evaluated is passive isolation, which means that no actuators, sensors or any active components are used. To minimise vibrations a heavy table mass m and a support spring with stiffness k are used, as in Figure 5.

The resonance frequency at which the table starts to reduce vibrations can be easily determined by Equation 1, where the isolation factor $U_{table} / U_{ceiling}$ is approximated by Equation 2:

$$f_{iso} = \frac{1}{2\pi} \sqrt{\frac{k}{m}} \tag{1}$$

$$Isolation \approx \frac{f_{iso}^2}{f_{iso}^2 - f^2} \tag{2}$$

In these equations, k and m denote the support stiffness and table mass, and f is the frequency in Hz. Note that damping is not taken into account to simplify the equation. From these equations, the following conclusions can be drawn:

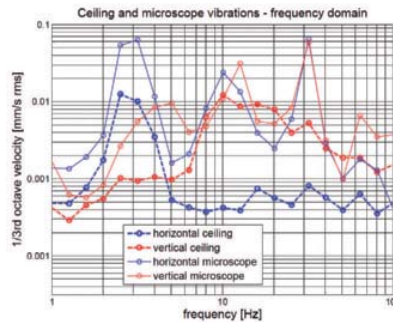
- In order to start isolating at low frequencies, a high-mass and low-stiffness design is necessary. However, these parameters are limited by the design:
 - The mass is limited due to available space and limitation in ceiling load.
 - The support stiffness is limited because of specification S2: when the support stiffness becomes too low, the table is sensitive to drift and ‘feels’ very unstable to the user.
- Equation 2 shows that isolating at least a factor of 10 is only possible at frequencies higher than three times the isolation frequency. Therefore, in practice, it is impossible to achieve 10x isolation of the microscope below 10 Hz with a passive system.

Typical passive vibration isolation systems start isolating at around 5 Hz. For this particular example, the system starts isolating at 7 Hz as is shown in the right side of Figure 5.

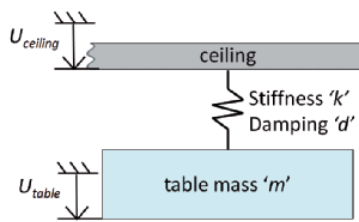
Overall, the passive vibration isolation solution is very effective to solve the higher-frequency problems, e.g. vibrations caused by air handling units. However, isolating the ceiling vibrations at frequencies of 2-4 Hz by a factor 10 is impossible with a passive vibration isolator alone.

Active vibration isolation

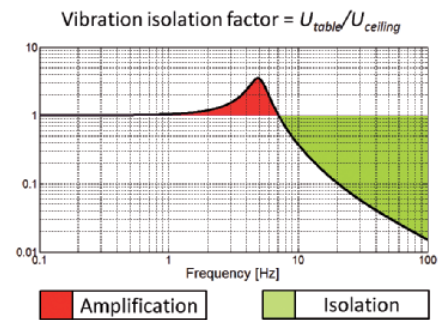
In active vibration isolation systems, sensors and actuators are used to measure and counter vibrations, often in combination with a passive isolation platform. The improvement with respect to the passive system is demonstrated in Figure 6.



4



5



The active system improves vibration isolation in the controller’s bandwidth, in this case between 0.5 and 30 Hz. Also, the passive part of this system can be designed with higher support stiffness, resulting in better performance of the microscope with respect to specification S2. Three major challenges exist when designing active vibration isolation in all directions:

- structural dynamics,
- sensor and electronic noise,
- tilt-to-horizontal coupling.

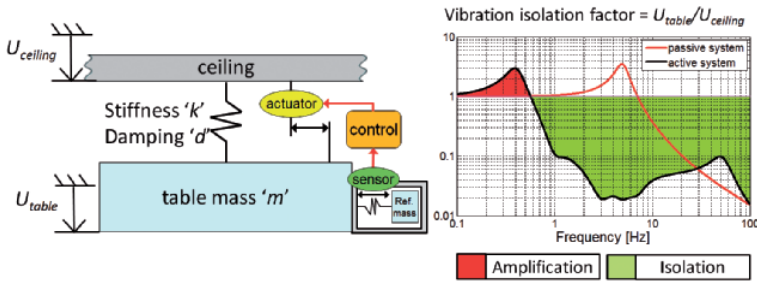
For a more detailed description of design properties of active vibration isolation systems, see [1].

Structural dynamics

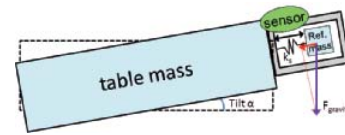
Structural dynamics concerns the natural frequencies and modeshapes of the entire system of ceiling, Hummingbird platform and microscope. Interaction exists between structural dynamics and the motion controller. This interaction can limit the controller’s bandwidth, and therefore reduce the frequency range in which the vibration isolator is effective.

In this case, structural dynamics has been evaluated by use of a Finite Element Model (FEM). This model is used in a virtual prototype with which the structural dynamics of the system is simulated in combination with the effects of the motion controller. These simulations include performance and stability calculations that predict whether the design will function according to the specifications. Typical trade-

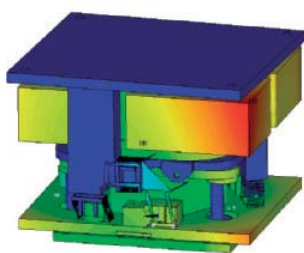
- 4 Frequency domain velocity results (left) and modal analysis measurement (right, sensors indicated with yellow dots).
- 5 Passive vibration isolation.



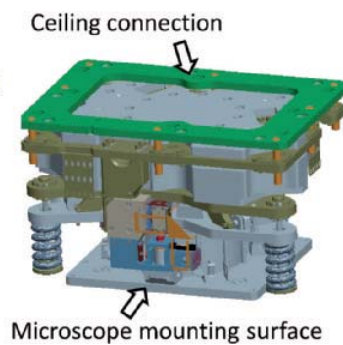
6



8



7a



7b

offs are seen for resonance frequency specifications, between mass, stiffness, and design dimensions.

An example of an FEM result is shown in Figure 7. On the left a calculated modeshape of an earlier version of the design is shown, with the various colours depicting the motion amplitude (blue = small, red = maximum). On the right, the optimised final design of the Hummingbird platform in CAD is shown.

Sensor and electronic noise

At low frequencies the velocity measured with a sensor (geophone) decreases to very low levels. Therefore, the sensor signal becomes very small and eventually the noise produced by the sensor and other electronic components becomes dominant. A low-noise sensor design in combination with low-noise high-accuracy electronics is required to achieve high vibration isolation performance in the Hz and sub-Hz frequency ranges.

Tilt-to-horizontal coupling

Inertia sensors, such as geophones, are suitable to measure motion at low frequencies. These sensors consist of a reference mass, suspended with a low-stiffness spring, which can move with respect to its housing. The reference mass is intended to move only in the direction in which motion is measured with that sensor.

A disadvantage of inertia sensors is the tilt-to-horizontal coupling problem, which limits the stability of the

- 6 Active vibration isolation.
- 7 The optimised final design of the Hummingbird platform.
 - (a) Example of a FEM-simulated modeshape.
 - (b) Final geometry in CAD.
- 8 Tilt-to-horizontal-coupling problem.
- 9 Hummingbird technology: solution for tilt-to-horizontal coupling.

controller at low frequencies, see Figure 8. This problem only occurs in active vibration isolation systems where not only vertical but also horizontal vibrations must be isolated. The gravity has a force component due to the tilt angle α , which presses against the sensor stiffness k_s . This results in movement of the reference mass in the horizontal motion sensor. Therefore, tilt will be misinterpreted as horizontal motion, causing cancellation errors of the controller. This effect becomes dominant at frequencies below the sensor resonance frequency and therefore limits the vibration isolation factor at low frequencies.

In cooperation with TNO, MECAL has successfully developed and patented a flexure mechanism to overcome this limitation, see Figure 9. The implementation of this mechanism in active vibration isolation is known as the Hummingbird technology, as described in [1].

The flexure mechanism prevents the horizontal sensor from tilting (Figure 9) and therefore eliminates the tilt-to-horizontal coupling problem. As a result, the Hummingbird platform provides isolation at much lower frequencies than other state-of-the-art active solutions and offers significantly better isolation performance in the 0.5-30 Hz range, which is critical for the microscope image quality.

Realisation

Figure 10a shows the Hummingbird active vibration isolation platform as realised for the surgery microscope at



azM. With its compact dimensions of 900 x 800 x 600 mm³ the Hummingbird platform was designed to fit in the available space between microscope interface and ceiling. Figure 10b shows the microscope mounted to the Hummingbird platform in the operation room. The microscope itself, including its interfaces, has not been adapted and functions as if it were mounted directly to the ceiling.

Results

After installation of the Hummingbird platform, all visible microscope image vibrations were eliminated, even for the highest microscope magnification factors. The vibrations of the microscope have been measured and compared to the original situation, see Figure 11. In Figure 11a the vibrations of the microscope tip are shown before and after installation of the Hummingbird platform. In Figure 11b the vibration levels as a function of frequency are depicted.

The main specifications have been met:

- S1) The improvement factor, highest peak to highest peak, ranges from 20 to 35 in both horizontal and vertical directions for the most dominant vibrations, exceeding the specification S1 of a factor of 10 improvement.
- S2) Due to the stiff support spring design, the microscope arm can be treated in the same way by the users as the original microscope. Also, due to the robustness of the Hummingbird platform, the microscope can be used in several positions without compromising image quality. Therefore, specification S2 is also met.

Conclusion

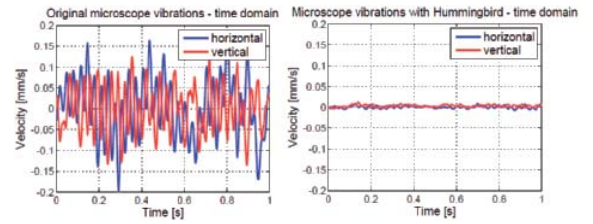
Building vibrations can cause image quality loss in today's high-sensitive microscope applications. At the azM academic hospital, the low resonance frequencies of the

building coincided with resonance frequencies of a microscope used for microsurgery. At high magnification factors of the microscope this resulted in unacceptable loss of image quality.

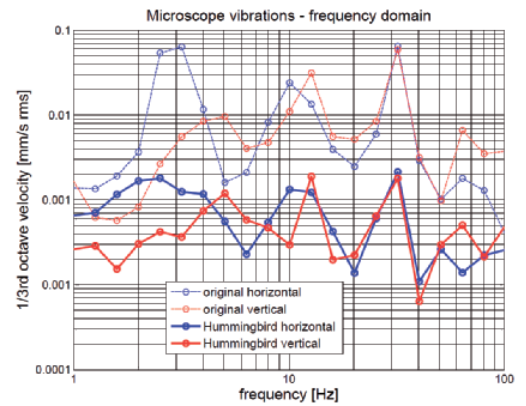
When disturbances at low frequencies are dominant, the conventional passive and active vibration isolation systems can no longer solve the problem. Based on Hummingbird technology, a robust six-degrees-of-freedom vibration isolation platform was implemented that counteracts vibrations at low frequencies better than any other state-of-the-art vibration isolation solution.

Both the horizontal and the vertical vibrations of the microscope are effectively isolated over the whole frequency range without deteriorating the microscope's user-friendly operation properties.

The Hummingbird platform is now used every day as a stable base for microsurgery operations to the full satisfaction of the surgeons at azM.



11a



11b

- 10 The Hummingbird active vibration isolation platform in the operation room at azM. (a) Mounted to the ceiling. (b) Microscope mounted on the platform.
- 11 Vibration isolation performance of the Hummingbird platform. (a) Time domain. (b) Frequency domain.

REFERENCES

[1] B. Bakker and J. van Seggelen, 2010, "The revolutionary Hummingbird technology", *Mikroniek* 50 (2), pp. 14-20.

INFORMATION

WWW.ACTIVE-VIBRATION-ISOLATION.COM

PROGRESS IN ENERGY TECHNOLOGIES, OPTICS AND MEASUREMENT

From 27 to 31 May 2013, the 13th International Conference of the European Society for Precision Engineering and Nanotechnology (euspen) was held in Berlin, Germany. Energy technologies (i.e. precision engineering advancements enabling progress in this field) and advanced optics technology were among the key topics covered. To illustrate the broad scope of euspen and its annual conference, the 2013 keynotes covered industrial measurement, micro-integrated diode laser systems and gas turbines.

AUTHOR'S NOTE

Raymond Knaapen works as a systems architect at TNO in Eindhoven, the Netherlands.

RAYMOND KNAAPEN

The 13th euspen conference (headline sponsor Heidenhain) was held in the Maritim Hotel in Berlin's city centre.

Some 370 people attended this year's conference and there were over 35 exhibitors at the commercial exhibition. A total of 160 papers were accepted for the conference, of which 38 were presented in oral presentations and the remainder in poster sessions. Technical workshops were also organised. After the final conference day, there were

company visits to Fraunhofer IPK, Helmholtz Zentrum Berlin and Siemens.

This year's conference topics included:

- Energy technologies (precision engineering advancements enabling progress in energy technologies)
- Nano- and micrometrology
- Ultra-precision machines and control
- High-precision mechatronics
- Ultra-precision manufacturing and assembly processes
- Important/innovative advances in precision engineering and nanotechnologies
- Advanced optics technology

The mix of research and industrial topics is one of euspen's strengths and was once again reflected in the participant population.

Tutorials

Preceding the conference itself, there was a one-day programme of morning tutorials and an afternoon workshop. The tutorial topics were "Advanced Mechatronic System Design" by Prof. Robert Munnig Schmidt (Delft University of Technology) and Adrian Rankers (Mechatronics Academy), and "Precision Flexures: Synthesis and Stiffness Design" by Jonathan Hopkins (Lawrence Livermore National Laboratory) and Nima



Tolou (Delft University of Technology). While the tutorials covered conceptual theories through best-practice applications, the workshop focused more on a review of technologies currently available in the market. The “Displacement Measurement Technology Products and Their Advancements” workshop was run by Denis Dontsov (SIOS), Lex Uittenbogaard (Agilent), Andreas Eberherr (Heidenhain) and Charlie Wallis (Renishaw).

Welcome to Berlin

On 28 May, the conference was opened by euspen President Prof. Paul Shore from Cranfield University. Euspen’s presidency was transferred to Dr. Wolfgang Knapp later during the conference. After the opening, Prof. Eckart Uhlmann (Fraunhofer IPK) welcomed the delegates to Berlin and also presented a brief history of science and technology in Berlin and introduced Technische Universität Berlin (TUB). One of the many universities in Berlin, TUB started as a school for mining in 1770, and after a number of mergers it was founded under its current name in 1946. Besides its universities, Berlin is also known for the companies that were founded in the city, like Siemens, AEG, Heidenhain and Fritz Werner. Berlin is home to



The welcome reception, sponsored by ASML, was in the Meistersaal at Potsdamer Platz.

many industrial sectors such as energy, aerospace, automotive, optics and microsystems.

Keynotes

Micro-integrated diode laser systems

The keynote “Micro-integrated diode laser systems: New applications in communication, sensing and production” was given by Prof. Günther Tränkle of Optec-Berlin-Brandenburg and Leibniz Ferdinand Braun Institute. Many optics companies in the Berlin area have joined the Optec-Berlin-Brandenburg initiative for joint development and application of optical technologies for such things as photonics, sensors, and communication.

An overview was given of micro-integrated diode laser systems, which can be used for communication, storage, display, space and materials analysis, etc., and in which different laser power levels (10 mW to 1 W) and semiconductor materials are used, such as InP, GaN, GaAs. Some space applications of quantum-optical sensors are light pulse atom interferometers and optical clocks.

Gas turbines

The keynote “Precision Engineering and Manufacturing in the Gas Turbine Industry” was given by Dr. Wolfgang Konrad of Siemens. Building complete power plants and manufacturing components for this industry accounts for 25% of Siemens’ turnover. By combining gas turbines with steam turbines, over 60% efficiency can be reached in power plants. Worldwide, Siemens has installed 1,200 gas turbines, the largest of which can produce 375 MW.

euspen

euspen, which was founded in 1999 with funding from the European Union, is a leading professional organisation in the field of ultra-precision/nanomanufacturing technologies. Linking leading industrialists and researchers worldwide, it has members in more than 32 countries. Euspen seeks to enable companies, research institutes and universities to more effectively develop and exploit leading-edge precision, micro- and nanotechnologies, to promote their products and services, and to keep up to date with important developments. Today, euspen is a self-sustaining non-profit organisation with private members as well as corporate memberships. euspen works together with the American and Japanese societies of precision engineering, ASPE and JSPE. They jointly publish the journal of Precision Engineering. euspen’s headquarters are located at Cranfield University in the UK. The organisation’s largest annual activity is the euspen conference. Past conferences were held in Bremen (1999), Copenhagen (2000), Eindhoven (2002), Glasgow (2004), Montpellier (2005), Baden (2006), Bremen (2007), Zürich (2008), San Sebastian (2009), Delft (2010), Lake Como (2011), Stockholm (2012) and Berlin (2013). The 14th euspen conference will be held in Dubrovnik, Croatia, from 2 to 6 June, 2014 and will focus on two key topics: renewable energy technologies and precision engineering for medical products.

WWW.EUSPEN.EU



One of the plenary sessions.

The move towards sustainable energy, in Germany often referred to as 'Energiewende', using such things as energy sources like wind, biomass, solar energy, and energy efficiency improvements, is a welcome change in the energy production industry. Some of the technical challenges that gas turbines face are high temperatures (over 1,500 °C), centrifugal forces 10,000 times the dead weight, mechanical parts moving at sonic speed and with high accuracy versus size, e.g. 50 to 100 µm over 5 m. To further improve efficiencies and reduce emissions, even higher temperatures are required.

Tomo-lithographic molding of blades is used to create freedom in gas turbine design. This molding technique uses a high-resolution master tool composed of lithographically micro-machined layers, precisely aligned and stack-laminated into a monolithic solid. By combining dissimilarly patterned layers or "toma", 3D cavities of otherwise unattainable sophistication and precision can be created.

Progress in industrial measurement

Nick Orchard from Rolls Royce presented "Industrial Measurement – A Reflection on Progress from 1960 to 2060". With the saying "If you can't measure it, you can't make it", he started off with a history of length standards, where copying or reproducing the standards was one of the major challenges. The relationship between length and time was first used by Michelson, who invented the interferometer.

Developments of measuring machines were also shown, such as the first coordinate measuring machine (CMM) by

Ferranti and the "Check-mate" CMM by Shelton. Tactile measurements were later extended or replaced by contactless measurement methods, using such things as lasers and even X-ray techniques.

Advanced optics technology

A few oral presentations will be highlighted. The first session, "Advanced Optics Technology", started with Prof. Alexei Erko of Helmholtz Zentrum Berlin giving a presentation about state-of-the-art X-ray optical systems and their manufacture. He showed the focusing of optical systems on the basis of glass capillaries, as well as optical systems based on diffraction gratings and reflection zone plates. The improvement of optical transport line efficiency was shown by reducing and improving optical elements. Blazed gratings were used, made with a ruling machine that can produce line densities of between 650 to 2,400 lines/mm. A new machine is being developed that can achieve densities of up to 5,000 lines/mm.

Prof. Qing Liang Zhao of the Harbin Institute of Technology talked about optical glass grinding with laser-structured coarse-grained diamond wheels. A smaller contact surface on grinding wheels is used to decrease machining forces. Laser machining is used to make grooves in grinding wheels for this purpose. The structured grinding wheels result in lower sub-surface damage.

Energy technologies

The next oral session was "Precision Engineering Advancements Enabling Progress in Energy Technologies". Christopher Sansom of Cranfield University discussed precision engineering for concentrating solar power, using line collimation to harvest thermal energy. Volker Herold of Friedrich-Schiller-Universität Jena presented an unconventional experimental set-up for testing the cutting performance and wear resistance of diamond cutting wires.

Nano- and micrometrology

The second conference day started with oral presentations on nano- and micrometrology. Prof. Liam Blunt of the University of Huddersfield gave a presentation about the in-line metrology of functional surfaces with a focus on defect assessment on large-area roll-to-roll substrates. This activity is part of the European NanoMend project and is about detecting and correcting micro- and nano-scale defects.

Gianluca Tristo of the University of Padua discussed the validation of on-machine microfeature volume measurement using a micro-EDM milling tool electrode as a touch probe. The ability of EDM tools to detect electrical contact between the electrodes is used to perform

dimensional measurements, using the tool electrode in a similar way to the touch probe in a CMM.

Alain Küng of METAS gave a presentation about a virtual CMM method applied to aspherical lens parameter calibration. A parametric fitting algorithm coupled with a virtual μ -CMM based on a realistic model of the machine was developed to perform simulations and provide the asphere parameter uncertainties.

Ultra-precision machines and control

Carsten Oberländer of Helmut Schmidt University demonstrated a concept for a miniaturised machine-tool module for manufacturing micro-components operated at its resonance frequency. In the context of 'square foot machining', a machine resonance frequency is used as feed motion as an alternative to ultrasonic machining.

Anindito Santoso of K.U.Leuven University showed a fast nanometer-positioning system that combines a fast resonant mode and an accurate piezostack direct drive. The advantages of small-stroke flexures, unlimited-stroke stick-

slip drives and ultrasonic piezomotors are combined in a hybrid concept. Elliptical piezo motion is used for long strokes, while linear motion is used for high accuracy. Both modes can be operated simultaneously.

Tat Joo Teo of the Singapore Institute of Manufacturing Technology discussed a geometrical-based approach for flexure mechanism design. Kinematic-based design for high natural stiffness versus low stiffness in motion direction requires human intuition. Optimised design based on required tasks and space constraints is done using topology optimisation. Conventional topology optimisation provides no guaranteed convergence. Therefore, a mechanism-based seeding approach using Grübler's criterion is used.

High-precision mechatronics

The "High Precision Mechatronics" session had a strong Dutch contribution. Jack van der Sanden of Philips Innovation Services talked about FEM model-based POD reduction for obtaining optimal sensor locations for thermo-elastic error compensation. Known heat loads on a construction line are used in an FEM model to obtain time-dependent temperature data. A proper orthogonal decomposition (POD) is used to determine temperature shapes, of which the dominant ones are selected. Sensor locations are then determined that can identify the most dominant temperature shapes. Because of the high computational load, an FEM model reduction is applied using the Arnoldi method to make POD practically possible.

Ruijun Deng of Delft University of Technology presented a 2-DoF magnetic actuator for a 6-DoF stage with long-stroke gravity compensation. A stage was developed for nano-imprint lithography using three times a 2-DoF actuator to obtain a total of six degrees of freedom (DoFs). Lorentz forces and reluctance forces were combined to obtain a combination of long-stroke motion with gravity compensation in one direction, and short stroke motion in a perpendicular direction. Constant-force optimisation was done to minimise actuator stiffness.

Johan Kruis of the Centre Suisse d'Electronique et de Microtechnique (CSEM) discussed the design and manufacture of a novel centimeter-scale three-dimensional silicon 'tip, tilt and piston mirror mechanism' (TTPmm), comprising delicate flexure mechanisms. For 'macro-MEMS', the advantages of silicon are used, e.g. the absence of fatigue, machining accuracy, the possible integration of sensors and actuators, and batch production on wafers. Because silicon processing is mostly planar (2D or 2.5D), assembly of different parts is required for silicon 'beyond 2.5D'.

euspen Challenge

During the conference, the results of the euspen Challenge 2012 were presented. Teams of students had been selected for the challenge which was held at ASML in Veldhoven, the Netherlands. The assignment was to develop a device to help people with one leg walk around the house. The goal of the euspen Challenge, which was initiated by former euspen President Prof. Ekkard Brinksmeier, is to identify outstanding students across Europe with the potential to be future leaders in the field of precision engineering and nanotechnology. Meanwhile, the euspen Challenge 2013 was held at the Technical University of Denmark in early July.



The winning entry of the euspen Challenge 2012 (a device to help people with one leg walk around the house) was demonstrated as a design prototype by Piet van Rens of Settels Savenije van Amelsvoort.



Ultra-precision manufacturing and assembly processes

Thomas Arnold of the Leibniz-Institut für Oberflächenmodifizierung presented plasma jet polishing of rough fused silica surfaces. Atmospheric plasma jet machining is used based on a microwave-powered atmospheric plasma jet source operating in CW mode and working with a noble gas mixture of He and Ar. The plasma tool FWHM is about 1.5 mm. Due to the highly localised working area, this process is applicable to plane, spherical, aspheric and micro-structured substrates.

Prof. Hirofumi Suzuki of Chubu University presented a study on the ultra-precision cutting of ceramics by a micro-milling tool of a single-crystalline diamond. Gustav Reichenbach of the University of Kaiserslautern discussed direct machining of microstructures in polymethylmethacrylate (PMMA) with single-edge micro-end mills with a diameter of 20 µm. Due to the increase of product variety in microfluidic devices and the demand for reductions in time-to-market, the fast manufacturing of microstructures at a prototype level is desired. This has become possible through direct micro-milling, providing a highly flexible manufacturing process with a high material removal rate. Micro-ball end mills of 20 µm diameter developed in-house were used.

Umang Maradia of ETH Zürich talked about EDM process analysis using high-speed imaging. To gain insight into the

Impression of the exhibition where euspen participants could visit company booths.

Electrical Discharge Machining process, high-speed imaging of up to 500,000 frames per second of the process is combined with electrical process signals. The correlation of visual and electrical information enables improvements in process control.

Important/innovative advances in precision engineering and nanotechnologies

Tim Götttsching of Leibniz University Hannover talked about the influence of micro-patterned grinding wheels on workpiece quality. In grinding processes, thermal load can be minimised when grinding with a reduced contact area between the grinding wheel and the workpiece. An experimental set-up and machining strategy for manufacturing micro-patterned grinding wheels were presented.

Peter Ekberg of Micronic Mydata discussed Z adjustment, a method for achieving an ultra-high absolute pattern placement accuracy of large-area photomasks. Photomasks used in the production of LCD, OLED and other kinds of displays can go up to 1.62 x 1.78 m² in size and 16 mm in thickness. The absolute placement accuracy of a pixel or line in the mask pattern needs to be better than 150 nm (3σ). Unflatness at the substrate backside or stage can easily generate geometrical errors in the X,Y plane. Z adjustment is used to correct this problem. ■

New euspen president

The newly appointed euspen president, Dr. Wolfgang Knapp of ETH Zürich, talked about precision engineering as an enabling technology for large science projects, high-tech systems, surface metrology and engineered surfaces (e.g. for energy savings, reduced wear, efficiency improvements of turbines and other equipment, and medical compatibility of parts in the human body), and new energy sources. Dr. Knapp felt that although the precision engineering community is aware of this potential, more awareness is needed among politicians, the public and especially the young. Finding young talent is difficult because of competition with other fields.



On the evening of the second conference day, a conference networking dinner was organised with a boat tour on the river Spree. During the tour, newly appointed euspen president Dr. Wolfgang Knapp took the microphone to express a number of things including his gratitude to his predecessor, Prof. Paul Shore, sitting in the front row on the right.



Miniature Encoders

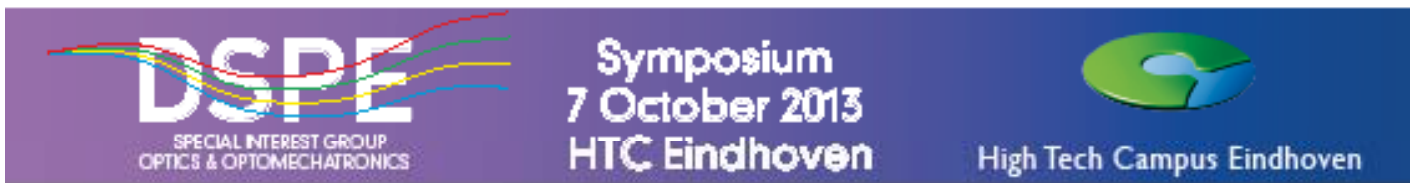
- Encoders – 2 Channel
- Encoders – 3 Channel

FAULHABER

WE CREATE MOTION

MINIMOTOR Benelux - www.faulhaber.com

FIRST DSPE SYMPOSIUM ON OPTICS & OPTOMECHATRONICS



On 7 October 2013, the first DSPE symposium on Optics & Optomechatronics will be held at the High Tech Campus Eindhoven conference centre, the Netherlands. This symposium is being organised by the newly established DSPE Special Interest Group Optics & Optomechatronics and it aims to bring together optical and optomechatronic experts so that they can learn from each other and increase the economic potential of this area of expertise.

The symposium is aimed at professionals researching, developing, engineering, producing and maintaining optics and/or optomechatronic parts, modules, products and systems. The programme will include excellent keynote speakers, business presentations and a preview of Chris Velzel's book "A Course in Lens Design". The symposium will also provide opportunities for networking, technical discussion, and sharing one's enthusiasm of working in this challenging field.

Speakers include (tentative):

- Wilhelm Ulrich, Senior Director Optical Design, Carl Zeiss: "Freeform Optics".
- Wolfgang Vollrath, Chief Scientist, KLA-Tencor MIE: "Optical design and manufacturing requirements for high-performance microscope objectives".
- Stefan Sinzinger, Head of Technical Optics, TU Illmenau: "Freeform surfaces in optical microsystems – from design to applications".

- Arie den Boef, Fellow, ASML: "Optical Metrology of Semiconductor Wafers in Lithography".
- Bert van der Pasch, Fellow, ASML: "System stability in a lithography wafer scanner".
- Jan Nijenhuis, Senior System Engineer, TNO.

- Paul Urbach, President of EOS & Head Optics Research Group, Delft University of Technology.
- Chairman of the day: Jan-Willem Martens, Vice President System Engineering, ASML. ■

WWW.DSPE.NL WWW.HIGHTECHCAMPUS.COM



■ The evening programme will include a dinner with a special treat, a visit to the Dr. A.F. Philips Observatory (sterrenwacht.dse.nl). There, participants will be invited to peer through the Newtonian telescope. Its concave parabolic primary mirror is 40 centimeters in diameter. The telescope is focused manually, with a special motor helping to keep the viewer focused on the object. The viewer magnifies up to 400 times and can detect distant objects down to magnitude 14.

RECOMMENDED: OPTO-MECHATRONICS SUMMER SCHOOL

The 2013 edition of the annual DSPE Opto-Mechatronics summer school, organised in cooperation with Mechatronics Academy and The High Tech Institute and held at the TNO offices in Eindhoven, the Netherlands, from 24 to 28 June, was again very successful. But how do you measure that success?

First of all, by reading the participants' feedback ("Very informative, practical", "Useful and enjoyable") and especially by looking at the scores on 'The Ultimate Question' (see Frederick F. Reichheld's book): "Would you recommend this training?". It's no coincidence that this year's participant from the Technical University of Denmark (DTU) happened to be a close friend of last year's participant from DTU (now, that's what you call 'word of mouth').

The fact that the summer school attracted almost 50% more participants than the previous two editions is also a good indicator. There were five different nationalities represented, twelve different companies (including Philips, ASML, Segula Technologies and Physik Instrumente) located in three European countries, and a range of positions (e.g. an optical engineer, a Ph.D. student, a design engineer, a junior architect, a chief researcher).

One final indicator of the success of the summer school was the great atmosphere at the event, especially during the summer school challenge. The challenge, by the way, was won by a team consisting of three nationalities and remarkably, just like last year, DTU took home one of the trophies.

The next edition is planned for 16-20 June 2014. ■

WWW.SUMMER-SCHOOL.NL



■ This year's Opto-Mechatronics summer school was again attended by a diverse group of participants.

We've Got It Together

A reliable source for plug and play motion systems, sub-assemblies and components

In-house design and manufacture, products can be readily modified to suit individual applications

Reliance
Precision Mechatronics

www.rpmechatronics.co.uk
sales@rpmechatronics.co.uk
NL +31 (0) 76 50 40 79 0
Tel +44 (0) 1484 601060

CPE COURSE CALENDAR

COURSE	CPE points	Provider	Starting date (location, if not Eindhoven)
--------	------------	----------	---

BASIC

Mechatronic System Design (parts 1 + 2)	10	HTI	30 September 2013 (part 1) 11 November 2013 (part 2)
Construction Principles	3	MC	29 October 2013 (Utrecht) 19 November 2013
System Architecting	5	HTI	4 November 2013
Design Principles Basic	5	HTI	25 September 2013
Motion Control Tuning	6	HTI	20 November 2013

DEEPENING

Metrology and Calibration of Mechatronic Systems	2	HTI	18 November 2013
Actuation and Power Electronics	3	HTI	23 September 2013
Thermal Effects in Mechatronic Systems	2	HTI	7 November 2013
Summer school Opto-Mechatronics	5	DSPE + HTI	16 June 2014
Dynamics and Modelling	3	HTI	25 November 2013

Specific

Applied Optics	6.5	MC	12 September 2013
	6.5	HTI	29 October 2013
Machine Vision for Mechatronic Systems	2	HTI	26 September 2013
Electronics for Non-Electronic Engineers	10	HTI	3 September 2013
Modern Optics for Optical Designers	10	HTI	13 September 2013
Tribology	4	MC	30 October 2013 (Utrecht) 27 November 2013
Introduction in Ultra High and Ultra Clean Vacuum	4	HTI	28 October 2013
Experimental Techniques in Mechatronics	3	HTI	15 April 2014
Design for Ultra High and Ultra Clean Vacuum	4	HTI	25 November 2013
Advanced Motion Control	5	HTI	7 October 2013
Iterative Learning Control	2	HTI	4 November 2013
Advanced Mechatronic System Design	6	HTI	5 February 2014

DSPE Certification Program

Precision engineers with a Bachelor's or Master's degree and with 2-10 years of work experience can earn certification points by following selected courses. Once participants have earned a total of 45 points (one point per course day) within a period of five years, they will be certified. The CPE certificate (Certified Precision Engineer) is an industrial standard for professional recognition and acknowledgement of precision engineering-related knowledge and skills. The certificate holder's details will be entered into the international Register of Certified Precision Engineers.

WWW.DSPEREGISTRATION.NL/LIST-OF-CERTIFIED-COURSES

Course providers

- The High Tech Institute (HTI)
WWW.HIGHTECHINSTITUTE.NL
- Mikrocentrum (MC)
WWW.MIKROCENTRUM.NL
- Dutch Society for Precision Engineering (DSPE)
WWW.DSPE.NL

THEME: ROBOTICS

This summer, from 26 to 30 June, the RoboCup 2013 event was held in Eindhoven, the Netherlands. Once again, the event proved that interest in non-industrial applications of robots is increasing steadily and presents new challenges for robot designers and engineers. The forthcoming issue of Mikroniek, due to be published on 12 October 2013, will be partly dedicated to robotics, both industrial and non-industrial.



The winning, Chinese goal in the Middle Size League final between Tech United Eindhoven (Eindhoven University of Technology) and Team Water (Beijing Information Science & Technology University; see the inset).

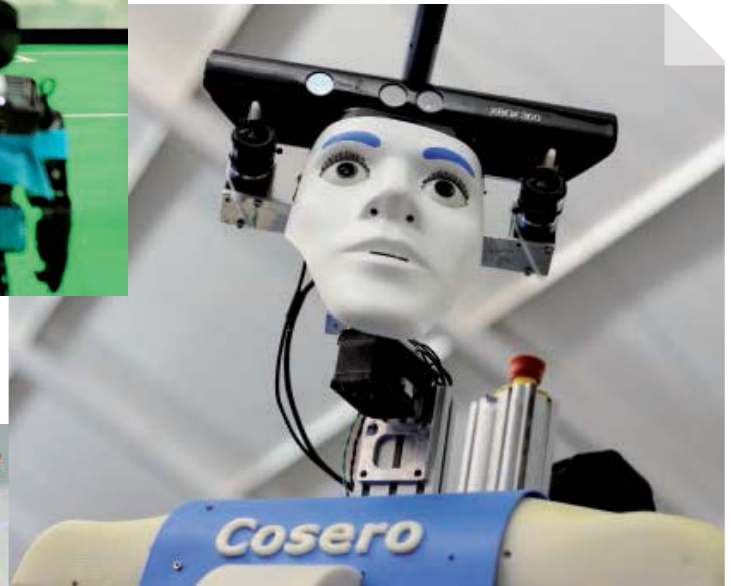
With some 2,500 participants, the international RoboCup event featured the robot soccer world championship (in various leagues, including the prestigious Middle Size League and the Humanoid League), the RoboCup Rescue and RoboCup@Home challenges and other robot-related competitions. The impressions of the event are courtesy of Bart van Overbeeke/RoboCup 2013. ■

INFORMATION

WWW.ROBOCUP2013.ORG



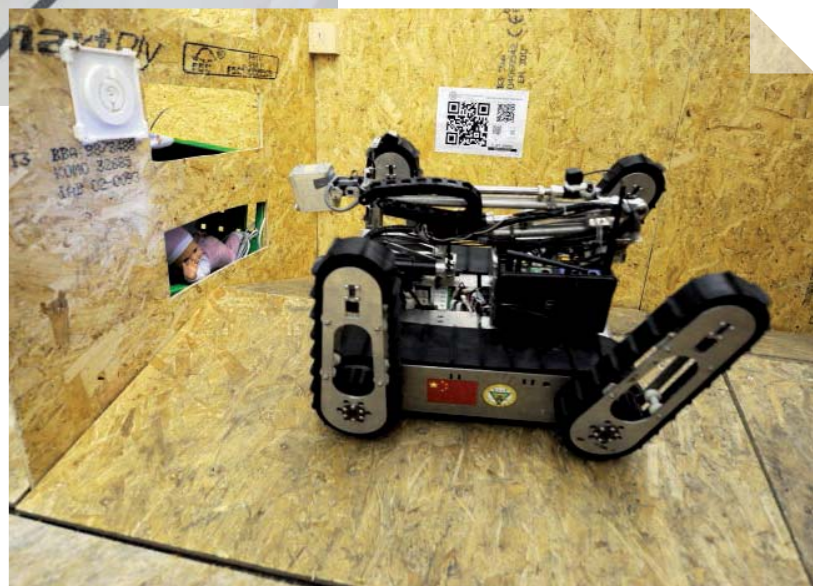
A match in the Humanoid KidSize League.



Care robot Cosero from Nimbro / University of Bonn.



Programmable robots for fast and accurate in-factory deliveries at the Festo Logistics League.



A rescue robot searching for babies.

NEWS

Promising single-piece and small-series production technologies

One of the trends outlined in the Dutch HTSM roadmap Mechatronics & Manufacturing (HTSM stands for the economic top sector High Tech Systems & Materials) is that of high-tech industrial components becoming smaller and more complex in their design, with production numbers steadily decreasing. This was the subject of a knowledge transfer meeting at the end of June in Nieuwegein, the Netherlands, organised by branch organisations Koninklijke Metaalunie and FDP and the innovation network Syntens (which is involved

with MKB-loket HTSM, the HTSM SME office). The meeting featured eight technologies for manufacturing single pieces and small series of products: friction welding, etching, metal casting based on 3D printing, electrochemical machining, metal injection moulding, electromagnetic pulse forming, additive manufacturing using metals, and electroforming. More information on these eight production technologies can be found in a booklet that was presented during the meeting. It provides a description of each

technology, constructional aspects, product dimensions, tolerances, surface roughness, smallest details, materials, production speed, prices, available suppliers, and promising fields of application.

The booklet was written by Syntens advisor Jo van der Put and published by MKB-loket HTSM (mkbloket@htsm.nl). Copies can also be obtained through Syntens (christa.gruijters@syntens.nl).

WWW.HOLLANDHIGHTECH.NL WWW.SYNTENS.NL

Electrical Discharge Machining seminar

On 1 October 2013, EDM market leader Ter Hoek Vonkerosie, based in Rijssen, the Netherlands, will be holding a seminar on the potential of Electrical Discharge Machining (EDM). Presentations will be given by IMS, Ceratizit, Ter Hoek Vonkerosie, AgieCharmilles and Mitutoyo, with the case of a micro cutting die serving as a common theme.

The presentations will cover:

- engineering a foil cutting die (5 x 8 mm, tolerances below 1 micron) for a specific end product;
- the choice of material for the die and EDM impact on the material;
- EDM process parameters for achieving constant quality;
- practical aspects of EDM production and

tolerances; and

- external influences on geometrical accuracy, and measurement techniques available.

As chairman of the day, Prof. Bert Lauwers of K.U.Leuven University (Belgium) hopes to ignite discussions on high-tech manufacturing. There will be ample networking opportunities during the day, along with a tour of Ter Hoek's production facilities, including the newly acquired Form 400, GF AgieCharmilles' largest die sinker EDM machine, and the WireDress extension to the Sarix micro-EDM machine, which was fitted with an ultrafine pulse shape generator as well.

WWW.TERHOEKVONKEROSIE.NL



■ The foil cutting die that serves as the common theme at the seminar.

Kennis verbreden en verdiepen www.pao.tudelft.nl

Lijmen als verbindingstechniek
9, 10 en 11 oktober 2013

Lichtgewicht Construeren voor Ontwerpers
4 dagen in het voorjaar 2014

Breukmechanica
op aanvraag

Diverse cursussen op het gebied van mechatronics
najaar 2013

Postbus 5048 015 278 83 50
2600 GA Delft info@paotechniek.nl
Kijk voor alle cursussen op www.pao.tudelft.nl

PAO Techniek
Techniek op maat

Attocube presents piezo-based industrial positioning drives

Focusing on the needs of today's nanotechnology industry for highly precise, reliable, and equally cost-effective positioning systems, attocube systems have established the ECS "Industrial Line". The piezo-based nanopositioning motors satisfy highest expectations in terms of precision and stability, according to a press release.

The compact drive units realise accurate positioning tasks, e.g. in precision machining, and are further successfully utilised for the nanoprecise alignment of optical and mechanical components. The "Industrial Line" product range consists of a variety of piezo-based linear, rotational, and goniometric positioning units. All products can simply be mounted on top of each other in order to achieve multi-degree-of-freedom motion devices offering up to six movement axes.

All positioning units can optionally be equipped with an opto-numeric position encoder, with a position resolution of 1 nm for linear and 10/1 µdeg for rotational/goniometric positioners, respectively. A compact three-axes drive electronics allows the user to operate the positioning units in both open- and closed-loop mode. The "Industrial Line" stages offer a repeatability of 50 nm for travel ranges of up to 50 mm (the positioner design can be customised for significantly larger travel ranges).

Integrated cross-roller bearings guarantee maximum load capacity – up to 20 kg depending on type and size. Angular travel errors are reduced to only 0.1 mrad (pitch, yaw, and roll). All positioners are manufactured from aluminum and dedicated for the operation at ambient conditions. For use in high-vacuum and UHV conditions all models can be modified in stainless-steel versions including corresponding cables, connectors and feedthroughs.

WWW.ATTOCUBE.COM



■ The attocube ECS series of piezo-based nanopositioning devices for industrial applications. From left to right a goniometer, a motion device with three degrees of freedom, and a rotator.

Printing technical ceramics

In December 2012, Formatec Ceramics, based in Goirle, the Netherlands, introduced ceramic printing technology. To continue the developments at the right pace, technology partners ECN and Innotech Europe joined the ADMATEC project, which seeks to develop a wide range of printing solutions for ceramics. Material, machine and process developments are all done within the group. The objective is to become the market leader for printing ceramic materials. To that end, the group decided to invest in a Cerafab 7500 3D printer from Lithoz. Adding Lithoz's LCM technology (i.e. lithography-based ceramic manufacturing) to the project underlines the group's ambition.

The main focus of the in-house development of the so-called ADMAFLEX® technology is to break down limitations on precision (currently 40 µm resolution), building size (80 x 80 x 150 mm³ platform) and building speed (> 10 mm/h). Secondly, materials research is a critical development factor. Reducing costs and widening the range of materials are clear objectives. These material developments will not be limited to ceramics; in the middle to long term, a pre-defined range of metals will be developed; and the process is suitable for all powder materials as well.

WWW.FORMATEC.NL

Dutch-Finnish Photonics 3D Printing partnership

The Institute of Photonics at the University of Eastern Finland (UEF) has launched a cooperation with Dutch company LUXeXcel, headquartered in Goes. Last year, UEF Professor Jyrki Saarinen discovered LUXeXcel, the Dutch inventor of the Printoptical Technology. LUXeXcel created a unique digital 3D printing method with the ability to print optical-quality components, such as lenses. With the known 3D printing processes, all parts need to be post-processed (grinding, polishing or painting). In contrast to conventional 3D printing, LUXeXcel's digital Printoptical manufacturing process is able to print smooth surfaces (without post-processing), can print lenses from a CAD file and is able to combine those optics with full-colour textures.

Both digital printing process and software will become important tools to drive the customisation and on-demand offering aspects of optics and photonics. "In my previous business life in the optics industry, there were so many product ideas but the tooling requested huge upfront investments, inventories and long inflexible R&D cycles. That kept us away from a lot of new product research. And small-volume productions usually had to be made by hand and were very expensive. Now I foresee that this 3D printing will become an important manufacturing method starting for small batches, single items and complex designed structures. It is a revolution as regards component availability, development and

manufacturing speed, and the concept of customisation", describes Prof. Saarinen.

The first phase of the project spans 18 months and the majority of funding comes from the EU through Tekes, the Finnish Funding Agency for Technology and Innovation. In addition to LUXeXcel and UEF, the project funders and partners include the (Finnish) companies Nanocomp, Oplatek Group, Thermo Fisher Scientific, Millog, Idman Airfield Lighting, and Nanobakers. An improved printing platform for 3D printing photonics is expected to be ready at the end of this year.

WWW.LUXEXCEL.COM WWW.UEF.FI

StartupBootcamp High Tech XL welcomes applications

High Tech Campus Eindhoven will host a unique programme, StartupBootcamp High Tech XL, designed to attract and accelerate promising high-tech start-ups from all over the world. The ten best high-tech teams for the 2013 programme will be selected in Eindhoven, the Netherlands, at the selection finals on 14 October 2013. Applications are still welcomed; on-line application closes on 8 September.

This mentorship-driven model is facilitated by providing start-ups with the essential tools needed to have a concrete focus during the three-month programme, including €15,000 towards living expenses for the team during the programme, six months co-working space, over €150,000 in sponsored services, and the platform to pitch to over 400 investors at Investor Demo Day.

StartupBootcamp is now running in Berlin, Amsterdam, Dublin, Copenhagen, Haifa, London, and Eindhoven, covering areas such as NFC & Contactless, Mobility, Health, and High Tech. In Eindhoven, StartupBootcamp High Tech XL focuses on Internet of Things, Advanced Materials, (Near) Autonomous Vehicles, Energy Storage, 3D Printing, Renewable Energy, Advanced Robotics, and Lifetech – Medtech.

WWW.STARTUPBOOTCAMP.ORG WWW.HIGHTECHXL.COM

StartupBootcamp is a mentorship-driven programme; mentors drive the start-up acceleration over the three-month program – and often for months or years afterwards.

The StartupBootcamp founders team, together with their group of international mentors, can open the door to nearly every investor, customer or partner. The value is the quality of that network. Mentors work closely with the start-ups to develop their product, validate their business model, get their first pilot customers and aim to get funding at the end of the programme.



■ High Tech Campus Eindhoven will host StartupBootcamp High Tech XL. (Photo courtesy of Marjolein Vugts)

Opening of ITRI High Tech Campus Eindhoven office

On 28 June 2013, the High Tech Campus Eindhoven office of the Taiwanese Industrial Technology Research Institute (ITRI) was officially opened. The mission of this office is to assist ITRI's research labs/centers to develop and maintain the research network and partnership with Dutch partners, as well as to initiate cross-disciplinary programmes. With the office serving as a conduit, ITRI can carry out complementary, innovative, collaborative research with Dutch supply chains, thus leading Taiwan's domestic industries to global markets. The office will initially target on Hightech Systems & Materials, Life Sciences & Health, and Green Energy.

At the same event, the Penrose Shared Research Programme kicked off with a signing ceremony.

Penrose joins Dutch applied research organisation TNO and ITRI, dedicated to the advancement of next generation additive manufacturing for high-tech, high-precision, high-complexity parts and products. More on Penrose in a forthcoming issue of Mikroniek.

Finally, the Taiwan-Netherlands Industry Innovation Collaboration Seminar was held, covering the latest developments and challenges in additive manufacturing and mechatronics. The keynote speech, delivered by Dr. Jon Hsu, the Executive Director of ITRI South Campus (HsinChu, Taiwan), introduced ITRI's latest development of Powder Bed Fusion technology in additive manufacturing and MEMS technology.

Industrial Technology Research Institute (ITRI) is one of the world's leading technology R&D institutions aiming to innovate a better future for society. Since 1973, ITRI has accumulated over 17,000 patents, cultivated more than 70 CEOs, and incubated 225 innovative companies, including global semiconductor leaders such as TSMC and UMC. In addition to its headquarters in Taiwan, ITRI has branch offices in Silicon Valley, Tokyo, Berlin, Moscow, and Eindhoven, in an effort to extend its R&D scope and promote opportunities for international cooperation around the world.

WWW.ITRI.ORG.TW/ENG

Facilitating additive manufacturing

Additive manufacturing and 3D printing are set to revolutionise multiple areas of technology and manufacturing, according to an Aerotech press release. The dispensing of compounds and coatings requires a 3D motion system to move either the printing head or the substrate with up to six degrees of freedom. Overall system accuracy and throughput are vitally important to creating complex structures with a commercially viable process.

Aerotech offers a full range of additive manufacturing motion systems and components to fit any application, and can engineer and build custom systems. Components include linear, rotary, lift and Z-axis stages, goniometers, motion controls, drives and motors.

Custom systems include multi-axis, gantry, air-bearing, cleanroom and vacuum-prepped. Minimum step sizes down to 1 nm are feasible, with in-position stabilities < 1 nm, and accuracies as good as 250 nm, while systems show a high dynamic performance.

WWW.AEROTECH.COM/INDUSTRIES-AND-APPLICATIONS/ADDITIVE-MANUFACTURING.ASPX



The advertisement banner for Ceramatec features a collage of images at the top showing various ceramic parts and manufacturing equipment. Below the images, the text reads "Ceramic on the right spot". The Ceramatec logo, which includes the text "ceramatec®" and "Technical Ceramics BV", is prominently displayed in the center. To the left of the logo, contact information is provided: "Poppenbouwing 35, 4191 NZ Geldermalsen, T: +31(0)345 - 58 01 01, F: +31(0)345 - 57 72 15". To the right, the website "WWW.CERATEC.NL" is listed, along with email "E: ceratec@ceratec.nl" and a website link "I: www.webshop.ceratec.nl".

Bearing and Linear Technology



Schaeffler Nederland B.V.

Schaeffler Nederland B.V.
Gildeweg 31
3771 NB Barneveld
T +31 (0)342 - 40 30 00
F +31 (0)342 - 40 32 80
E info.nl@schaeffler.com
W www.schaeffler.nl

Schaeffler Group - LuK, INA and FAG - is a world wide leading company in developing, manufacturing and supplying of rolling bearings, linear systems, direct drives and maintenance products. Applications: automotive, industrial and aerospace.

Development



TNO
T +31 (0)88-866 50 00
W www.tno.nl

TNO is an independent innovation organisation that connects people and knowledge in order to create the innovations that sustainably boost the competitiveness of industry and wellbeing of society.

member **DSPE**

Development and Engineering



ACE ingenieurs- & adviesbureau
werktuigbouwkunde en elektrotechniek BV
Dr. Holtropaan 46
Postbus 7030, 5605 JA Eindhoven
5652 XR Eindhoven
T +31 (0)40 - 2578300
F +31 (0)40 - 2578397
E info@ace.eu
W www.ace.eu

ACE has developed into a leading engineering and consultancy firm with a strong focus on mechanics and mechatronics. Services include conceptualization, development, engineering and prototyping.

member **DSPE**

Education



Leiden school for Instrument-makers (LiS)
Einsteinweg 61
2333 CC Leiden
The Netherlands
T +31 (0)71-5581168
F +31 (0)71-5681160
E info@lis-mbo.nl
W www.lis-mbo.nl

The LiS is founded in 1901 by the famous scientist prof. Kamerlingh Onnes. Nowadays the LiS is a modern school for vocational training on level 4 MBO-BOL. The school encourages establishing projects in close cooperation with contractors and scientific institutes, allowing for high level "real life" work.

member **DSPE**

Education



PAO Techniek
Stevinweg 1, 2628 CN Delft
Postbus 5048, 2600 GA Delft
T +31 (0)15 27 88 350
F +31 (0)15 27 84 619
E info@paotechniek.nl
W www.cursus.paotechniek.nl

Lasers and Light



Laser 2000 Benelux C.V.
Voorbancken 13a
3645 GV Vinkeveen
Postbus 20, 3645 ZJ Vinkeveen
T +31(0)297 266 191
F +31(0)297 266 134
E info@laser2000.nl
W www.laser2000.nl

Laser 2000 Benelux considers it her mission to offer customers the latest available photonics technologies.

Our areas of expertise:

- Lasers and laser systems for industry and research
- Light metrology instruments for LED and luminaire industry
- Piezo- and stepper motion products for nano- and micro-positioning
- LED illumination and high speed inspection in machine vision

Laser Systems



Applied Laser Technology
De Dintel 2
5684 PS Best
T +31 (0)499 375375
F +31 (0)499 375373
E techsupport@alt.nl
W www.alt.nl

member **DSPE**

3D Measurement Services



Mitutoyo Nederland B.V.
Storkstraat 40
3905 KX Veenendaal
T +31 (0)318-534911
F +31 (0)318-534811
E info@mitutoyo.nl
W www.mitutoyo.nl

Mechatronics Development



CCM Centre for Concepts in Mechatronics
De Pinckart 24
5674 CC Nuenen
T +31 (0)40 2635000
F +31 (0)40 2635555
E info@ccm.nl
W www.ccm.nl

CCM translates technology into technique. Commitment, motivation, education and skills of our employees are the solid basis for our business approach.

member **DSPE**



Janssen Precision Engineering
Azielaan 12
6199AG Maastricht-Airport
T +31 43 3585777
F +31 43 3580036
E huub.janssen@jpe.nl
W www.jpe.nl

Precision engineering and mechatronic solutions in ambient, vacuum and cryogenic environment

member **DSPE**

Metal Precision Parts



Etchform BV
Arendstraat 51
1223 RE Hilversum
T +31 (0)35 685 51 94
F info@etchform.com
W www.etchform.com

Etchform is a production and service company for etched and electroformed metal precision parts.

member **DSPE**

Micro Drive Systems

maxon motor
driven by precision

Maxon Motor Benelux

The Netherlands

Head Office
maxon motor benelux bv
De Giem 22
7547 SV Enschede

South
High Tech Campus 9
5656 AE Eindhoven
T +31 (0)53 486 47 77
F +31 (0)53 486 47 88
E info@maxonmotor.nl
W www.maxonmotor.nl

Belgium / Luxembourg
maxon motor benelux bv
Schaliënhoevedreef 20C
2800 Mechelen - Belgium
T +32 (15) 20 00 10
F +32 (15) 27 47 71
E info@maxonmotor.be
W www.maxonmotor.be

maxon motor is the worldwide leading supplier of high precision drives and systems. When it really matters! Try us.

Micro Drive Systems



Minimotor Benelux

Belgium
Dikberd 14/6c
B-2200 Herentals
T +32 (0)14-21 13 20
F +32 (0)14-21 64 95
E info@minimotor.be

The Netherlands
Postbus 49
NL-1540 Koog a/d Zaan
T +31 (0)75-614 86 35
F +31 (0)75-614 86 36
E info@minimotor.nl
W www.faulhaber.com

Faulhaber is a leading manufacturer of miniature drive systems based on ironless micromotors with the highest power-to-volume ratio.

member **DSPE**

Micromachining



Reith Laser bv
Bijsterhuizen 24-29
6604 LK Wijchen
The Netherlands
T +31 (0)24 3787564
F +31 (0)24 3787586
E info@reithlaser.nl
W www.reithlaser.nl

For more than 22 years Reith Laser bv is the leading supplier of laser-processed products in Europe. We can offer you a great diversity of lasermaterialprocessing activities:

- Laser- (micro-) cutting
- Laser drilling
- Laser welding
- Laser micromachining

Reith Laser is active in precision industry, medical industry, aerospace, semiconductor- and automotive industry.

Motion Control Systems



Aerotech LTD
Jupiter House, Calleva Park
Aldermaston
Berkshire
RG7 8NN England
T +44 (0)118 9409400
F +44 (0)118 9409401
E sales@aerotech.co.uk
W www.aerotech.co.uk



Applied Laser Technology
De Dintel 2
5684 PS Best
T +31 (0)499 375375
F +31 (0)499 375373
E techsupport@alt.nl
W www.alt.nl

member **DSPE**



IBS Precision Engineering
Esp 201
5633 AD Eindhoven
T +31 (0)40 2901270
F +31 (0)40 2901279
E info@ibspe.com
W www.ibspe.com

IBS Precision Engineering is a high-tech company in precision metrology components, systems and machines. Our solutions include special metrology machines, machine tool calibration systems, non-contact measuring systems and porous media air bearings.

member **DSPE**

Motion Control Systems



Newport Spectra-Physics B.V.
 Vechtensteinlaan 12 - 16
 3555 XS Utrecht
 T +31 (0)30 6592111
 E netherlands@newport.com
 W www.newport.com

Newport Spectra-Physics BV, a subsidiary of Newport Corp., is a worldwide leader in nano and micropositioning technologies.

member **DSPE**



Reliance Precision Mechatronics
 Florijnstraat 20
 4879 AH Etten-Leur
 The Netherlands
 T +31 (0)76 5040790
 F +31 (0)76 5040791
 E sales@rpmechatronics.co.uk
 W www.rpmechatronics.co.uk

- Positioning systems
- Drives
- Standard components
- Mechatronic assemblies

Manufacturer of among others: gears, rack, couplings and linear systems

Motion Control Systems



Rotero Holland bv
 Pompmolenaan 21
 3447 GK Woerden
 Postbus 126
 3440 AC Woerden
 T +31 (0)348 495150
 F +31 (0)348 495171
 E info@rotero.com
 W www.rotero.com

Rotero is specialized in small electrical motors and mechanical drives. Products: AC-, DC-, stepper- and servo motors up to 1.5 kW, actuators and small leadscrews.

Optical Components



Applied Laser Technology
 De Dintel 2
 5684 PS Best
 T +31 (0)499 375375
 F +31 (0)499 375373
 E techsupport@alt.nl
 W www.alt.nl

member **DSPE**

Optical Components



Molenaar Optics
 Gerolaan 63A
 3707 SH Zeist
 Postbus 2
 3700 AA Zeist
 T +31 (0)30 6951038
 F +31 (0)30 6961348
 E info@molenaar-optics.nl
 W www.molenaar-optics.eu

member **DSPE**

Piezo Systems



Applied Laser Technology
 De Dintel 2
 5684 PS Best
 T +31 (0)499 375375
 F +31 (0)499 375373
 E techsupport@alt.nl
 W www.alt.nl

member **DSPE**

Piezo Systems



Heinmade B.V.
 High Tech Campus 9
 5656 AE Eindhoven
 T +31 (0)40 8512180
 F +31 (0)40 7440033
 E info@heinmade.com
 W www.heinmade.com

HEINMADE develops and supplies piezo system solutions for positioning and vibration damping. HEINMADE cooperates with and is distributor of Nanomotion, Noliac and Piezomechanik.

YOUR COMPANY PROFILE IN THIS GUIDE?

Please contact:

Sales & Services / Gerrit Kulsdom / +31 (0)229 211 211 / gerrit@salesandservices.nl

Dutch Society for Precision Engineering

DSPE

YOUR PRECISION PORTAL

Your button or banner on the website www.DSPE.nl?

The DSPE website is the meeting place for all who work in precision engineering.

The Dutch Society for Precision Engineering (DSPE) is a professional community for precision engineers: from scientists to craftsmen, employed from laboratories to workshops, from multinationals to small companies and universities.

If you are interested in a button or banner on the website www.dspe.nl, or in advertising in Mikroniek, please contact Gerrit Kulsdom at Sales & Services.

T: 00 31(0)229-211 211 ■ E: gerrit@salesandservices.nl

ADVERTISERS INDEX

■ Coralis	58
www.coralis.nl	
■ DSPE Symposium	2
www.dspe.nl	
■ Helmholtz Institute EM	64
www.helmholtz-em.nl	
■ Mikroniek Extra	68-72
■ Mikroniek Special	35-50
www.mikroniek.com	
■ PAU Technik - optischen en elektronen	56
www.pau-technik.nl	
■ Precision Precision Electronics	52
www.precisionelectronics.co.uk	
■ Vainola	23
www.vainola.com/instruments	

DSPE

YOUR PRECISION PORTAL

μ MIKRONIEK

Mikroniek is the professional journal on precision engineering and the official organ of the DSPE, The Dutch Society for Precision Engineering.

Mikroniek provides current information about technical developments in the fields of mechanics, optics and electronics and appears six times a year.

Subscribers are designers, engineers, scientists, researchers, entrepreneurs and managers in the area of precision engineering, precision mechanics, mechatronics and high tech industry. Mikroniek is the only professional journal in Europe that specifically focuses on technicians of all levels who are working in the field of precision technology.

Publication dates 2013:

nr:	deadline reservation	publication date:
5	06-09-2013	11-10-2013 - Robotics
6	11-10-2013	22-11-2013 - (Preceding the Precision Fair) - Thermo-Mechanics

**For questions about advertising
please contact Gerrit Kulsdom**

Dial: 00 31(0)229-211 211 ■ E-mail: gerrit@salesandservices.nl





HEIDENHAIN

How much extra time does an absolute encoder offer you?

Time is priceless. That's why HEIDENHAIN absolute linear and angular encoders for machine tools set new standards for time and functionality – Without costing more. They obviate referencing runs and reduce the non-productive time of your machines. This feature plays an essential role when putting linked automatic production machines into operation. Should servicing or maintenance ever become necessary, our encoders issue warning signals that provide you with ample time not only to react, but also to plan. In a word, our absolute encoders give you and your machines more time. HEIDENHAIN NEDERLAND B.V., Postbus 92, 6710 BB Ede, Telephone: (0318) 58 1800, www.heidenhain.nl, E-Mail: verkoop@heidenhain.nl



Absolute linear and angular encoders

ask motion + linear scales + rotary graticules + digital readouts + length gauges + rotary encoders